

University of Nottingham
UK | CHINA | MALAYSIA

Evaluating the effects of climate change and biotic interactions on terrestrial ectotherms through time and space

Simon Tarr

MSci (Hons)

Thesis submitted to the University of Nottingham
for the degree of Doctor of Philosophy

August 2019

Acknowledgements

Sometime in 2008, having worked in my old IT job for around 2 years, I came home from work—a little nervous and despondent—and told my parents that I wanted to quit work and go to university. By this point I had been out of their hair for a while but knew I'd need their support if I was to just drop everything and become a student again. I needn't have been nervous - they didn't bat an eye. O*f course we will support you, we think it's a great idea to go to university!* And with that I handed in my notice and started a degree in Zoology. To be here now, almost 10 years later—and submitting my PhD thesis, no less—is testament to the support they have provided me throughout university and, frankly, my entire life. So, to my parents—Wendy and Simon—I owe an enormous thank you.

I also owe an enormous thank you to Ruth. She never complained as I routinely disappeared on fieldwork, jetted off to conferences and indulged me in my passion for science. She allowed me to maintain my fantasy as a gentleman scientist and naturalist for four whole years and ultimately made this PhD possible. I also thank her for keeping me sane throughout this work, insisting that I don’t stay up coding until 2am and ensuring that I had quality weekend time to decompress after a mentally taxing week. I think that returning to a lovely home, free from the influence of academia, went a long way to making this PhD such a fulfilling and (mostly) stress-free experience, and I thank her for providing me with that physical and mental security.

Thanks are in order for *many* people within the School of Geography. First I must thank my supervisor, Adam, for entertaining—with good humour—my

many questions, half-baked ideas and often questionable logic. I've lost count of the number of hours we spent talking science; Adam with a look of concentration (or perhaps confusion) on his face while I ramble on about my work. I thank him for imparting upon me his knowledge, wisdom and passion for science. But not his coding practices. If I have become a good scientist it is because of him. If I haven't, then it is my own doing. Second I must thank my office pals – Catherine, Chloe, Phil and Savannah (in alphabetical order so I can't be accused of favouritism) – for their emotional support throughout my time here. It's been a pleasure to experience the rollercoaster of emotions that is a PhD with them and I would be lying if I said I'd have been able to do this without them. Third, I must thank the department, and everyone in it, for making my time here fun and memorable. This endeavour would have been a far less fulfilling experience without my friends and colleagues in Geography.

I am also grateful to my three cats—Pippa, Peanut and Monty. Although they have no concept of a PhD, data or the stress of giving academic talks, they were nonetheless there for me, providing unwavering emotional support whenever I need it.

Finally, doing a PhD is tough. But it's not as tough as being diagnosed with cancer, enduring treatment and surviving. I must mention my sister, Charlotte, who stood strong and overcame the worst with more than a modicum of perseverance and resilience. Her situation certainly put my PhD-related difficulties into perspective.

Table of Contents

Acknowledgements 2

List of Figures 6

List of Tables 7

Abstract 9

Chapter 1: Introduction 11

Chapter 2: Literature Review 14

2.1 Species distribution modelling 14

2.1.1 Correlative species distribution models 15

2.1.2 Mechanistic species distribution models 16

2.2 Why is understanding range limits and distributions important? 18

2.3 Research Questions 19

2.3.1 How does climate alter the spatial distribution of ectotherm activity budgets? 19

2.3.2 What are the relative contributions of biotic interactions, dispersal limitations and availability of preferred habitat type in limiting species' ranges through geographic space? 22

2.3.3 Does climate generate repeatable and predictable patterns of biodiversity? 23

2.4 A note on the papers 24

Chapter 3: The ticking clock: a global analysis of ectotherm activity budgets under anthropogenic climate change 26

3.1 Introduction 26

3.2 Methods 30

3.3 Results 36

3.4 Discussion 46

3.5 Supporting Information 53

Chapter 4: Revealing effects of biotic interactions on species' ranges using ecological traits and mechanistic niche modelling 58

4.1 Introduction 58

4.2 Methods 67

4.3 Results 74

4.4 Discussion 82

4.5 Supporting Information 91

Chapter 5: Testing for macroecological convergence of climate-richness relationships in replicated island radiations 105

5.1 Introduction 105

5.2 Methods 109

5.3 Results 114

5.4 Discussion 125

5.5 Supporting Information 133

Chapter 6: General conclusions and future directions 136

References 143

Appendix 1: A biogeographic reversal in sexual size dimorphism along a continental temperature gradient 173

1.1 Abstract 174

1.3 Introduction 175

1.4 Methods 180

1.5 Results 185

1.6 Discussion 193

1.7 References 200

1.8 Supporting Information 201

Appendix 2: Fossils, phylogenies and the evolving climate niche 220

List of Figures

Figure 1-1 Conceptual representation of a species' niche in geographic space 12

Figure 3-1 Change in activity hours (relative to 1661) across all taxa between 1661 and 2100. 37

Figure 3-2 Change in activity hours (relative to 1661) for reptiles between 1661 and 2100. 39

Figure 3-3 Reptile disharmony maps under RCP 6.0. 40

Figure 3-4 Change in activity hours (relative to 1661) for amphibians between 1661 and 2100. 42

Figure 3-5 Amphibian disharmony maps under RCP 6.0. 43

Figure 3-6 Change in activity hours (relative to 1661) for insects between 1661 and 2100. 45

Figure 3-7 ISIMIP2b percentage change in rainfall between 1661 (pre-industrial baseline) and 2100 under RCP 6.0 for both IPSL and GFDL climate scenarios. 57

Figure 4-1 Predicted relationships depicting a fundamental niche boundary and the detection of distributional debt from biotic interactions. 62

Figure 4-2 Fundamental niche (FN), geographically accessible realised niche (GARN) and distributional debt plots (DEBT) 76

Figure 4-3 Estimated Probability of Presence (EPP; from Maxent species distribution models) against activity hours (a proxy for fundamental niche suitability) 77

Figure 4-4 Relationships between morphological similarity and fundamental niche residuals (residuals from the 90th percentile) 80

Figure 4-5 Relationships between percentage canopy cover and fundamental niche residuals.....81

Figure 4-6 Morphological similarity surfaces (MSS).....103

Figure 4-7 Activity hours/estimated probability of presence plots with cost surface (dispersal constraint) removed from MaxEnt models.....104

Figure 5-1 Potential species richness for 74 species of *Anolis* lizard across the Greater Antilles at 1x1km resolution.....116

Figure 5-2 Relationships between observed richness and fitted species richness on each island.....122

Figure 5-3 Predictions of climate richness relationships on independent islands.. 123

Figure 5-4 Estimated species richness on Cuba.....134

Figure 5-5 Relationships between species richness and climate on each island of the Caribbean.....135

List of Tables

Table 4-1 Replacement climate layers for *NicheMapR's* microclimate sub-model.....91

Table 4-2 Thermal parameters for *NicheMapR* obtained from an extensive literature search.....92

Table 4-3 Default ectotherm sub-model parameters for NicheMapR.....96

Table 4-4 Summary statistics for MaxEnt species distribution models……. 98

Table 4-5 List of the 18 traits used in this analysis.....99

Table 4-6 Euclidean morphological distances between all 10 species of *Anolis* on Puerto Rico.....100

Table 4-7 Fundamental niche summary statistics for 8 *Anolis* species across Puerto Rico.....101

Table 4-8 ANOVA test of slope differences between upper and lower quantiles. 102

Table 5-1 Summary statistics for species occurrence data and species distribution models.....115

Table 5-2 Summary statistics of the ‘best’ model for each island (lowest Bayesian Information Criterion value, BIC).....118

Table 5-3 Environmental predictor coefficients for the ‘best’ fitting model on each island.....119

Table 5-4 Summary statistics for model predictions.....124

Table 5-5 Summary AUC statistics for MaxEnt species distribution models across Cuba, Hispaniola, Jamaica and Puerto Rico. 133

Abstract

Understanding the limits to species ranges and distributions remains a difficult and long-standing problem in the field of macroecology. This difficulty exists because species' range limits reflect several complex and interacting processes including; physiological responses to abiotic conditions, biotic interactions and species' dispersal abilities across geographic space. This complexity is increased further under rapid anthropogenic climate change which is predicted to affect all these processes simultaneously. Nonetheless, recent advances in species distribution modelling—particularly mechanistic species distribution models which can estimate a species' fundamental niche—have provided novel means to further understand how species distributions manifest across large geographic extents. Despite these methodological breakthroughs, there remain substantial gaps in our knowledge of species' distributions including: (1) How does climate alter the spatial distribution of ectotherm activity budgets through time and space? (2) What are the relative contributions of biotic interactions, dispersal ability and availability of preferred habitat type in limiting species' ranges across geographic space? and (3) Does climate generate repeatable and predictable patterns of biodiversity?

Here—within a species distribution modelling framework—I use both correlative and mechanistic species distribution models to address these questions. I reveal how climate, biotic interactions and species' dispersal abilities limit ranges across large spatial extents and that by integrating correlative and mechanistic species distribution models we may tackle questions that have, until very recently, been out of reach. I predict that over the next decade macroecology will witness an increased use of correlative and

mechanistic models in tandem to leverage the strengths of both approaches. Despite continued anthropogenic pressures on species across the globe limiting where species can survive, it is nonetheless an exciting time to be working in the field of macroecology and species distribution modelling.

Chapter 1: Introduction

Macroecology's primary aim is to understand and predict the abundance and distribution of organisms across the planet, ultimately linking patterns of species diversity to the underlying processes which generate them (Pearse et al., 2018; Peters, 1991). The discipline has surprisingly ancient roots with Aristotle commenting as far back as 350 B.C.E. on the distribution of scorpions in Caria and Pharos (Fet et al., 2009) but it wasn't until the nineteenth century—with the arrival of early naturalists such as Alexander von Humboldt, Alfred Russell Wallace and Charles Darwin, amongst others—that macroecology would begin to develop into the quantitative subject that it is known as today. Central to our modern understanding of species' range limits and distributions is the niche concept. The niche has been defined in many ways (Chase and Leibold, 2003; Holt, 2009; Hutchinson, 1957; Leibold, 1995; Soberón, 2007) but it is the Hutchinsonian niche concept, which views the niche as a property of an organism—rather than as a property of a particular environment—is arguably the most useful in the context of understanding species' ranges. The Hutchinsonian niche concept proposes that species' ranges reflect fundamental niche limits set by species' physiological tolerances to abiotic conditions and/or realised niche limits set by biotic interactions such as competition or predation (Algar et al., 2013; Bruno et al., 2003; Bulleri et al., 2016; Hutchinson, 1957; Pulliam, 2000; Soberón and Nakamura, 2009). A third component—dispersal limitation—futher restricts where a species can exist in geographic space (Algar et al., 2013; Glor and Warren, 2011; Pulliam, 2000; Soberón and Nakamura, 2009). The challenge faced by researchers wanting to understand species' distributions is to identify

where these components of the niche overlap and thus manifest as a species' range in geographic space (Figure 1).

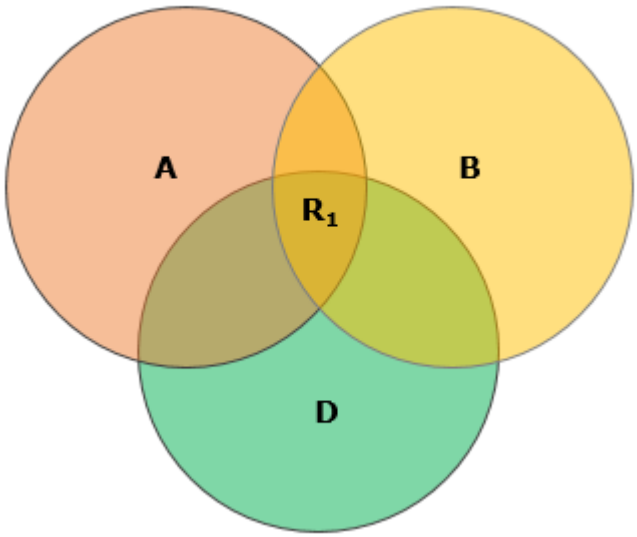


Figure 1-1 Conceptual representation of a species' niche in geographic space. Circle A represents all abiotic conditions which are suitable for a focal species. Circle B represents regions where biotic conditions (e.g. competition, predation etc.) permit survival. Circle D represents dispersal and is the region in geographic space accessible to a species. R_1 represents areas where the species is actually found in geographic space. Diagram adapted from Figure 2 in Soberón and Nakamura (2009).

Using niche theory as an overarching framework for this work, I identify three unresolved questions regarding species' range limits and distributions and address them within a species distribution modelling framework:

(1) How does climate alter the spatial distribution of ectotherm activity budgets through time and space?

(2) What are the relative contributions of biotic interactions, dispersal ability and availability of preferred habitat type in limiting species' ranges across

geographic space?

(3) Does climate generate repeatable and predictable patterns of biodiversity?

I provide a more detailed summary of each research question in Section 2.3 Research Questions starting on page 19.

Chapter 2: Literature Review

2.1 Species distribution modelling

The Hutchinsonian niche concept is both elegant and intuitive, but it has taken many decades of research to package these ideas into practical tools which enable ecologists to better understand the limits to species' ranges and how they are distributed across geographic space (Soberón and Nakamura, 2009). These tools, referred to collectively as species distribution models, have become the most widely-implemented method in biogeography and macroecology to quantify species' ranges (Fois et al., 2018; Soberón and Nakamura, 2009). Within the literature, the terms *species' distribution model*, *habitat suitability model* and *ecological niche model* have routinely been used interchangeably (Soberón and Nakamura, 2009). To provide a clear definition throughout this thesis, I define a *species distribution model* as an n-dimensional niche space which is projected across geographic space. Given that a species' range must be defined in reference to an area in geographic space, I use the terms *species distribution model* and *species range* interchangeably throughout, as both are approximations of a species' niche in geographic space. I consider an ecological niche model as a representation of a species' niche in environmental space which is not projected into geographic space.

All SDMs have a similar purpose: to identify an environmental space which permits survival. Within this definition, the 'environment' can be any factor external to an organism which influences survival, whether this be abiotic (e.g. climatic) or biotic (e.g. competition, predation, disease etc.). Two general

methodological approaches have been developed to quantify different aspects of a species' niche which have helped to improve our understanding of species ranges through geographic space; correlative and mechanistic species' distribution models.

2.1.1 Correlative species distribution models

Most species distribution modelling approaches are correlative and estimate potential distributions given a set of environment predictors (e.g. climate, land cover) and observed presences and/or absences (Elith et al., 2011, 2010, 2006; Guisan and Zimmermann, 2000). Environmental predictors are (ideally) chosen based on *a priori* expectations regarding the factors hypothesised to be important in limiting the distribution of the focal species. For example, temperature is key determinant of reptile distributions (Angilletta, 2009; Deutsch et al., 2008; Huey et al., 2009; Kingsolver et al., 2013; Sunday et al., 2014) while precipitation levels can influence the distribution of amphibian species (Araújo et al., 2006; Buckley and Jetz, 2007; Feder and Burggren, 1992). The environmental conditions are extracted at the locations where the species is known to occur, and a suitable environmental space is described statistically (e.g. using a model such as BIOCLIM or Maxent), which can then be mapped onto geographic space to infer distributions. This approach is powerful because the processes influencing the distribution are implicit in the model; even if we do not know the exact mechanism underlying an observed pattern, if the process is related in some way to the chosen predictor variables, a good model may nonetheless be produced. Indeed, correlative SDMs have been applied successfully to a wide range of theoretical and practical applications (Fois et al., 2018) from understanding niche evolution (Warren et

al., 2008) to assessing the impacts of future climate change (Fois et al., 2016) and identifying suitable conservation areas (Kaky and Gilbert, 2016). The main advantages of this modelling approach are mature modelling and software environments (e.g. running Maxent within R) plus reasonably modest data requirements. With an increasingly rich array of interpolated climate data (e.g. Worldclim) and remotely-sensed environmental data (e.g. MODIS Leaf Area Index), along with ever-expanding databases of observation records (e.g. the Global Biodiversity Information Facility; GBIF), it can be a reasonably straightforward process to parameterise a model.

The starting point of any correlative SDM are observation records. For a species to be observed at a location, it must have been able to survive given the local abiotic environmental conditions (e.g. temperature, precipitation, humidity) plus any biotic interactions which facilitate survival at that location. As such, observation records contain, implicitly, information on the complex milieu of biotic interactions which allow survival at a location. Correlative SDMs are therefore quantifying both the direct influences of the abiotic environment plus climate-related biotic interactions (Kearney and Porter, 2004). Thus, although correlative distribution models may provide some information on a species' fundamental (abiotic) niche, it becomes difficult to unpick the relative contributions of abiotic and biotic interactions. In this respect, correlative SDMs are approximating a species' realised niche (Anderson, 2017; Kearney and Porter, 2009, 2004).

2.1.2 Mechanistic species distribution models

Mechanistic SDMs are fundamentally different to correlative SDMs. The approach here is to instead model a whole organism, explicitly linking species'

morphological, physiological and behavioural traits with microclimate data to gain a mechanistic, processed-based, understanding of species' distributions (Kearney and Porter, 2009). At the most fundamental level, all organisms are constrained in where they can survive by physiological limitations to outside conditions (Kearney and Porter, 2004). A key goal of mechanistic species distribution modelling is to incorporate these physiological limits into models so that ranges can be inferred across a landscape (Kearney and Porter, 2009).

All organisms are tied intimately to their surrounding climatic conditions via exchanges of energy and mass. The field of biophysical ecology arose throughout the 1970s and 1980s (Gates, 1980; Porter and Gates, 1969; Tracy, 1982) to quantify and model key 'transfer processes' between organism and environment—primarily heat and mass transfer. Energy and mass are constantly flowing between organism and environment. Energy moves *via* conduction, convection, evaporation and radiation and is influenced, in the case of terrestrial organisms, by local environmental conditions such as wind speed, humidity, radiation and air temperature (Gates, 1980). Mass is transferred *via* the flow of gases (e.g. respiration) as well as food and water ingested and excreted by an organism. Survival of an organism will only be possible within a subset of the entire *n*-dimensional climate space, with successful reproduction occurring within a smaller subset of those conditions that permit survival (Kearney and Porter, 2004).

The flow of energy and mass between the environment and organism is mediated by the morphological and physiological characteristics of the individual. An organism's size, shape, mass, solar reflectance and permeability to water all contribute to the regions in which survival and

reproduction is possible (Gates, 1980; Kearney and Porter, 2004). By solving thermodynamic heat and mass balance transfer equations—using both environmental conditions and organismal traits as inputs—key organismal properties such as metabolic rate, water balance and core body temperature can be calculated and, when integrated across a landscape, distributions can be inferred (Kearney et al., 2008, 2013; Kearney and Porter, 2009, 2017).

A key advantage to modelling organismal responses to climate from first principles is that predictions of species' distributions can be made with no information on where the species currently lives (i.e. observation records are not required). Such models are modelling the response to abiotic conditions only, with no confounding effects of biotic interactions or dispersal limitations, and are therefore approximating a species' fundamental niche (Kearney and Porter, 2009, 2004). The trade-off for a detailed, mechanistic, understanding of a species' response to climate is the high initial data requirements such as species-level morphological and physiological data plus detailed microclimatic data.

2.2 Why is understanding range limits and distributions important?

Understanding species' range limits and distributions is important for two main reasons. The first is scientific interest. Although theory is quite clear on the factors which can limit species' ranges (i.e. abiotic, biotic and dispersal factors) substantial knowledge gaps still exist, particularly regarding how biotic interactions limit species' distributions at macroecological scales (Anderson, 2017; Gilman et al., 2010; Wisz et al., 2013) and how species'

ranges shift through time (Maguire et al., 2015; Nogués-Bravo et al., 2018; Parmesan, 2006). The second is practical. Anthropogenic climate change is predicted to alter species' distributions (Urban, 2015), generate novel communities (Algar et al., 2009; Gilman et al., 2010; Stralberg et al., 2009; Williams and Jackson, 2007; Wisz et al., 2013) and cause extinctions across the globe (Parmesan, 2006; Poloczanska et al., 2013; Sinervo et al., 2010; Urban, 2015). If society is to stand any chance of mitigating the effects of climate change on biological diversity, we must improve our understanding of how species' niches manifest as distributions across geographic space. These two reasons—scientific and practical—are not mutually exclusive. A better theoretical understanding of species ranges, and improved methods to quantify them, will ultimately provide the tools necessary for conservation practitioners to potentially mitigate the worst effects of anthropogenic climate change upon biodiversity.

2.3 Research Questions

Below I present an overview of each research question along with the rationale behind each analysis. Full and detailed methodologies can be found within respective chapters (Chapters 3, 4 and 5). I refer the reader to the introduction within each data chapter for the broader scientific context surrounding each topic.

2.3.1 How does climate alter the spatial distribution of ectotherm activity budgets?

Anthropogenic climate change is widely regarded as one of the greatest threats to biodiversity. Ectothermic organisms are particularly susceptible to climate

change because their physiology and metabolism is tied intimately to outside environmental conditions (Araújo et al., 2006; Deutsch et al., 2008; Gilman et al., 2010; Lenoir and Svenning, 2015; Poloczanska et al., 2013; Sinervo et al., 2010; Sunday et al., 2014; Urban, 2015). Most projections of the thermal implications of climate change on organisms compare current conditions to future ones (Urban, 2015). However, rapid climate change has been occurring for at least half a century (Diffenbaugh and Field, 2013), meaning that species' ranges could have already changed substantially. Shifting baselines syndrome describes the general phenomena where present-day measurements are assumed to be reliable historical reference points (Soga and Gaston, 2018). However, these present-day measurements may themselves represent a change from an earlier state in a system. In the context of global climate change, shifting baselines present a considerable barrier to understanding how species distributions have changed through space and time; without a fixed reference point with which to compare contemporary distributions, it is impossible to determine the full effect of climate change upon them. In short, without historical context, it is not possible to determine whether predicted range contractions—and potential extinctions—are first relaxing back to a 'pre-industrial norm' or represent novel and unprecedented changes.

Establishing a reliable baseline to quantify species' responses to climate change is challenging. Most attempts quantify species' distributions under future climates use correlative models (Urban, 2015), despite known issues with extrapolation (Elith et al., 2010; Fitzpatrick and Hargrove, 2009; Maguire et al., 2015; Urban, 2015; Urban et al., 2013; Veloz et al., 2012). These same issues will also preclude accurate hindcasting. The extrapolation of correlative

models could be avoided with the use of time-series observation records, parameterising models at snapshots in time and observing how distributions change. However, while observation records extend back many decades for some taxa (e.g. birds and some mammals) for the overwhelming majority of species, such data are absent, making this method unworkable.

To predict species' past, and future, responses to climate, we must therefore move beyond a purely correlative-based framework to species distribution modelling. Biophysical mechanistic models offer a logical way forward as such methods do not require observation records for model parameterisation. Instead, suitability can be calculated from the first principles, avoiding the issues intrinsic to correlative species distribution models (Kearney and Porter, 2009). Biophysical ecological models (e.g. NicheMapper; Kearney and Porter 2009) can quantify activity time (Gunderson and Leal, 2015) at a particular point in space and time given empirical data on an organism's morphology and physiology and the microclimate conditions at a location. Activity time can then be used as a proxy of relative habitat suitability with a greater number of hours being 'better' than fewer hours.

In **Chapter 2** I model geographic and temporal variation in activity budgets for 262 ectotherm species from the year 1661 to the present day to quantify changes in activity budgets that have already occurred due to recent climate change. I then forecast changes in activity budgets to the year 2100 under three different climate change scenarios to determine whether time for life has changed across taxa and through space. Finally, I evaluate congruence between activity budget estimates and species diversity to test for growing

'spatial disharmony' in the conditions favourable for life and how biodiversity is distributed—and may be distributed in the future—across the globe.

2.3.2 What are the relative contributions of biotic interactions, dispersal limitations and availability of preferred habitat type in limiting species' ranges through geographic space?

Understanding the factors and processes limiting species' ranges and distributions has long been a goal in biogeography and ecology. Central to our current understanding of species ranges is Hutchinsonian niche theory (Hutchinson, 1957). Within this theoretical framework, three factors are considered critical in delimiting species ranges (1) abiotic factors (e.g. climate) which determine a species' fundamental niche (2) biotic interactions (e.g. competition, predation) which exclude species from areas of the fundamental niche or extends beyond the fundamental niche limit via positive biotic interactions such as facilitation (Pulliam, 2000) and (3) dispersal limitiation which prevents access to otherwise suitable areas (Algar et al., 2013; Glor and Warren, 2011; Pulliam, 2000; Soberón and Nakamura, 2009). Although theory is clear on how these factors should interact to manifest as a species' geographic range (Soberón and Nakamura, 2009), the relative contribution of each of these three processes is generally unknown, especially for entire fauna. Often, studies seek to address one or two of these factors, thus presenting an incomplete picture of a species' range.

In **Chapter 3**, I use mechanistic and correlative niche models to map areas of distributional debt (i.e. where species fail to fill their fundamental niches) for *Anolis* lizards on Puerto Rico. Here, distributional debt is defined as locations which are within a species' fundamental niche, but which are uninhabited by

that species. I then move on to test whether dispersal limitation, access to preferred habitat type or biotic interactions can explain mismatches between realized and fundamental niches across geographic space.

2.3.3 Does climate generate repeatable and predictable patterns of biodiversity?

A criticism often applied to the field of macroecology is the lack of controlled, replicated, experiments necessary to reliably infer causation. The scope and breadth of many macroecological analyses makes a traditional experimental approach practically impossible. Even if such a manipulation were possible, considerable ethical issues may also arise. As a solution to this inferential barrier, naturally replicated systems—such as islands—can provide an opportunity to test predictions when manipulative experiments are not possible. Such an approach has been used successfully for decades by evolutionary biologists who retrospectively infer the drivers and processes of evolution using islands and exploiting them as 'natural laboratories' (Diamond, 1986; Losos and Ricklefs, 2009). In **Chapter 4,** I use this approach to better understand the processes determining species richness patterns within islands. Although total species richness on islands varies in predictable ways within archipelagos, the processes determining intra-island patterns of richness remains largely unknown. Using the 4 large islands of the Greater Antilles as a naturally replicated experiment, I ask three questions: (i) how does species richness vary within islands? (ii) are species richness gradients within individual islands related to climate? (iii) are climate–richness relationships repeatable and predictable between islands?

2.4 A note on the papers

The papers within this thesis are at various stages of the publication process, as outlined in the table below. Where a paper has been published, I include the final version of the paper in 'Word format', prior to the journal's typesetting process to keep formatting consistent throughout the document. There may therefore be minor discrepancies between the online PDF version of each paper and the text included here due to the journal's copy-editing process.

Throughout the course of my PhD I was also involved in a number of different projects related to my core research but which cannot be included as main chapters in my thesis. The first paper in this bracket is an extension of my master's dissertation which was published in 2018 in *Ecography* (Appendix 1). The second paper is a short 'News & Views' article which appeared in *Nature, Ecology and Evolution* (Appendix 2) where I am second author. These manuscripts can be found at the end of the thesis.

Title	Status	Journal (Target Journal)	Page No.
The ticking clock: a global analysis of ectotherm activity budgets under anthropogenic climate change	In prep	*(TBC)*	26
Revealing effects of biotic interactions on species' ranges using ecological traits and mechanistic niche modelling	In prep	*(Ecography)*	58
Testing for macroecological convergence of climate-	In prep	*(Journal of the Linnean Society B)*	105

richness relationships in replicated island radiations			
Appendix 1: A biogeographic reversal in sexual size dimorphism along a continental temperature gradient	Published (2018)	*Ecography*	173
Appendix 2: Fossils, phylogenies and the evolving climate niche	Published (2018)	*Nature, ecology & evolution*	220

Chapter 3: The ticking clock: a global analysis of ectotherm activity budgets under anthropogenic climate change

3.1 Introduction

All animals need time to carry out critical activities such as sleeping, feeding and, most importantly, mating. At an individual level, a reduction in time to carry out these activities can result in reduced fitness (Grant and Dunham, 1988; Sunday et al., 2014), while decreases in time across many individuals in a population could manifest as local extinctions and range contractions across geographic space (Sinervo et al., 2010; Sunday et al., 2014). Climate change may alter the duration within which conditions are suitable for a species to remain active. In areas where climate change alters body temperatures (T_b) so that they approach or surpass critical thermal minima (CT_{min}) or maxima (CT_{max}), activity times—and fitness—will decline, while changes that allow body temperatures to remain within critical limits for longer periods may be beneficial (Jayatilaka et al., 2011; Kingsolver et al., 2013; Sinclair et al., 2016; Sunday et al., 2014).

Climate change is not homogenous through time and space (Diffenbaugh and Field, 2013). Increasing temperatures at mid– to high latitudes could increase the length of the growing season or the frequency that species experience optimal temperatures (Kingsolver et al., 2013), making available a wider range of locations and habitats (Algar et al., 2018; Araújo et al., 2006; Buckley and Kingsolver, 2012; Deutsch et al., 2008; Huey et al., 2009). However for many

species, increasing temperatures may lower thermal safety margins (Deutsch et al., 2008; Huey et al., 2009) or surpass thermal tolerances entirely (Huey et al., 2009; Sunday et al., 2014). In tropical regions, which harbour the vast majority of the world's biodiversity, species—especially cool-adapted forest dwellers—have lower thermal safety margins compared to species at higher latitudes (Deutsch et al., 2008; Huey et al., 2009; Sunday et al., 2014), making them particularly sensitive to warming temperatures (Bonebrake and Deutsch, 2012; Diamond et al., 2012; Sunday et al., 2014; Urban, 2015). To mitigate the increasing frequency of higher and more extreme temperatures, time may be diverted away from activities which contribute directly to fitness, such as finding mates, and toward behaviours such as shade-seeking and burrowing to lower body temperatures to within physiological limits (Kearney and Porter, 2009; Sunday et al., 2014).

Most projections of the thermal implications of climate change for organisms compare future and current conditions (Urban, 2015). However, rapid climate change has been occurring for almost half a century (Diffenbaugh and Field, 2013), meaning that animal activity budgets—defined here as the time within which an animal can be active (Gunderson and Leal, 2015)—for many species may have already declined. Alternatively, recent anthropogenic warming could have increased activity budgets throughout the recent past, meaning that projected declines are a relaxation back to pre-industrial activity budgets, rather than unprecedented reductions in activity time. Furthermore, because climate change and biodiversity are unevenly distributed across the globe, gains and losses in activity time worldwide may not be spatially concordant with biodiversity, i.e. the places where most species live. Resolving these

unknowns requires reconstructing historic, current and future variation in thermally-dependent animal activity budgets across the globe.

Establishing a reliable historical baseline for animal activity time against which to evaluate future changes is challenging. A key barrier is a shortage of continuous historical climate data extending from the present day to the period preceding the Industrial Revolution and the onset of anthropogenic greenhouse gas emissions. The climate datasets popular with ecologists typically come from a small handful of sources which often span less than 40 years of contemporary climate. For example, WorldClim v2 (Fick and Hijmans, 2017) provides climate data between 1970 and 2000 and CHELSA (Karger et al., 2017) spans 1979 to 2013. CRU TS datasets (various versions) span a greater temporal range between 1901 to 2017 (Harris et al., 2014; New et al., 2002, 1999) but do not extend back prior to the start of the Industrial Revolution. While WorldClim v1.4 (Hijmans et al., 2005) does provide historical climate data, these datasets capture a snapshot in time at 6,000 and 22,000 years ago, rather than detailed time-series that would permit the quantification of activity budgets through time. The ISIMIP2b climate simulations (Frieler et al., 2017) address these temporal shortfalls and provide daily climate estimates between the years 1661 and 2100. As the dataset spans a substantial amount of the recent past, it is possible to use these data to understand how activity budgets have changed prior to industrialisation and then forward to the year 2100 under a range of different climate change scenarios.

Biophysical ecological models (e.g. NicheMapper; Kearney and Porter 2009) can quantify activity budgets at a particular point in space and time given empirical data on an organism's morphology and physiology, the microclimate

conditions at a location, and a definition of what constitutes ‘active’ time. Several different definitions have been proposed to measure the time within which animals can be active, which vary in the degree of thermal constraints they impose on activity (Gunderson and Leal, 2015). At the most restrictive level, an animal is considered active only when it is within the bounds of a preferred range of temperatures (Hertz et al., 1993; Kearney and Porter, 2009; Sinervo et al., 2010). Grounded in work on behavioural thermoregulation (Hertz et al., 1993), preferred temperatures are the temperatures that organisms actively locate through geographic space. Less restrictive definitions of activity time use either minimum and maximum field and body temperatures or critical thermal minima and maxima (CT_{min} and CT_{max}). Within these thermal limits an animal is considered active, regardless of the level of activity that may be attained across a thermal spectrum (Gunderson and Leal, 2015). In other words, an animal is considered to be equally active at any point within these thermal boundaries, despite the fact that ectothermic species have optimum temperatures under which locomotion and metabolism (and therefore activity) is most efficient or effective (reviewed in Angilletta 2009). The type of thermal thresholding selected will often cause an over- or underprediction of true activity budgets; a restrictive activity time will tend to underestimate activity budgets, while less restrictive thresholds will tend to over predict activity budgets (Gunderson and Leal, 2015).

Choosing an appropriate thermal thresholding method to quantify activity budgets—particularly when analysing multiple species across large geographic extents—necessitates trade-offs. Preferred thermal activity levels are not known for many species of ectotherm, making it challenging to

threshold activity budgets using this metric. Further, it has been observed that for at least one species of tropical ecotherm (*Anolis cristatellus*) that individuals can be active far outside their preferred temperature range (Gunderson and Leal, 2015) thus questioning the utility of this thresholding approach when quantifying activity budgets. Systematically applying this method across species will likely substantially underestimate true activity budgets. A pragmatic alternative is to use CT_{min} and CT_{max} data (Bennett et al., 2018), counting hours when T_b is within this range as 'active' time. This classification will likely over-predict activity budgets but has the advantage that one can quantify the maximum number of hours an animal could feasibly be active.

Here, I model geographic and temporal variation in activity budgets for 262 ectotherm species from the year 1661 to the present day to quantify changes in activity budgets that have already occurred due to recent climate change. I forecast changes in activity budgets to the year 2100 under three different climate change scenarios to determine whether time for life has changed across taxa and through space. Finally, I evaluate congruence between activity budget estimates and species diversity to test for growing spatial disharmony' in the conditions favourable for life and how biodiversity is distributed—and may be distributed in the future—across the globe.

3.2 Methods

Overview

I used the biophysical model *NicheMapR* (Kearney and Porter 2009b, 2017) to estimate the activity budgets, in hours, for 262 species of terrestrial ectotherm

across the globe (excluding Antarctica) at a resolution of 0.5 x 0.5 degrees between the years 1661 and 2100 across a range of different climate change scenarios. The animal dataset included species from three taxonomic classes: insects (74 species), amphibians (31 species), and reptiles (159 species). Due to computing constraints, I first averaged each month's climate values within a decade (1661-1670, 1671-1680, etc.) and computed the activity budget for each species for the middle day of each month, thus providing yearly activity budgets at the decadal scale. I performed these calculations across the globe and summed the values across all species and within classes, to produce a global estimate of variation in activity time in each decade from 1661 to 2100.

Biophysical modelling

NicheMapR is a mechanistic niche model which can estimate various organismal properties including water budgets, body temperature and activity hours (Kearney and Porter, 2009, 2017). The model solves balanced heat and mass transfer equations for every hour in a day to estimate, in the present case, the number of hours within a 24-hour period where an animal's body temperature falls within its critical thermal limits (CT_{min} and CT_{max}), i.e. maximum potential activity hours, given the interaction between the local microclimatic conditions and the organism's physiology.

To compute activity hours, *NicheMapR* requires data on several aspects of an organism's physiology including body shape and mass, CT_{min}, CT_{max} and preferred body temperature (T_{pref}). Data on CT_{min} and CT_{max} were obtained from the GlobTherm database (Bennett et al. 2018). To calculate the maximum potential activity hours, i.e. when activity is limited by physiology rather than behaviour, I set each species' voluntary thermal minimum and

maximum temperatures to equal CT_{min} and CT_{max} respectively. I arbitrarily set a species' preferred body temperature at 75% of its CT_{max} as a sensitivity analysis determined that this parameter did little to affect the number of predicted activity hours across a year (see supplementary material). Emergence and basking temperatures were set to equal CT_{min}. This ensured that when an individual's CT_{min} threshold was passed, the animal was immediately set as active. The animal then remained active unless its T_b surpassed either CT_{min} or CT_{max}, at which point it becomes inactive. As temperature changes throughout the day, the organism can perform a range of behaviours including shade seeking and climbing. I ensured that the organism could always find the maximum amount of shade (100%) to potentially buffer extremes in daytime temperatures. I also allowed the organism to climb or burrow to a maximum height/depth of 15 cm in order to mitigate thermal stress and keep T_b as close as possible to T_{pref}. When climbing, the organism was still considered active if the act of climbing reduced T_b to within CT_{min} and CT_{max}. Should the animal select to burrow, its activity state was set to inactive. I did not compute hourly estimates for every day in the year (n=365) due to computing constraints. The maximum number of hours available to each species within a year in our study was therefore 12 * 24 = 288 hours per grid cell.

I supplemented thermal data with mass data from several different sources (see supplementary materials). Where empirical mass data was not available for amphibian species, I used the organism's mean snout-vent length (SVL) measurement and allometric equations to estimate body mass (see supplementary material). Mass data at the species level for insects were

difficult to procure, so I used family-level mass data from Chown et al. (2007). Although these data are at a high taxonomic level, at the organismal scale changes in body mass made little difference to the number of available activity hours when predicted across the globe and at this resolution (see supplementary material).

All organisms lose water to their surroundings via cutaneous water loss (Gates, 1980). To account for the difference in water loss between reptiles, amphibians and insects I modified the 'skinwet' parameter within *NicheMapR*. For all species of lizard and insect I left this at *NicheMapR*'s default (2% of the surface acting as a free water exchanger). For amphibians, I set 'skinwet' to 100% as almost the entire body surface is able to act as a free water exchanger (Kearney et al., 2008). I further limited amphibian's scope for activity by allowing activity only when it had rained. This ensured that highly xeric habitats, while potentially suitable in terms of temperature, are not counted.

My estimates of activity hours represent the maximum potential activity hours when an animal could be active, given its physiological constraints, and is therefore conservative with respect to changes in activity budgets in response to climatic changes (Gunderson and Leal, 2015). It does not consider behavioural thermal limits which may further reduce activity times, nor does it restrict access to shade or consider activity constrained within shaded (or sunny) environments. As such, I counted any hours during the day, night or dawn/dusk when conditions are suitable, regardless as to whether a particular species is considered diurnal, nocturnal or crepuscular. I did not define an activity hours threshold over which an organism can persist at a location as my

goal was not to delimit distributions, but rather measure the potential time - and thus the overall climatic favourability - for life at particular locations and times.

Thermal threats due to climate change are expected to vary across the globe, with tropical species more at risk (Deutsch et al., 2008; Huey et al., 2009; Sunday et al., 2014). Thus, in addition to our global analysis, I evaluated changes in activity hours within individual broad-scale climatic zones. I divided the world into equatorial, arid, warm temperate, snow and polar using the Köppen-Geiger climate classification system (Kottek et al., 2006).

Climate data

By default, *NicheMapR* uses mean monthly climate data provided by the Climate Research Unit CL v2.0 between the years 1961 and 1990 to downscale macroclimate to the microclimatic conditions experienced by an organism (Kearney and Porter, 2017; New et al., 2002). While this temporal resolution is suitable for present-day analyses, these data are insufficient for understanding species' responses to past climatic conditions. To resolve this, I created a custom climate database between the years 1661 and 2100 using ISIMIP2b climate simulations (Frieler et al., 2017) at decadal intervals for two different climate scenarios (GFDL-ESM2M and IPSL-CM5A-LR) and 5 different climate scenarios representing different greenhouse gas emissions levels (pre-industrial, historical, RCP2.6, RCP4.5 and RCP6.0). I chose to run the models across the two climate scenarios to capture the uncertainty associated with different climate change projections. Here, GFDL-ESM2M can be thought of as a simulation representing cooler and drier climatic conditions compared to IPSL-CM5A-LR whereas IPSL-CM5A-LR represents

hotter and wetter conditions compared to GFDL-ESM2M. Full details on how the custom climate databases were built can be found within the supplementary materials. Hereafter I abbreviate IPSL-CM5A-LR and GFDL-ESM2M to ‘IPSL’ and ‘GFDL’, respectively.

Time-Diversity Disharmony

To quantify disharmony—where predicted increases in activity hours are in locations with lower species richness (or vice versa)—I created global reptile and amphibian species richness maps with data from the Global Assessment of Reptile Distributions (GARD; Roll et al. 2017) for reptiles and IUCN version 6.1 for amphibians. I did not perform this analysis for insects as there are no global insect diversity maps at appropriate resolution of which I am are aware. For each cell across the globe I computed species richness and the percentage change in activity hours between three different timeframes under RCP 6.0. Timeframe 1 is the difference in activity hours between 1661 and 2100 and illustrates change between pre-industrial times and the worst future climate change scenario in the present study at the year 2100. Timeframe 2 is from 1861 and 2001 and demonstrates the change in activity hours from the approximate beginning of the industrial revolution to the start of the future RCP future climate change projections in 2001. Timeframe 3 is from 2001 to 2100 and presents the change in activity hours from the start of RCP 6.0 in 2001 to when it finishes in 2100.

3.3 Results

All Species

Across all taxa, prior to the start of the Industrial Revolution (*circa* 1860), activity budgets remained consistent through time globally and within individual climate regions, changing little relative to 1661 across this time period (Figure 3-1). Global activity budgets began to increase in approximately 1900 and are projected to continue increasing until at least 2100. However, there is considerable variability across the globe. Within equatorial (i.e. tropical) regions, activity budgets began declining sharply from 1900 until the present day with these declines predicted to continue to 2100. These declines are unprecedented compared to changes from 1661 to 1900. In all other regions, models predict an increase in activity budgets across taxa (Figure 3-1).

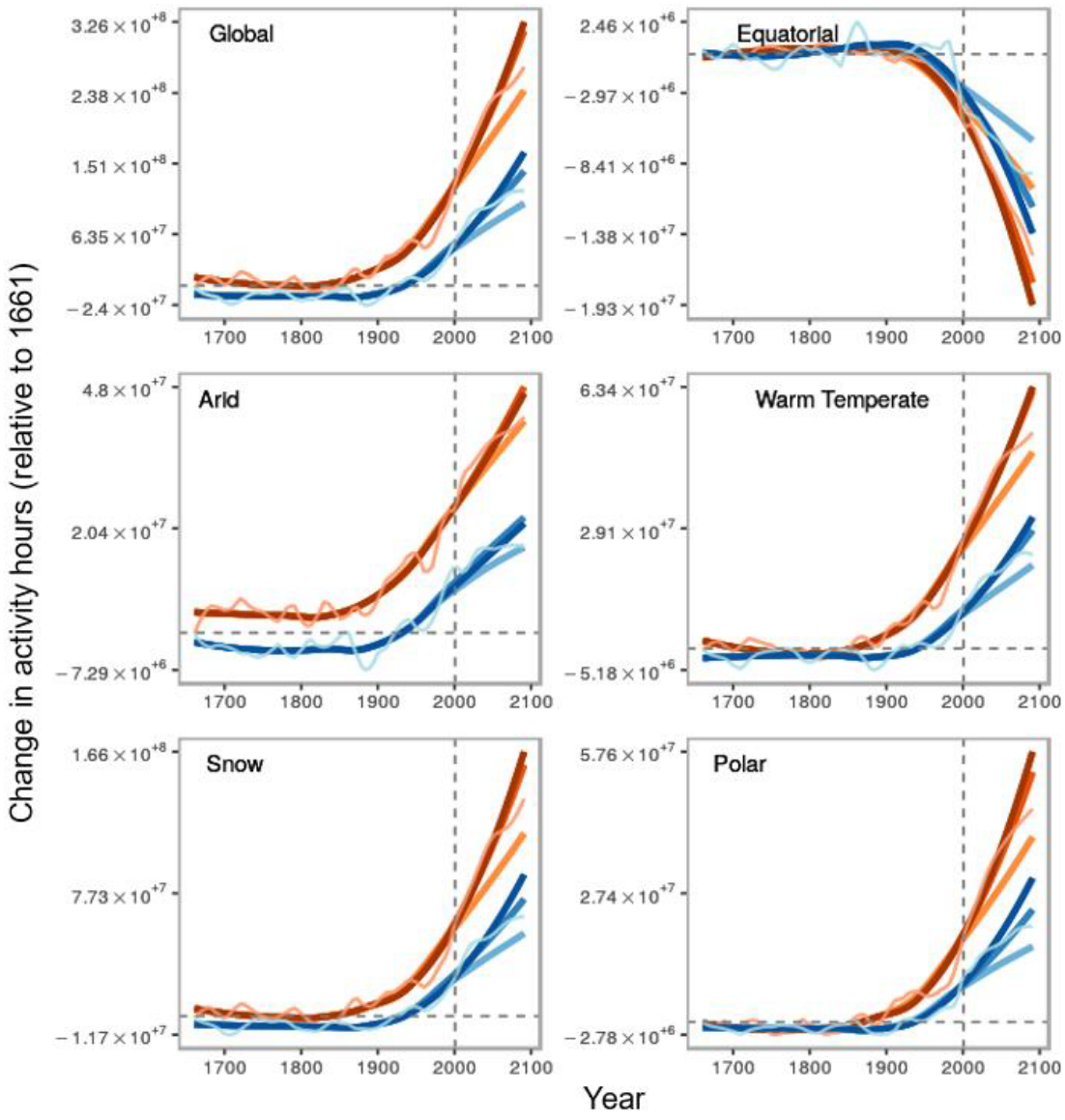


Figure 3-1 Change in activity hours (relative to 1661) across all taxa between 1661 and 2100. Orange lines are a warmer and wetter climate change scenario (IPSL), blue lines are a cooler and drier scenario (GFDL). Line shading from (lightest to darkest) represent different RCP scenarios (2.6, 4.5 and 6.0 respectively). Horizontal dashed line represents 0% change in activity hours relative to 1661. Vertical dashed line signifies where future RCP projections begin in 2001. All lines are loess smoothed for plot clarity. Thin coloured lines superimposed on the IPSL/GFDL predictions are relative change in activity hours but with less smoothing to show inter-decadal variability; mean change in activity hours calculated across RCP scenarios beyond the vertical dashed line.

Reptiles

Overall activity budget patterns for reptiles (Figure 3-2) are largely consistent with those observed for all species combined (Figure 3-1). Prior to the start of the 20th century, activity time remained highly consistent at a global scale and within all climate regions with little variability between decades (thin colour lines; Figure 3-2). Within equatorial regions, models predict a small increase in activity budgets between 1900 and ~1980 with a greater increase under a warmer and wetter climate change scenario (IPSL; orange lines Figure 3-2). However, after the start of the 21st century, predicted activity hours decline sharply towards 2100. These declines are particularly noticeable under RCP 6.0 which models the highest concentration of atmospheric CO_2 in the present study.

Qualitatively, the greatest decreases in activity budgets are in those regions of the globe which contain the highest levels of biodiversity (dark purple shading, Figure 3-3). Conversely, the biggest gains in activity budgets are in regions which currently harbour relatively low species diversity. There is therefore high discordance between species richness and activity hours observed here.

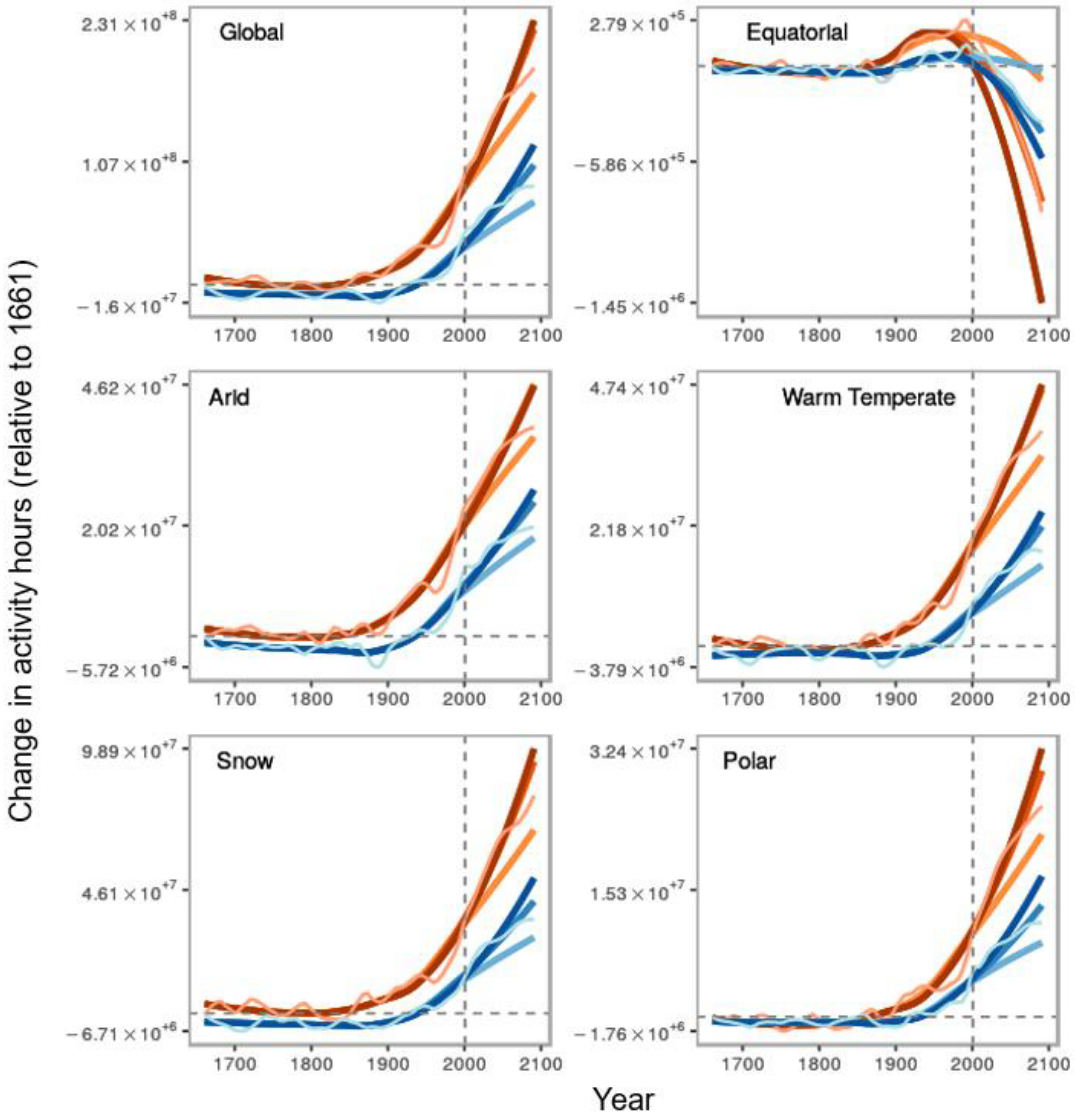


Figure 3-2 Change in activity hours (relative to 1661) for reptiles between 1661 and 2100. Orange lines are a warmer and wetter climate change scenario (IPSL), blue lines are a cooler and drier scenario (GFDL). Line shading from (lightest to darkest) represent different RCP scenarios (2.6, 4.5 and 6.0 respectively). Horizontal dashed line represents 0% change in activity hours relative to 1661. Vertical dashed line signifies where future RCP projections begin in 2001. All lines are loess smoothed for plot clarity. Thin coloured lines superimposed on the IPSL/GFDL predictions are relative change in activity hours but with less smoothing to show inter-decadal variability; mean change in activity hours calculated across RCP scenarios beyond the vertical dashed line.

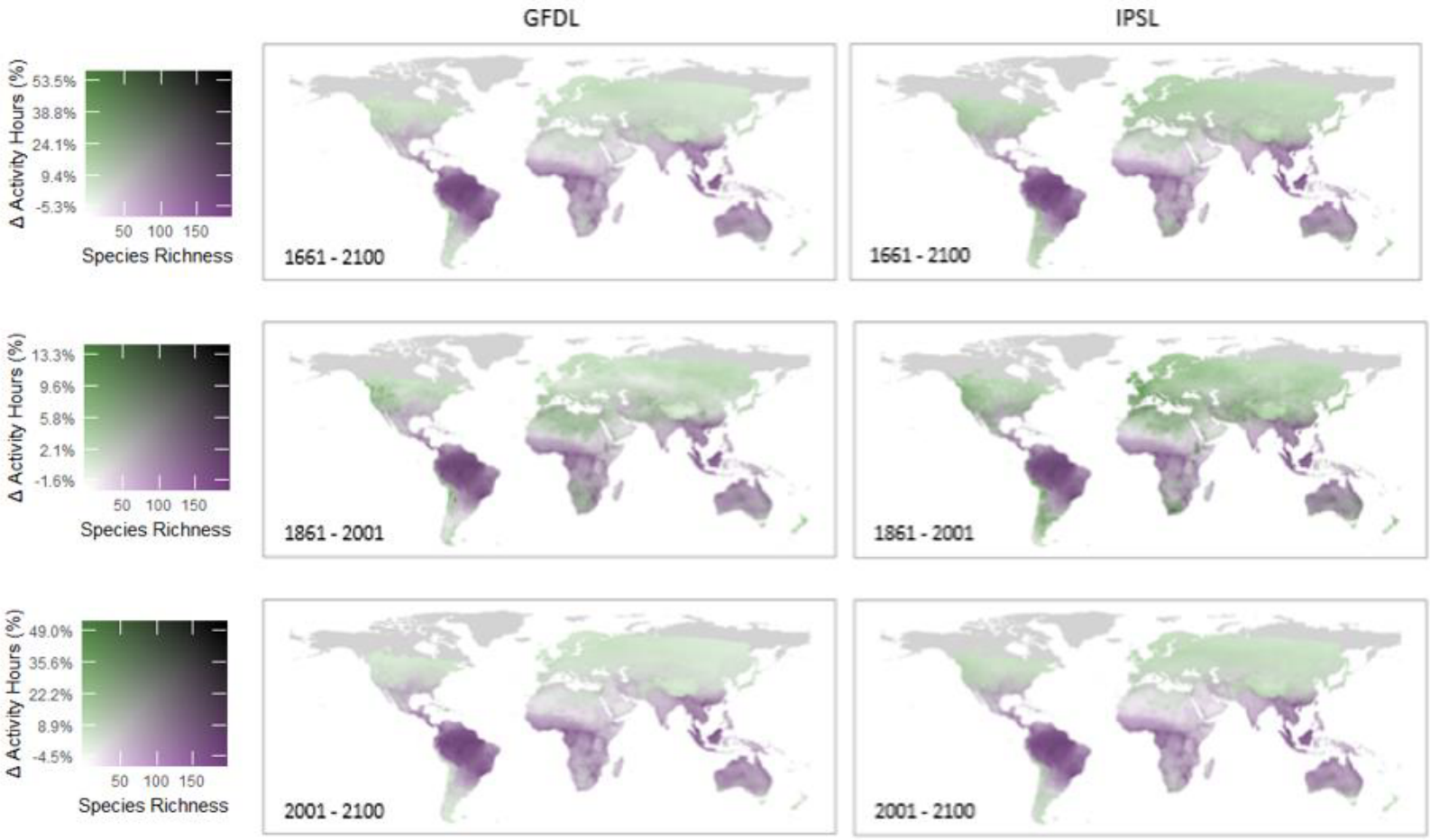


Figure 3-3 Reptile disharmony maps under RCP 6.0. Each map displays the percentage change in activity hours between different start and end decades. Row 1 (1661 – 2100) shows the difference between pre-industrial times (1661) and the worst future climate change scenario (RCP 6.0) in 2100. Row 2 (1861 – 2001) shows the difference between the start of the industrial revolution ~1860 and the start of the RCP projections in 2001. Row 3 (2001 – 2100) shows future climate change and the difference between 2001 and 2100 under RCP 6.0. The dark purple shades show that the greatest decrease in activity hours are in locations with the highest species richness. The green shades show where activity hours are predicted to increase in regions of the globe where species richness is lower. Note the different scaling (y-axis) for each row.

Amphibians

Activity budget relationships for amphibians (Figure 3-4) are more complex than those of reptiles (Figure 3-2) and insects (Figure 3-6) while also demonstrating greater inter-decadal variability in relative activity change, particularly within arid regions (thin colour lines; Figure 3-4). However, the general trend is of reasonably stable activity budgets during pre-industrial times (i.e. before 1860) within all climate regions. Overall declines in activity budgets are predicted for amphibians within equatorial regions but the decline starts sooner than for reptiles; between ~1880 (IPSL) and ~1950 (GFDL) depending on the climate scenario. While the decline in activity budgets is not as steep as that observed for reptiles (Figure 3-2) or insects (Figure 3-6), the overall trend mirrors that of the other taxa in this study with large losses in activity hours by the year 2100, particularly under high CO_2 concentration RCP scenarios (e.g. RCP 6.0).

Within arid regions, the warmer and wetter climate scenario (IPSL; orange lines Figure 3-4) predicts substantially higher activity hours than the cooler and drier scenario (GFDL; blue lines Figure 3-4). While both scenarios ultimately predict a decrease in activity budgets by the year 2100, this is expected much sooner for GFDL scenario (Figure 3-4). Warm temperate, snow and polar regions are all predicted to gain activity hours from the start of the industrial revolution onwards

Similar to reptiles, the greatest losses in activity hours are in those regions with the greatest amphibian biodiversity (i.e. the tropics) while the biggest gains are in those regions with relatively low amphibian richness (Figure 3-5). This suggests there is a similarly high level of time-life disharmony within the amphibian clade.

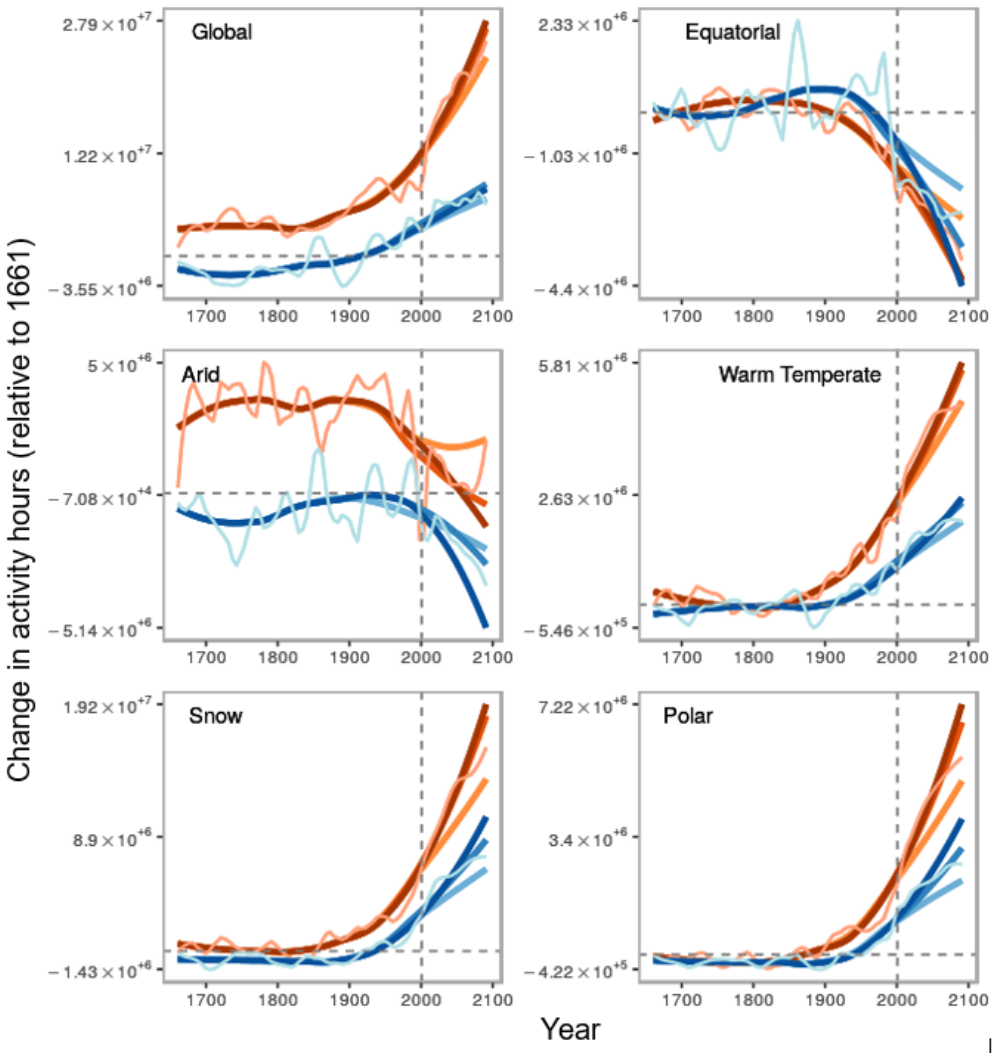


Figure 3-4 Change in activity hours (relative to 1661) for amphibians between 1661 and 2100. Orange lines are a warmer and wetter climate change scenario (IPSL), blue lines are a cooler and drier scenario (GFDL). Line shading from (lightest to darkest) represent different RCP scenarios (2.6, 4.5 and 6.0 respectively). Horizontal dashed line represents 0% change in activity hours relative to 1661. Vertical dashed line signifies where future RCP projections begin in 2001. All lines are loess smoothed for plot clarity. Thin coloured lines superimposed on the IPSL/GFDL predictions are relative change in activity hours but with less smoothing to show inter-decadal variability; mean change in activity hours calculated across RCP scenarios beyond the vertical dashed line.

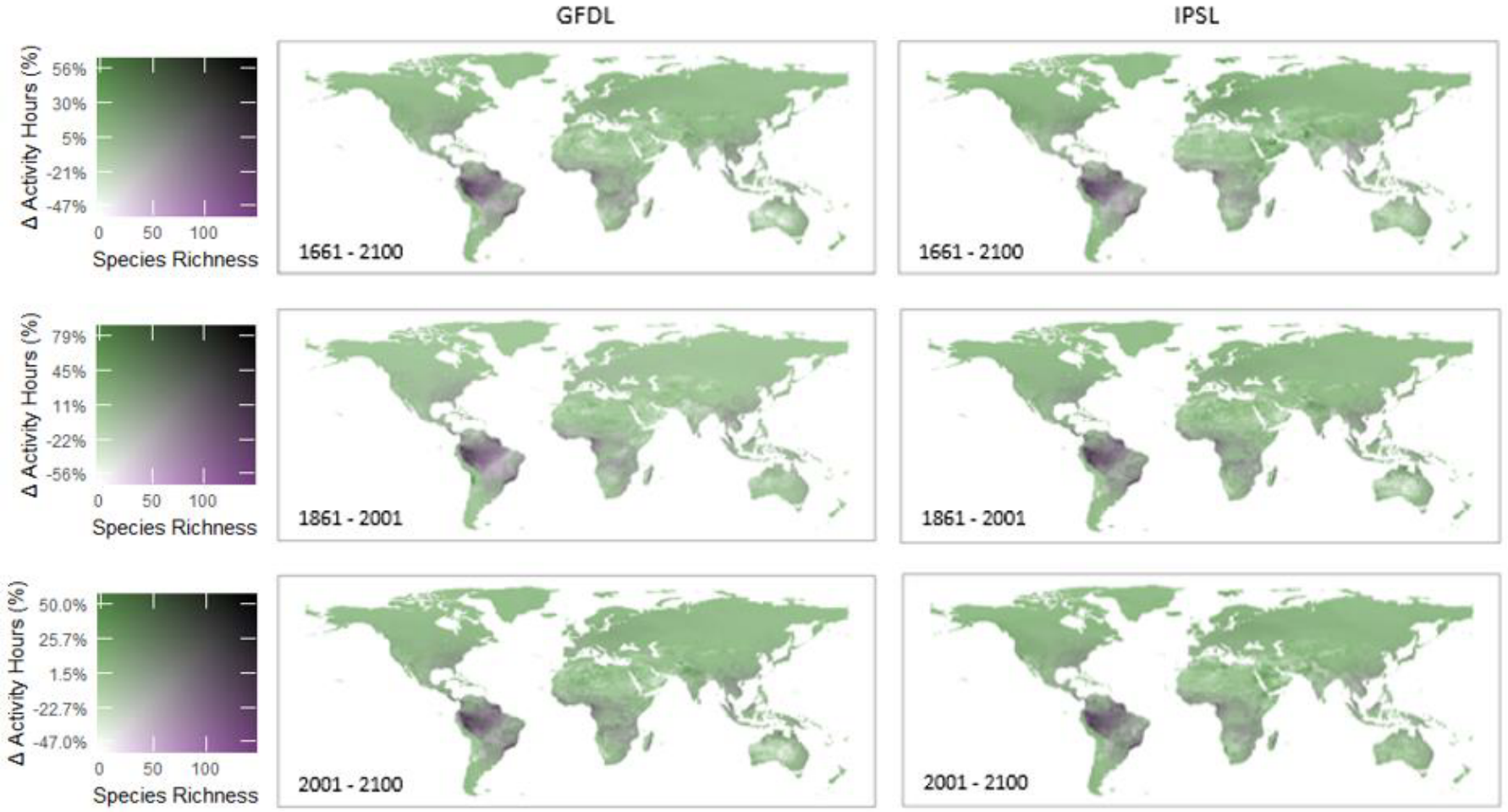


Figure 3-5 Amphibian disharmony maps under RCP 6.0. Each map displays the percentage change in activity hours between different start and end decades. Row 1 (1661 – 2100) shows the difference between pre-industrial times (1661) and the worst future climate change scenario (RCP60) in 2100. Row 2 (1861 – 2001) shows the difference between the start of the industrial revolution ~1860 and the start of the RCP projections in 2001. Row 3 (2001 – 2100) shows future climate change and the difference between 2001 and 2100 under RCP 6.0. The dark purple shades show that the greatest decrease in activity hours are in locations with the highest species richness. The green shades show where activity hours are predicted to increase in regions of the globe where species richness is lower. Substantial decreases in activity hours are predicted within tropical regions (purple) with modest (at best) gains apparent across much of the rest of the globe (greens). Note the different scaling (y-axis) for each row.

Insects

Insect activity budgets (Figure 3-6) within climate regions and through time are consistent with those observed for reptiles (Figure 3-2) and all taxa (Figure 3-1) with the exception of arid regions. While reptile activity budgets are predicted to increase within arid regions between the start of the industrial revolution and the year 2100, insect activity budgets are predicted to peak mid-21st century before declining by 2100 (Figure 3-6). However, with the exception of GFDL RCP 6.0 (dark blue line), activity budgets are not predicted to decline below levels seen in 1661.

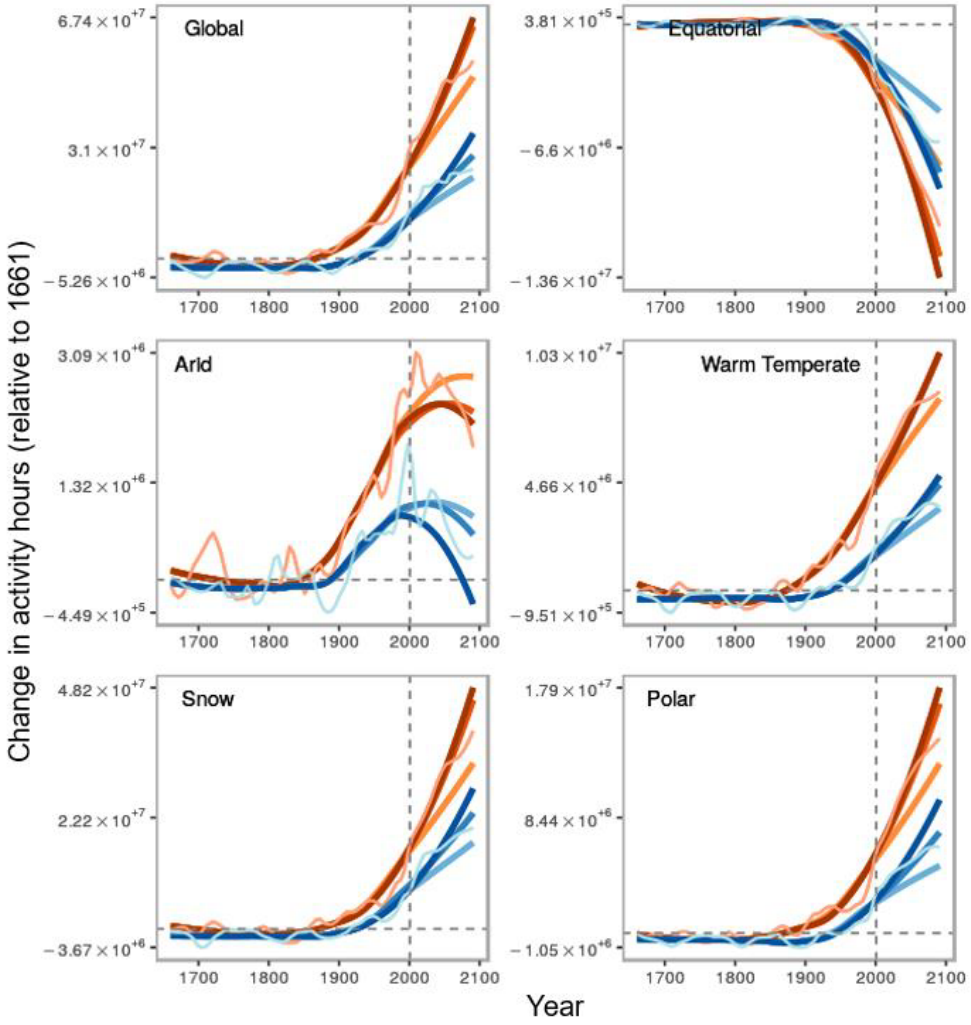


Figure 3-6 Change in activity hours (relative to 1661) for insects between 1661 and 2100. Orange lines are a warmer and wetter climate change scenario (IPSL), blue lines are a cooler and drier scenario (GFDL). Line shading from (lightest to darkest) represent different RCP scenarios (2.6, 4.5 and 6.0 respectively). Horizontal dashed line represents 0% change in activity hours relative to 1661. Vertical dashed line signifies where future RCP projections begin in 2001. All lines are loess smoothed for plot clarity. Thin coloured lines superimposed on the IPSL/GFDL predictions are relative change in activity hours but with less smoothing to show inter-decadal variability; mean change in activity hours calculated across RCP scenarios beyond the vertical dashed line.

3.4 Discussion

I found that from 1661 to the start of the industrial revolution (*circa* 1860), activity budgets remained remarkably consistent, with little variation across taxa, climate regions, or between climate scenarios (Figure 3-2, Figure 3-4 and Figure 3-6). In contrast, post-industrial variation in activity time far surpasses any that occurred in the preceding two hundred years, a result that is robust regardless of variation in climate reconstructions, and across taxa. Across much of the globe, climate warming has increased the duration of favourable conditions for life for most taxa, but future warming is predicted to degrade the time for life within tropical regions, regardless of taxa (see also Huey et al. 2009, Sinervo et al. 2010, Sunday et al. 2014; Figure 3-2, Figure 3-4 and Figure 3-6). Moreover, tropical amphibians and insects have already experienced substantial reductions in their pre-industrial activity budgets which are similar in magnitude to the projected future declines. Although, overall, available time is increasing at a global scale, it is increasing in areas that currently harbour few species, leading to high spatial discordance between where most biodiversity resides and where conditions for life are becoming increasingly favourable.

Previous forecasts of the impact of climate change on activity budgets have projected substantial decreases in activity times of tropical ectotherms (Sinervo et al., 2010; Sunday et al., 2014), due to the erosion of thermal safety limits (Deutsch et al., 2008; Huey et al., 2009) and/or species' exceeding their physiological thermal limits (Sunday et al., 2014). However, these forecasts use current climate conditions as a baseline and thus may over-estimate their

importance of activity time losses if, in fact, they represent a relaxation back to a ‘pre-industrial norm’; alternatively, they could underestimate the scale of impact if substantial amount of activity time has already been lost, i.e. shifting baseline syndrome (Soga and Gaston, 2018). My results suggest that both may be occurring. Activity time for amphibians and insects has been declining in tropical regions since the early 1900s and will be compounded by further losses. Alternatively, in arid regions, projected declines in insect activity budgets under future climate change scenarios will counteract the increases that have occurred since the industrial revolution for these taxa, returning their activity budgets to close to baseline (i.e. 1661) levels by 2100.

Tropical reptiles have experienced stable activity budgets for several hundred years (prior to the start of the industrial revolution) but they are predicted to decline under future climate change (Figure 3-2). The declines observed here are congruent with previous studies documenting a decrease in activity budgets within tropical regions (Sinervo et al., 2010; Sunday et al., 2014). It is thought that tropical ectotherms are more susceptible to warming than species at higher latitudes due to narrower thermal tolerance breadths (Deutsch et al., 2008; Sunday et al., 2014) thought to be driven by differential exposure to greater ranges (and extremes) in climate toward the poles. Similar declines in activity budgets are also predicted for amphibians (Figure 3-4) and insects (Figure 3-6). For amphibians, the decreases I observe here are possibly due to their strong physiological dependence on water – especially for reproduction (Feder and Burggren 1992) – and the parameterisation of my models. The climate data I used predicts decreases in precipitation between 1661 and 2100,

particularly within tropical regions (see Figure 3-7 in supporting information) which may explain the observed and projected declines in activity budgets observed here. Decreased water availability as a result of anthropogenic climate change is predicted to be highly detrimental to amphibian survival (Araújo et al., 2006; Buckley and Jetz, 2007); our results provide further support that this is likely to be the case. The observed declines for tropical insects are likely due to a combination of temperature and desiccation rate increases within this region. Previous work has highlighted tropical insect's sensitivity and vulnerability to small changes in temperature (Deutsch et al., 2008) and their lower desiccation tolerance—especially compared to their temperate relatives (Chown et al., 2011; Thorat and Nath, 2018)—may be highly detrimental to this taxon as temperatures continue to rise and water availability decreases (Breshears et al., 2005; Diffenbaugh and Field, 2013).

The predicted decreases in time for life within the tropics are highly conservative. Previous projections of the thermal ecological implications of global warming have shown that terrestrial ectotherms will need to thermoregulate more, by seeking shade, to avoid overheating (Kearney and Porter, 2009; Sunday et al., 2014). Our results show that even these behavioural adjustments will be insufficient to buffer the effects of warming tropical conditions. In my models, I allowed animals to burrow and climb (± 15 cm) or seek shade (to a maximum of 100%) to mitigate thermal stress, and still remain ecologically active. However, animal activity is unlikely to be 'all or nothing' and performance and activity can vary greatly within activity thresholds and may be limited by voluntary/behavioural thermal limits that are

narrower than physiological limits (Gunderson and Leal, 2015). Additionally, I counted all climatically suitable hours within a 24-hour period to measure activity time, regardless of whether a species was diurnal, nocturnal or crepuscular, i.e. animals could shift their daily activity times without constraint. Nascent research exploring the diel time axis as an ecological resource has indicated that, at least for diurnal mammals, shifting to nocturnality can mitigate the stresses of future summers (Levy et al., 2019), and given differences between day and night time temperatures and solar radiation inputs, should also allow ectotherms to extend activity hours. However, if such changes occur, it is not guaranteed that fitness will be maintained at levels prior to climate change. For example, a diurnal species may lack the anatomical adaptations to thrive in low-light conditions (e.g. low-light adapted retinas).

Despite allowing considerable behavioural freedom to mitigate thermal stress, the results here suggest that behavioural changes alone will be unable to counteract the negative effects of future warming on activity budgets in the tropics. The same behavioural freedoms could also mean that the predicted gains in activity time outside tropical regions may be over-estimated, resulting in smaller gains in activity time than predicted here. In contrast, acclimation of animals' physiological limits could, at least partially, restore activity budgets under future climate warming. Evidence suggests that the adaptive evolution of critical thermal limits is constrained, at least over longer time scales (Araújo et al., 2013; Muñoz et al., 2014). In the short term, however, acclimation could allow for increases in CT_{max} that permit additional activity time (Morley et al. In Press) though the potential for acclimation-rescue is

limited, especially in the tropics (Gunderson and Stillman, 2015; Rohr et al., 2018). Future work should look to investigate the complex interactions between behavioural thermal regulation and acclimation as a buffer to anthropogenic climate change.

Land use change and degradation will likely compound the physiological responses to climate demonstrated here, further reducing available time for life in tropical and arid regions, but possibly enhancing it in colder areas. Canopy shade generates cooler microclimates within forests, providing species with refuges from overheating (Algar et al., 2018; Scheffers et al., 2014), while partial shade in more open areas allows for efficient thermoregulation (Sears et al., 2016). Even in the absence of wholesale deforestation, fragmentation of habitat increases temperatures at patch edges (Tuff et al., 2016), and canopy thinning can also raise body temperatures via increased radiation (Algar et al., 2018). Shade availability also plays an important role in reducing water loss (Kearney and Porter, 2009; Levy et al., 2019) and continued changes to forest habitat could make shade an ever-limited and contested resource for animals to exploit, particularly for strongly water-dependent taxa like amphibians.

Recent warming has stimulated a global redistribution in time for life, with losses in tropical areas counteracted by increases in cooler, high latitude regions. These shifts have produced a growing spatial disharmony between the thermal conditions favourable for life and high biodiversity. As climate change continues, this disharmony is predicted to increase, shifting the areas thermally favourable for life further from where most species occur. Currently,

terrestrial species – including plants, mammals, birds and invertebrates - are moving poleward at a rate of about 17km per decade in response to climate change (Chen et al., 2011), demonstrating at least some capacity for species to track climate change and potentially exploit an increase in favourable climatic conditions at higher latitudes (Chen et al., 2011; Poloczanska et al., 2013). However, the rate of climate change is rapid and many species are failing to move fast enough, resulting in observable lags between distributions and climate change (Lenoir and Svenning, 2015). The causes of these lags are complex and multi-faceted but include physiological, behavioural and evolutionary responses (Williams et al., 2008) as well as connectivity issues resulting in a matrix of unfavourable microhabitat and microclimatic conditions (Pecl et al., 2017; Scheffers et al., 2014). Taken together, it seems doubtful that climate tracking will fully mitigate the decreases in time for life compared to present-day 'native' ranges.

The majority of previous research investigating the role of anthropogenic climate change on organisms compares current conditions to future ones (Urban, 2015). However, rapid climate change has been happening for at least 50 years (Diffenbaugh and Field, 2013), meaning that animal activity budgets and distributions could have already changed substantially compared to the present day. I found that, since the start of the Industrial Revolution, variation in activity time far surpassed any that occurred in the two hundred years prior. In the tropics—which harbour much of the world's biodiversity—activity budgets are predicted to decline markedly, with amphibians and insects having already experienced substantial reductions in their pre-industrial activity budgets. Behavioural thermoregulation is unlikely to buffer species from the

magnitude of future warming. While climate warming has increased available activity times globally, the gains are in areas which currently support few species, further limiting life's capacity to respond to rapid climate change. Without substantial mitigation—whether through acclimation or adaptation—or by exceptional dispersal ability, fitness is likely to decline into the future in highly diverse areas, ultimately resulting in range contractions and possible extinctions.

3.5 Supporting Information

Body mass data

Amphibians

Empirical body mass data at the species level were available for 9 of the 33 amphibian species in this study. For the remaining species I estimated mass using allometric equations and snout-vent length measurements from various sources. Please refer to the supplied CSV files for all data, equations and references.

Insects

Body mass data for insects at the species level is rarely available. I therefore calculated mean body mass at the family level for 69 species and at order level for 3 species. With the exception of Psocoptera, all family/order body mass data are from Chown et al. (2007) 10.1111/j.1365-2435.2007.01245.x. Psocoptera body mass was estimated from Table 3 in 10.2307/3543566.

Reptiles

As a very well-studied taxonomic group, species-level mass data were available for all 159 species of reptile in our study. All mass data used were obtained from Feldman et al. (2016) 10.1111/geb.12398

Sensitivity analyses

Insect body mass sensitivity analysis

Obtaining species-level data on insect body mass was not possible for species in this analysis. However, I was able to obtain family-level mass data from Chown et al. (2007). Given that body mass can differ substantially between species within the same fazmily, I ran a sensitivity analysis to determine

whether large changes in body mass made an appreciable difference to the number of predicted activity hours across the globe. I randomly sampled 1000 points across the globe and ran *NicheMapR* at these locations. I kept all parameters constant except body mass which I varied. I ran the model across three orders of magnitude in body mass: 0.5g, 0.05g and 0.0005g. Predicted activity hours across these 1000 points were: 149,791 (0.5g), 149,036 (0.05g) and 147,727 (0.005g). This represents a change in activity hours of 1.4% between the greatest and smallest mass.

T_{Pref} sensitivity analysis

Data on species' preferred body temperatures are rarely empirically derived, for example with controlled thermal gradient experiments. Often, the mean field body temperature (T_b) of a species is used to infer preferred temperature which may or may not represent a species' true preferred temperature, particularly if sample sizes are low or if a species thermoconforms. Given the large number of species in this analysis, I performed a sensitivity analysis to determine how altering T_{pref} affects predictions of activity hours across the globe. If I observed large differences in predicted activity hours with minor changes to Tpref then I would have been required to limit our study to just those species where empirical/mean field T_b data were available in the literature.

I randomly sampled 5000 locations across our study area. I then modelled a small lizard-shaped organism with a CT_{Max} of 40°C and a CT_{Min} of 10°C at these locations. I allowed the organism to be active during the day, night and dawn/dusk, as well as permitting climbing and/or burrowing to mitigate thermal stress. The animal was also permitted to move between 0 and 100%

shade cover, as required. All other settings within the ectotherm sub-model remained at default.

I ran three different T_{pref} scenarios:

(1) $T_{pref} = CT_{Max}$ i.e. $T_{pref} = 40℃$

(2) $T_{pref} = 0.75 * CT_{Max}$ i.e. $T_{pref} = 30℃$

(3) $T_{pref} = 0.50 * CT_{Max}$ i.e. $T_{pref} = 20℃$

I found that there was no difference in predicted activity hours. Given this, I arbitrarily set T_{pref} to $0.75 * CT_{Max}$ for all species analysed.

Custom climate database

Construction of custom *NicheMapR* climate database

By default, the *NicheMapR* package (Kearney and Porter, 2017) uses climate data from the Climate Research Unit (CRU CL v2; New et al. 2002) which comprises of monthly climate averages between the years 1961- 1990 at a 10-minute spatial resolution. To estimate available time for life prior to anthropogenic climate change, it was necessary to construct a custom climate database prior to the start of the industrial revolution. To do this I constructed my own climate database from the ISIMIP2b simulation round (Frieler et al., 2017). ISIMIP2b provides daily climate surfaces from 1st January 1661 to 31st December 2100 for a range of different climate forcings and scenarios. I created climate databases for both IPSL-CM5A-LR and GFDL-ESM2M for the following climate scenarios: pre-industrial control, historical, RCP2.6, RCP4.5 and RCP6.0.

I downloaded near-surface, bias-corrected, daily climate data from 01/01/1661 to 31/12/2100 for the following variables: maximum air temperature, minimum air temperature, mean air temperature, relative humidity, wind speed and precipitation. From these daily estimates I computed the mean monthly estimates by decade (e.g. 01-JAN-1661 to 31-DEC-1670, 01-JAN-1671 to 31-DEC-1680 and so on). To ensure consistency with *NicheMapR* so that the functions micro_global() and ectotherm() receive the correct climate data as input, I adjusted relative humidity to the minimum and maximum air temperatures to generate minimum and maximum relative humidity estimates, respectively, following Kearney and Porter (2017). I calculated the number of wet days per month by summing the number of days per month where rainfall exceeds 0.1mm. I took elevational data from the original *NicheMapR* database but aggregated this to 0.5 degrees while taking the mean. Percentage cloud cover was not available from the ISIMIP2b simulations so I therefore assumed that cloud cover has remained constant over this study's time period and used cloud cover provided in the original *NicheMapR* climate database, again aggregated to 0.5 degrees resolution. This resulted in the following climate layers, in line with the default *NicheMapR* climate database: elevation, precipitation, wet days, wind speed, minimum temperature, maximum temperature, minimum relative humidity, maximum relative humidity and percentage cloud cover.

Koppen-Geiger climate classification

Climate classification

To test whether time for life differs between different climate zones, I simplified the Koppen-Geiger climate system, taking the top-level climate types from the updated classification of Peel et al. (2007). This resulted in 5 main climate types: tropical, arid, temperate, cold and polar. The broad-level climate types used here have been shown to be relatively insensitive to temperature trends (Peel et al., 2007; Triantafyllou and Tsonis, 1994), making it useful for the present analysis across a substantial period of time.

ISIMIP2b rainfall differences

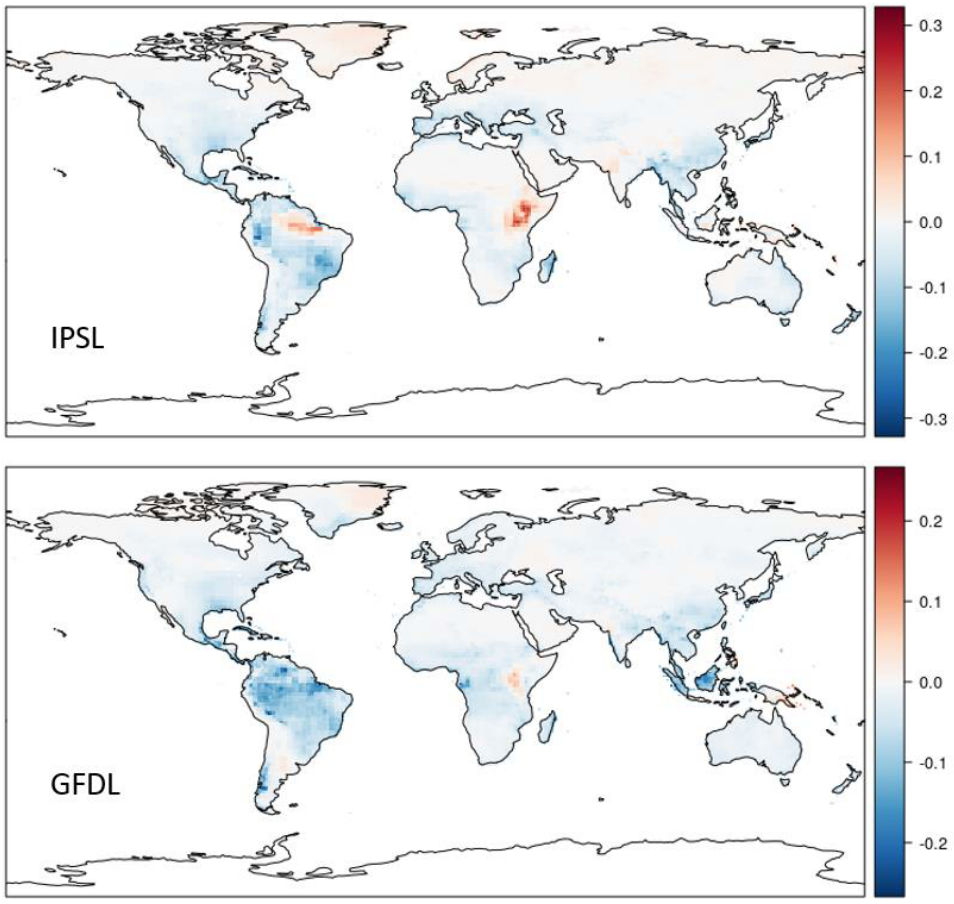


Figure 3-7 ISIMIP2b percentage change in rainfall between 1661 (pre-industrial baseline) and 2100 under RCP 6.0 for both IPSL and GFDL climate scenarios.

Chapter 4: Revealing effects of biotic interactions on species' ranges using ecological traits and mechanistic niche modelling

4.1 Introduction

Since the time of Alfred Russell Wallace, understanding the factors and processes limiting species' distributions has been a fundamental goal in biogeography and ecology. More recently, climate change-related shifts in species' ranges (Lenoir and Svenning, 2015; Parmesan and Yohe, 2003) and the need to predict the spread of invasive species have given this topic considerable conservation and management importance (Pacifici et al., 2015). Central to our current understanding of range limits is the Hutchinsonian niche concept (Hutchinson, 1957). It proposes a fundamental niche within which a species can persist in the absence of biotic interactions, and a realized niche that either excludes portions of the fundamental niche due to negative biotic interactions (Bruno et al., 2003; Bulleri et al., 2016; Hutchinson, 1957; Pulliam, 2000) or extends beyond the fundamental niche via positive interactions such as facilitation (Pulliam, 2000). A third component—dispersal limitation—further restricts where a species can exist in geographic space (Algar et al., 2013; Glor and Warren, 2011; Pulliam, 2000; Soberón and Nakamura, 2009). Although Hutchinson's theory explicitly recognizes a role for abiotic factors and biotic interactions in determining niche—and thus distribution—limits, we still have limited understanding of how all these processes occur together across large spatial extents to generate observed species' ranges.

Although biotic interactions are central to Hutchinsonian niche theory, debate continues regarding their importance in limiting species ranges at macroecological scales (Pearson and Dawson, 2003; Wiens, 2011) and methods to quantify and understand these interactions remain underdeveloped (Anderson, 2017; Kissling et al., 2012). This is due in part to a long history of research which emphasizes climate as the primary explanation for species' range limits (Pearson and Dawson, 2003; Sexton et al., 2009; Soberón, 2007), but also uncertainty in how to appropriately model biotic interactions across landscapes (Algar et al., 2013; Anderson, 2017). Nonetheless, recent empirical evidence suggests that biotic interactions can have detectable effects on species distributions at large spatial extents (Algar et al., 2013; Araújo et al., 2014; Blois et al., 2013; Gilman et al., 2010; Gutiérrez et al., 2014; Wisz et al., 2013).

One way to evaluate the effects of biotic interactions on species' distributions has been to extend correlative species distribution models by including predictors that represent the constraining effects of biotic interactions (Algar et al., 2013; Anderson, 2017; Wisz et al., 2013). However, correlative niche models, which take known species occurrences and correlate them with environmental conditions to predict relative suitability across a landscape (Elith and Leathwick, 2009), may underestimate the impact of biotic interactions on range limits. In the absence of frequent dispersal into sink habitats (see Pulliam 2000), the presence of a species at a location means it is able to persist given the abiotic environmental conditions plus any negative (or positive) biotic interactions at that location. Correlative niche models, therefore, draw on data from a species' realized niche (Anderson, 2017;

Kearney and Porter, 2009) and thus may fail to account for effects of biotic interactions that prevent it from filling its potential range in the absence of biotic interactions (Algar et al., 2013).

Resolving the problem outlined above requires information on where a species could survive in the absence of biotic interactions (i.e. its fundamental niche). Estimating and mapping the fundamental niche is non-trivial, but recent developments in mechanistic niche models have made it feasible (Kearney and Porter, 2009, 2020, 2017). While the term 'mechanistic model' has been applied to a range of modelling approaches within the ecological literature (Bugmann, 2001; Friend et al., 1997; Haxeltine and Prentice, 1996; Neilson, 1995; Scheller et al., 2007), here I focus on those based on coupled energy and mass balance transfer equations, which can estimate body temperature and water balance for an organism and therefore provide a mechanistic link between an organism's physiology and the surrounding environment (Kearney and Porter, 2009; Kearney et al., 2013). Locations that permit positive energy and water balances will enable survival and reproduction and are considered to be within the organism's fundamental niche (Kearney and Porter, 2009). Such models can infer a species' potential distribution across a landscape from first principles and do not require observation records to parameterise a model. Consequently, they are free from many of the issues associated with correlative models in that predicted distributions are in response to abiotic factors only and thus contain no confounding effects of biotic interactions (Kearney and Porter, 2009).

Here, I introduce a framework to map a species' fundamental niche boundary (i.e. where the distribution is limited by the fundamental niche) and identify

areas of ‘distributional debt’, defined here as areas where a species fails to fill its fundamental niche. I explore whether species can fill the entirety of their fundamental niche or rather inhabit a subset of potentially available niche space. In areas where a species’ distribution is limited by the fundamental niche, a species’ probability of presence—as derived from a correlative niche model—should be tightly correlated with its fundamental niche suitability, with higher probability of presence in fundamentally more suitable areas and lower probability of presence in marginal areas. However, based on Hutchinsonian niche theory (Hutchinson, 1957), this correlation will degrade if other processes prevent a species from entirely filling its fundamental niche. For example, the presence of competitor species, dispersal limitations imposed by the landscape (e.g. a mountain range) or intrinsic to a species (e.g. an inability to travel far) or the availability of suitable habitat, could all prevent a species from inhabiting areas which are otherwise physiologically suitable (Algar et al., 2013; Allouche et al., 2008; Soberón and Nakamura, 2009). The fundamental niche, therefore, imposes a constraining upper bound on species’ probability of presence, with biotic interactions, dispersal limitations or availability of suitable habitat causing probability of presence to fall below this boundary. The bounded nature of this relationship makes a series of predictions that can be detected using quantile regression. If a species’ distribution is entirely limited by the fundamental niche, then fundamental niche suitability and probability of presence will be highly correlated (Figure 4-1a), and upper and lower quantile regression will have similar slopes. However, if species are limited in some areas by factors other than their fundamental niche limits (e.g. biotic interactions or dispersal limitation), then

probability of presence will be lower than expected based on the fundamental niche boundary (Figure 4-1b and c), leading to a triangular, bounded relationship between fundamental niche suitability and probability of presence. How these factors prevent species from reaching their fundamental niche boundary will influence the shape of this triangular relationship. Specifically, if a species' distribution is determined by fundamental niche limits in marginal conditions, but other factors—like competition, dispersal or available habitat—set distributional limits when conditions are more favourable, then I predict a triangular relationship between fundamental niche suitability and probability of presence, with a widening of the triangle in more climatically suitable regions and a shallow lower-quantile slope (Figure 4-1b). Alternatively, the opposite relationship could occur, with a widening of the triangle in fundamentally marginal areas if species in these areas are on tight energy budgets and are thus more easily excluded by these same potentially limiting factors than in more fundamentally suitable areas, leading to a steeper lower-quantile slope (Figure 4-1c).

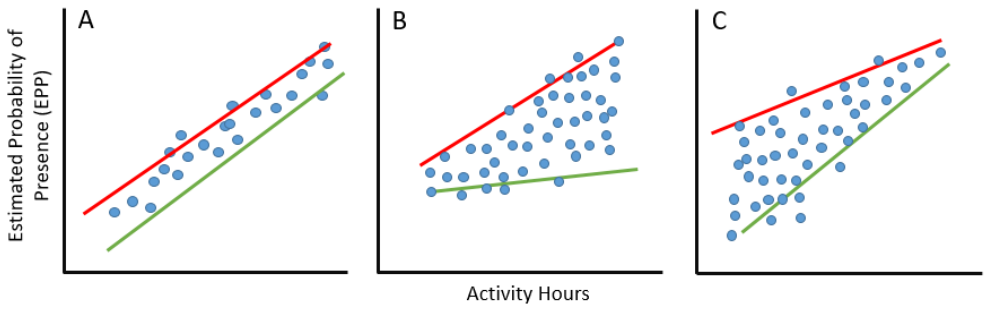


Figure 4-1 Predicted relationships depicting a fundamental niche boundary and the detection of distributional debt from biotic interactions. Red lines depict the constraining effect of the fundamental niche on probability of presence, detected

using quantile regression on the 90th percentile. The green line is the quantile regression on the 10th percentile. **(A)** If a species' distribution is limited by its fundamental niche throughout its range, probability of presence will be highly correlated with fundamental niche suitability. **(B)** If a species' distribution is determined by fundamental niche limits in fundamentally marginal areas (i.e. low values on the x-axis and areas potentially outside a species' fundamental niche), but other processes such as biotic interactions, dispersal limitation or the availability of preferred habitat set distributional limits in fundamentally favourable areas, I predict a widening of the triangle as fundamental suitability increases, as species are excluded from otherwise favourable areas. **(C)** If species are more easily excluded from fundamentally marginal areas where they exist on tight energy budgets, then biotic interactions, dispersal limitation or habitat availability may produce a widening of the triangle in fundamentally marginal areas (low values on the x-axis).

To test whether the triangular relationships hypothesised above are the result of biotic interactions or another process not accounted for in climate-based niche models—for example, access to preferred land cover or dispersal limitation—I make additional predictions based on the magnitude of the residuals from the fundamental niche boundary (upper quantile regression line); the magnitude of these negative residuals indicates the degree of distributional debt. First, species may be excluded from otherwise suitable geographical areas by competition from ecologically and morphologically similar species (Algar et al., 2013; MacArthur, 1972; Williams, 1965). If this is the case, I predict that, for a focal species, the magnitude of distributional debt should be greatest in areas where an ecologically and morphologically similar species occurs. Second, additional habitat conditions not included in the niche models (e.g. habitat structure or type), may also prevent species from

filling their fundamental niches. In this scenario I predict that distributional debt is greatest in areas where preferred habitats (e.g. closed versus open) are lacking. If dispersal limitation prevents species from filling their fundamental niche, then distributional debt should be greatest in areas that are isolated, either by distance or barriers, from other fundamentally suitable areas (Algar et al. 2013; see Glor and Warren 2011 for a similar argument).

I apply this framework to the *Anolis* lizard fauna of Puerto Rico to identify areas of distributional debt, and test whether they arise from biotic interactions, dispersal limitation, or unmeasured habitat variables. The ten Puerto Rican species of these small, mostly arboreal, lizards are a useful system for testing these ideas for multiple reasons. They include widespread and range-restricted species, including lowland and highland specialists (Schwartz and Henderson, 1991). They are found across xeric/open and mesic/closed habitats (Gunderson and Leal, 2012) and have diverged in physiological thermal tolerance traits (Gunderson et al., 2018) linked to the fundamental niche. Despite this divergence, species still overlap in geographical space (Schwartz and Henderson, 1991), and in their thermal tolerance breadths (Gunderson et al., 2018). Puerto Rican (and other Greater Antillean) anoles have adaptively radiated into distinct ecomorphs with morphology adapted to specific microhabitats with body size differences within ecomorphs linked to prey size (reviewed in Losos 2009). This tight link between anole morphology, microhabitat use and prey size influences the strength of competition amongst anole species (Pacala and Roughgarden, 1985), and means that morphological similarity can be used as a proxy for

ecological similarity, allowing for the strength of biotic interactions among anole species to be quantified through space (Algar et al., 2013).

To estimate fundamental niche suitability for anoles, I use a behavioural and physiological mechanistic niche model to estimate potential activity time for each species (Kearney and Porter, 2009, 2017; Porter and Mitchell, 2006). Activity time in lizards has been linked to population persistence and extinction (Sinervo et al., 2010; Sunday et al., 2014), suggesting that it is tightly linked to the fundamental niche. The advantage of the quantile-regression based framework identified above is that it does not require identifying a specific threshold (fundamental niche limit) where number of activity hours translates to non-negative population growth rates. Identifying such a threshold would require additional detailed information on resource availability, and reproductive rates not available for most species at broad scales. As probability of presence is problematic to determine using presence only data on species' localities (Phillips and Elith, 2013), I calculate a proxy by fitting a correlative niche model that includes climate and distance constraints (Algar et al., 2013; Allouche et al., 2008; Glor and Warren, 2011). This approach estimates the distribution as the geographically accessible realized niche (GARN), i.e. it estimates the realized niche and eliminates those areas where dispersal limitation may prevent a species from occurring (Algar et al., 2013; Allouche et al., 2008).

I test the above hypotheses for eight species of *Anolis* lizard on Puerto Rico (two species, *A. cuvieri* and *A. occultus,* had insufficient data). For each species, I identify and map fundamental niche boundaries and areas of distributional debt using mechanistic and correlative models and test for

triangular relationships consistent with a lack of fundamental niche filling. I then test hypotheses based on negative biotic interactions (i.e. competition), canopy cover (i.e. habitat availability) and dispersal limitation to explain areas of distributional debt.

4.2 Methods

Study System

I test hypotheses for eight of the ten species of *Anolis* lizards on the island of Puerto Rico. There were insufficient thermal data to parameterise fundamental niche models for *A. cuvieri* and *A. occultus*. Puerto Rico is the most easterly of the four main islands of the Greater Antilles and the smallest by area, covering approximately 9,100 km^2. High elevation areas (>1,000 m.a.s.l.) form much of the island's centre. This system has several advantages in that it has clearly defined geographical boundaries, is composed of an ecologically diverse lizard assemblage, and is well studied in terms of its anole thermal ecology which is necessary to parameterise mechanistic niche models.

Quantifying the fundamental niche

I used the biophysical mechanistic model *NicheMapR* version 1.1.4 (Kearney and Porter, 2017; Porter and Mitchell, 2006) to estimate the fundamental niche for eight *Anolis* species; *A. cooki, A. cristatellus, A. evermanni, A. gundlachi, A. krugi, A. poncensis, A. pulchellus* and *A. stratulus*. *NicheMapR's* default macroclimatic data are from the Climate Research Unit (CRU) version 1.0 and 2.0 datasets at ~17 x 17 km resolution. While this spatial resolution is suitable for analyses at broad-scales (e.g. continents), it is insufficient when applied to an island the size of Puerto Rico. To resolve this, I created a custom climate dataset at ~1 x 1km resolution using climate surfaces from various sources (see Table 4-1 in supporting information). It was not possible to find alternative relative humidity estimates at 1 x 1 km resolution. Therefore, to downscale relative humidity from 17 x 17 km to 1 x 1 km, I took the original

CRU mean relative humidity data and recomputed minimum and maximum values using *NicheMapR's* built-in 'Wetair' and 'VAPRRS' functions. These functions require as input mean relative humidity (from CRU), minimum and maximum temperature (from Worldclim v2 Fick and Hijmans 2017) and output minimum and maximum relative humidity respectively

A range of behavioural and physiological data for each species are required to accurately parameterise the *NicheMapR's* ectotherm sub-model (Table 4-2 in supporting information). All data were obtained by searching the literature or by deriving estimates based on empirical data from the literature (Table 4-2 in supporting information). I enabled diurnal activity, shade seeking and climbing but prevented burrowing, crepuscular and nocturnal activity. I allowed the model to provide shade between 0 - 100% for all species, enabling the organism to always locate a level of shade necessary to maintain preferred body temperatures (unless external temperatures are so high that shade is unable to buffer the organism from overheating). All other model parameters were left at default (see Table 4-3 in supporting information for a list of the remaining default parameters).

Using the ectotherm sub-model output table environ, I calculated total activity hours for the middle day of each month for 1 year, i.e. the sum for 12 days. A lizard is considered 'active' within a given hour if the model determines the organism is either basking (ACT=1 in *NicheMapR*) or foraging (ACT=2). In essence, if the environmental conditions are suitable and the modelled organism is within its physiological tolerances, the animal is considered active and "foraging". Included within this definition of activity is when an animal is utilising shade or climbing to mitigate thermal stress. I use activity hours as a

proxy for fundamental niche suitability, where longer activity time is inferred to be more suitable.

Quantifying the Geographically Accessible Realized Niche (GARN)

I used climate predictors and dispersal-cost surfaces to estimate the GARN. Occurrence data were available for all 10 species of anole so I estimated the GARN of all species using Maxent version 3.4.1 (Phillips et al., 2017, 2006) and the R package '*dismo*' (Hijmans et al., 2016). Estimating the GARN for all species enabled a more accurate quantification of morphological similarity across the island (see 'Morphological similarity' below). Occurrence records for each species were obtained from a database of previously published observations (Algar et al., 2013) and thinned to 3 km to reduce the effects of spatial sampling bias using the R package '*spThin*' (Aiello-Lammens et al., 2015). Sample sizes for each Maxent model can be found in Supporting Information Table 4-4. I chose five bioclimatic variables from the Worldclim version 2 database (Fick and Hijmans, 2017) which are expected to affect ectotherm physiology; mean diurnal temperature range (BIO2), maximum temperature of the warmest month (BIO5), minimum temperature of the coldest month (BIO6), precipitation of the wettest month (BIO13) and precipitation of the driest month (BIO14).

Dispersal limitation is documented for *Anolis* lizards on Hispaniola (Algar et al., 2013; Wang et al., 2013) and thus could also prevent individuals from accessing all climatically suitable areas across Puerto Rico. To account for this, I generated dispersal-cost surfaces for each species (Algar et al., 2013; Glor and Warren, 2011) to use as additional predictors in my distribution models. I did this by summing overland distances for each observation record

to all other points across the landscape using the R package gDistance (van Etten, 2015) and including this surface as a predictor in each Maxent model. My models can therefore constrain a species' predicted distribution to those areas which are inferred to be both climatically suitable and accessible. Background locations for each species' model were selected at random across the island (n = 10,000).

I used *ENMeval* v0.3.0 (Muscarella et al., 2014) to tune Maxent's regularisation multiplier and feature classes to balance distribution model complexity and goodness of fit. For species with fewer than 25 observation records I used k-1 ('jackknife') to partition training and test data and for all other species I used random k-fold partitioning (k=10;Table 4-4 in supporting information). After spatial thinning, *A. cooki* and *A. poncensis* were represented by fewer than 10 observation records. Despite these low sample sizes, it is possible to construct meaningful distribution models with careful consideration of model tuning and selection procedures (Galante et al., 2018; Morales et al., 2017). I selected the 'best' model for each species by sorting on lowest omission rate and then selecting the model with the highest AUC, as per recommendations by Galante et al. (2017). Estimating probability of presence from Maxent requires estimates of prevalence (Elith et al., 2011). I estimated prevalence for each species by dividing the number of unique cells each species occurred in by the total number of unique cells occupied by any species. This method assumes that species with a low number of observation records are geographically rarer than those with a greater number of observations, which is reasonable given the extensive sampling of *Anolis* over

the preceding decades. I use the clog-log output from Maxent as this is more appropriate when estimating probability of presence (Phillips et al., 2017).

Distributional Debt

I mapped distributional debt across the island for each of the eight focal species. I define debt as areas where a species does not occur despite high predicted fundamental niche suitability. Because distributions and fundamental niches are in different units (estimated presence probabilities and activity hours, respectively), I first converted each species' activity hours and estimated probability of presence (EPP) into a proportion of maximum by dividing each cell across the landscape by the maximum value found across all cells. I then subtracted the map of fundamental niche suitability from the GARN map, so that negative values indicate areas of distributional debt where a species is unlikely to occur despite a high fundamental niche suitability.

Quantile regression analysis

To identify fundamental niche boundaries on species' distributions, I extracted activity hours and estimated probability of presence across Puerto Rico for each of our eight focal *Anolis* species. Using the R package *quantreg* (Koenker, 2017), I performed quantile regression on the 90th percentile to identify areas where EPP was limited by the fundamental niche. I then tested for slope differences between the 90th and 10th percentiles to identify triangular, constraining relationships. Next, for each species, I extracted the residuals from the upper quantile regression (n=10,673) and refer to these as fundamental niche residuals.

Morphological similarity

I computed morphological similarity between species by conducting principal component analysis (centred and scaled) on 18 morphological measurements for all 10 Puerto Rican species of *Anolis* from Mahler et al. (2010). I quantified overall size and shape, head size, leg length, foot morphology and tail length (see Table 4-5 in supporting information for a complete list), all of which have been implicated in microhabitat specialization and adaptive radiation of *Anolis* (Losos, 2009; Mahler et al., 2010). Full details on traits are given in Mahler et al. (2010). Note that I include both *A. cuvieri* and *A. occultus* here because complete morphological data were available for these species. I retained the first four principal components which explained 93% of the variation in morphology. I then calculated the Euclidean distance between principal components for each species to generate morphological distance scores between all species (Table 4-6 in supporting information).

Using the Euclidean morphological distances and each species' EPP surface, I created a 'morphological similarity surface' for each species to measure the degree of morphological similarity between the focal species and all other species within each grid cell (Algar et al., 2013). If there is a single species within a grid cell which is highly morphologically similar to the focal species, this may be more important in reducing fundamental niche filling than the contribution of several other species which are morphologically dissimilar. I therefore computed a 'maximum similarity score' at each cell in the landscape. At each location, I weighted each species' morphological similarity to the focal species by their estimated probability of presence at that location and extracted the maximum value across species for use in subsequent regression

modelling. I took the inverse of each score such that higher values are interpreted as being more morphologically similar to the focal species. Morphological similarity scores were then extracted from each cell across the landscape for use in subsequent regression modelling (see Figure 4-6 in supporting information for maps of each species' morphological similarity surfaces).

Canopy cover

Differences in modelled distributions could be the result of processes unrelated to biotic interactions, such as the availability of preferred habitat type. Anoles are known to differ in their use of closed (forest) and open habitats, thus anole distributions may be related to the availability of forested habitat and extent of canopy cover. To test this I extracted percentage canopy cover from the USGS Global Tree Canopy Cover dataset (Hansen et al., 2013) at a 1x1km resolution. Canopy cover was then regressed against the fundamental niche residuals for all cells across the island.

Testing dispersal limitation

To test whether dispersal limitation generates distribution debt and eliminates the predicted triangular relationships between measures of the fundamental and GARN, I omitted the dispersal-cost surface from the GARN while retaining all other climatic predictors. This provided a predicted distribution for each species which was not constrained by dispersal. I then tested whether the upper and lower quantile slopes became more similar, indicating a breakdown of the predicted triangular relationship.

4.3 Results

Fundamental niche predictions

In general, the majority of Puerto Rico had high predicted activity hours (my proxy for fundamental niche suitability) for all species, except at the highest elevations (Figure 4-2). *A. gundlachi* differed in that fundamental niche suitability was predicted to be greater at mid- to high elevations but lower around low-lying coastal areas. Activity hours predicted across all species of *Anolis* on Puerto Rico ranged from 83 to 144 hours within an individual grid cell. *Anolis cristatellus* had the highest overall mean activity hours across the island per grid cell (141.69 ± 3.47) and *Anolis poncensis* had the lowest (121.21 ± 9.44; see Table 4-4 in supporting information). *A. poncensis* and *A. pulchellus* had relatively low fundamental niche suitability at mid- to high elevation areas compared to the other six species.

GARN predictions

Estimated probability of presence differed markedly within and between species across the island. Individual species' distribution models had mean area under the curve of the receiver operating characteristic (AUC) values ranging from 0.44 to 0.98 (Table 4-4 in supporting information). Two species—*A. cooki* and *A. poncensis*—were highly range restricted; both were confined to the south west of the island where conditions are typically hotter and more xeric than the rest of the island. Three species exhibited little to no variation in relative suitability across the island: *A. cristatellus*, *A. pulchellus* and *A. stratulus* (Figure 4-2). Three species (*A. evermanni*, *A. gundlachi* and

A. krugi) were predicted to have the greatest probability of presence at mid- to high elevations (Figure 4-2).

Distributional Debt

I compared activity hours and probability of presence for each species to evaluate the degree of fundamental niche filling across the island. I found that for the three most abundant and wide-ranging species (*A. cristatellus, A. pulchellus* and *A. stratulus*), the degree of fundamental niche filling was high (Bottom panels; Figure 4-2). In contrast, the remainder of species (*A. cooki, A. evermanni, A. gundlachi, A. krugi* and *A. poncensis*) had large areas of the island in which the fundamental niche is under filled, i.e. fundamental niche models predict high suitability but realized niche models predict low suitability (Figure 4-2).

Quantile regression between fundamental and realized niche estimates revealed a range of different relationships. For two highly range-restricted species (*A. cooki* and *A. poncenis*) I uncovered clear triangular relationships between fundamental and realized niche estimates (Figure 4-3). A similar, yet weaker, triangular relationship was also observed for *A. gundlachi*. An unexpected negative correlation between fundamental and realized niche estimates was uncovered for *A. evermanni, A. krugi* and *A. stratulus.* Two species demonstrated little covariation between activity hours and EPP*: A. cristatellus* and *A. pulchellus* (flat relationships), predominantly because there was little variance in EPP across Puerto Rico. Upper and lower quantile slopes were significantly different for all species except *A. stratulus* (Table 4-8 in supporting information).

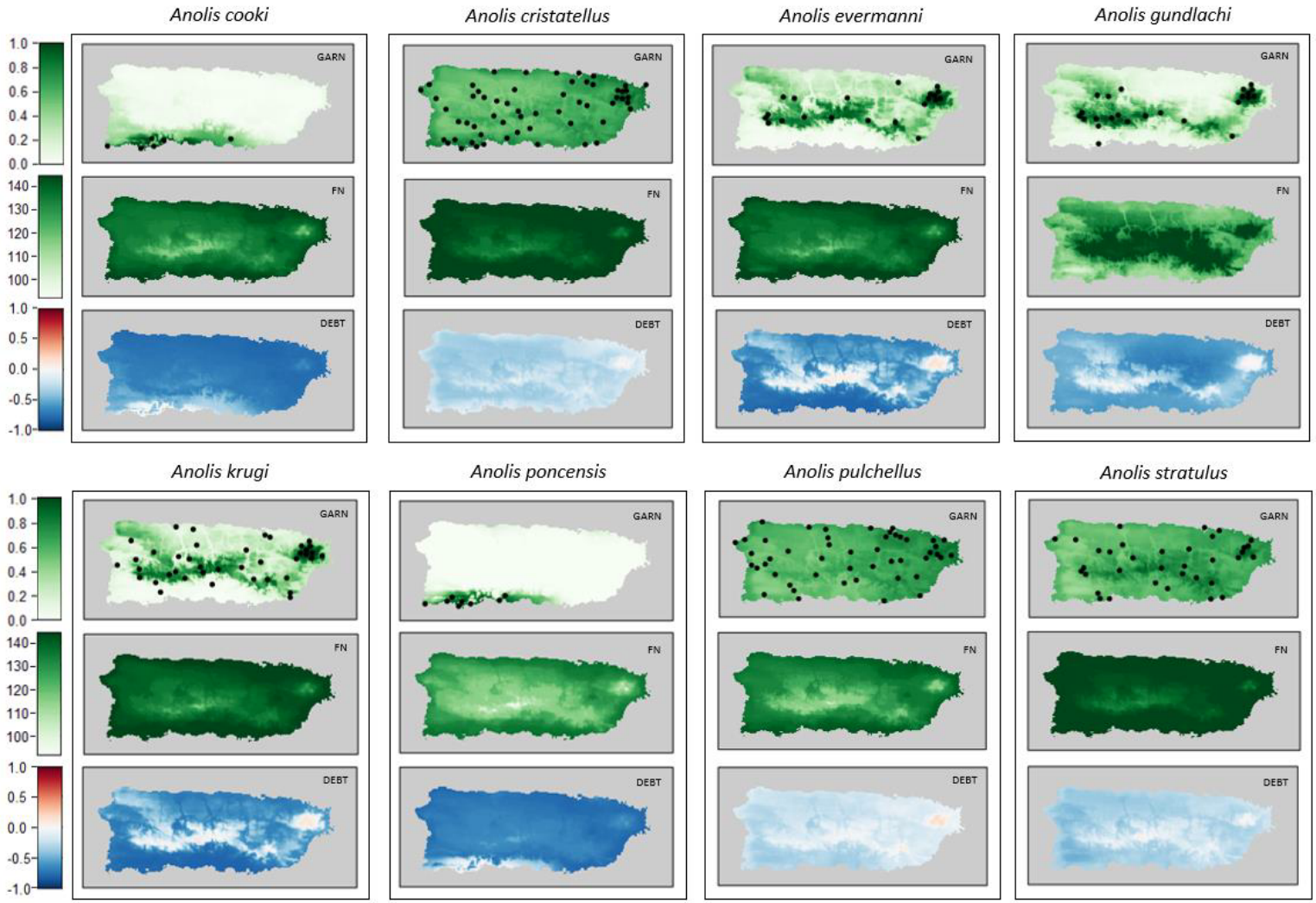


Figure 4-2 Fundamental niche (FN), geographically accessible realised niche (GARN) and distributional debt plots (DEBT). Debt maps are presented on a diverging colour scale where zero (white) indicates areas where the fundamental niche is filled. Blue areas are locations where distributional debt is estimated to be greatest; fundamental niche suitability is high but estimated GARN is low (i.e. the fundamental niche is under filled). Black points on GARN plots are observation records used when training Maxent models.

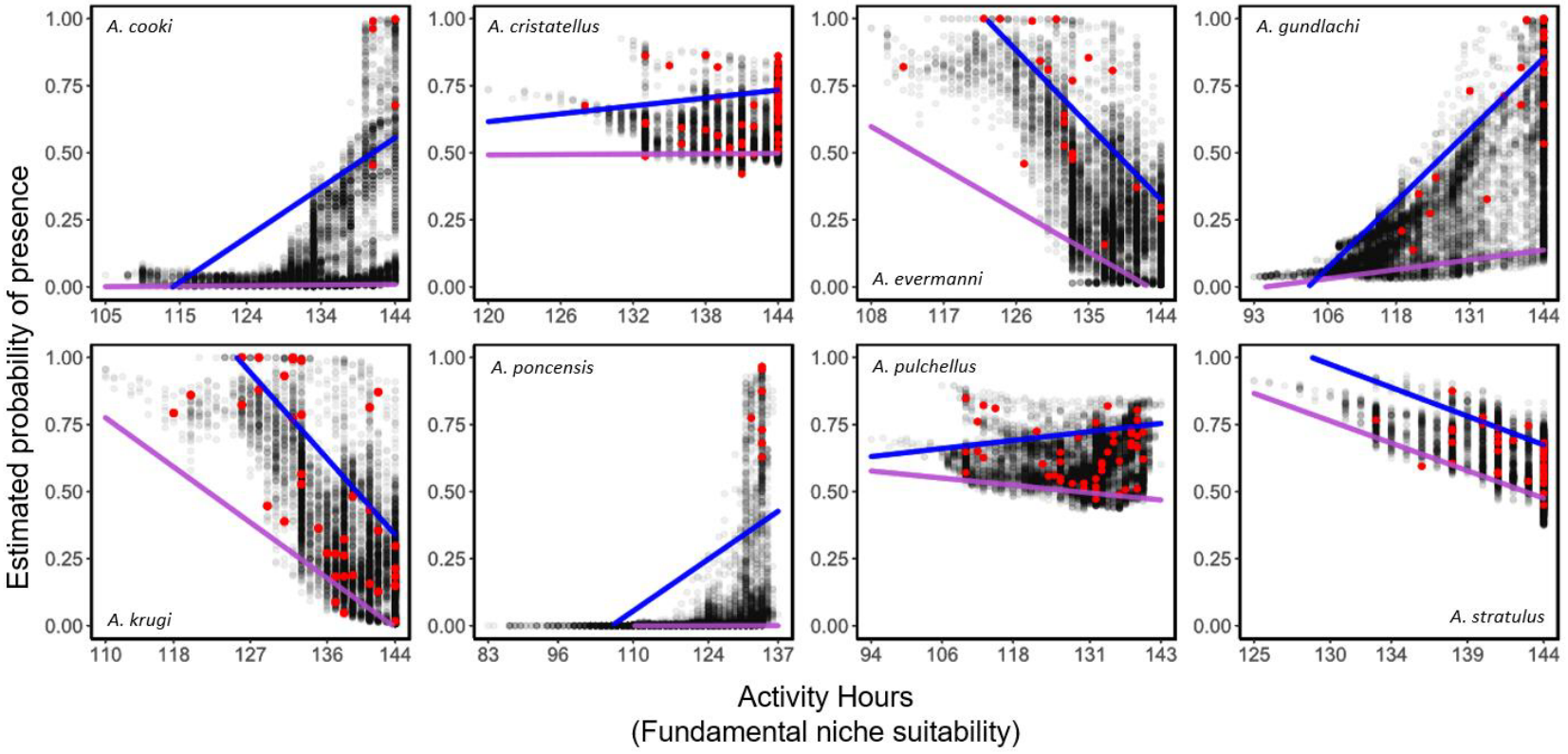


Figure 4-3 Estimated Probability of Presence (EPP; from Maxent species distribution models) against activity hours (a proxy for fundamental niche suitability). Higher activity hours are inferred to be areas which are more abiotically suitable. Blue line is the upper quantile (90th percentile) which we have arbitrarily set as a fundamental niche boundary – points below this line are within a species' fundamental niche. Purple line is the lower quantile (10th percentile). Red points are locations on Puerto Rico where the species has been observed (and are the same points that were used during Maxent modelling).

Morphological similarity

I regressed fundamental niche boundary residuals (upper quantiles in Figure 4-3) against morphological similarity scores to determine whether the presence of other morphologically similar species reduces fundamental niche filling. Given the very large sample size for each model (n = 10, 643), significant relationships were expected even if very little variation was explained by the model. I therefore focus primarily on the variance explained by each model and whether this relationship is positive or negative. I found that between 0 and 50% of the variation in fundamental niche residuals can be explained by morphological similarity (Figure 4-4). For all but one of the species (*A. evermanni*, $R^2 = 0.00$), there were positive relationships between fundamental niche residuals and morphological similarity (Figure 4-4) with morphological similarity explaining 50% of the variation in fundamental niche filling for *A. poncensis*. These results are opposite to my original predictions if the presence of other morphologically similar species limit the distribution via competitive exclusion.

Canopy cover

Given the extensive sample size within each model, significant relationships are expected even when explaining little of the variation between canopy cover and fundamental niche boundary residuals. I found that canopy cover explained little of the variation in fundamental niche model residuals for any species (R^2 ranging between <0.01 and 0.05) with correlations being both positive and negative (Figure 4-5).

Dispersal constraints

I removed dispersal cost surfaces as predictors when generating EPP surfaces so that each species' prediction was not constrained by dispersal. I found that there was little difference in the shape of relationships between activity hours and EPP (Figure 4-7 in supporting information), indicating that dispersal is not responsible for the observed patterns of distributional debt.

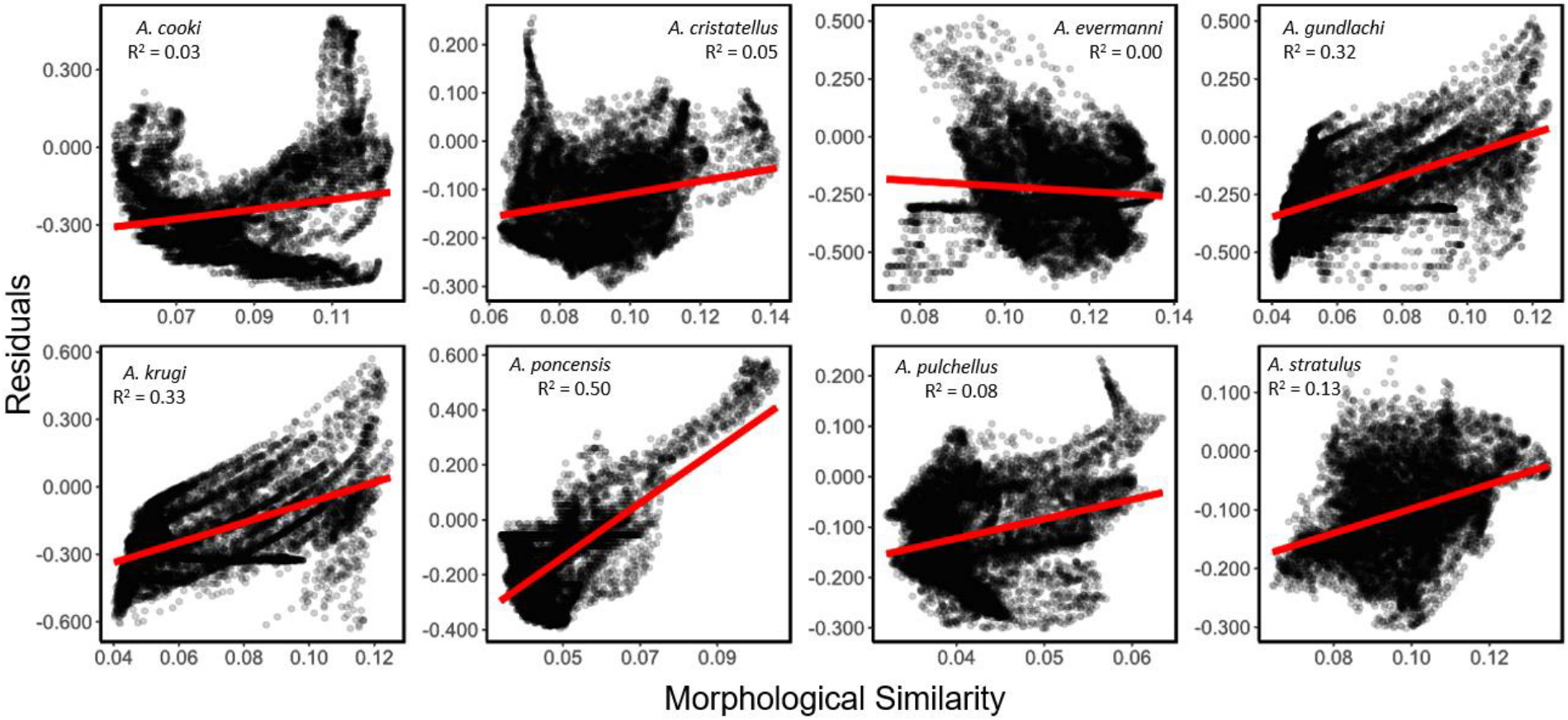


Figure 4-4 Relationships between morphological similarity and fundamental niche residuals (residuals from the 90th percentile). Higher morphological similarity values indicate locations where other species are more similar to the focal species based on principal components analysis on 18 morphological traits (see methods).

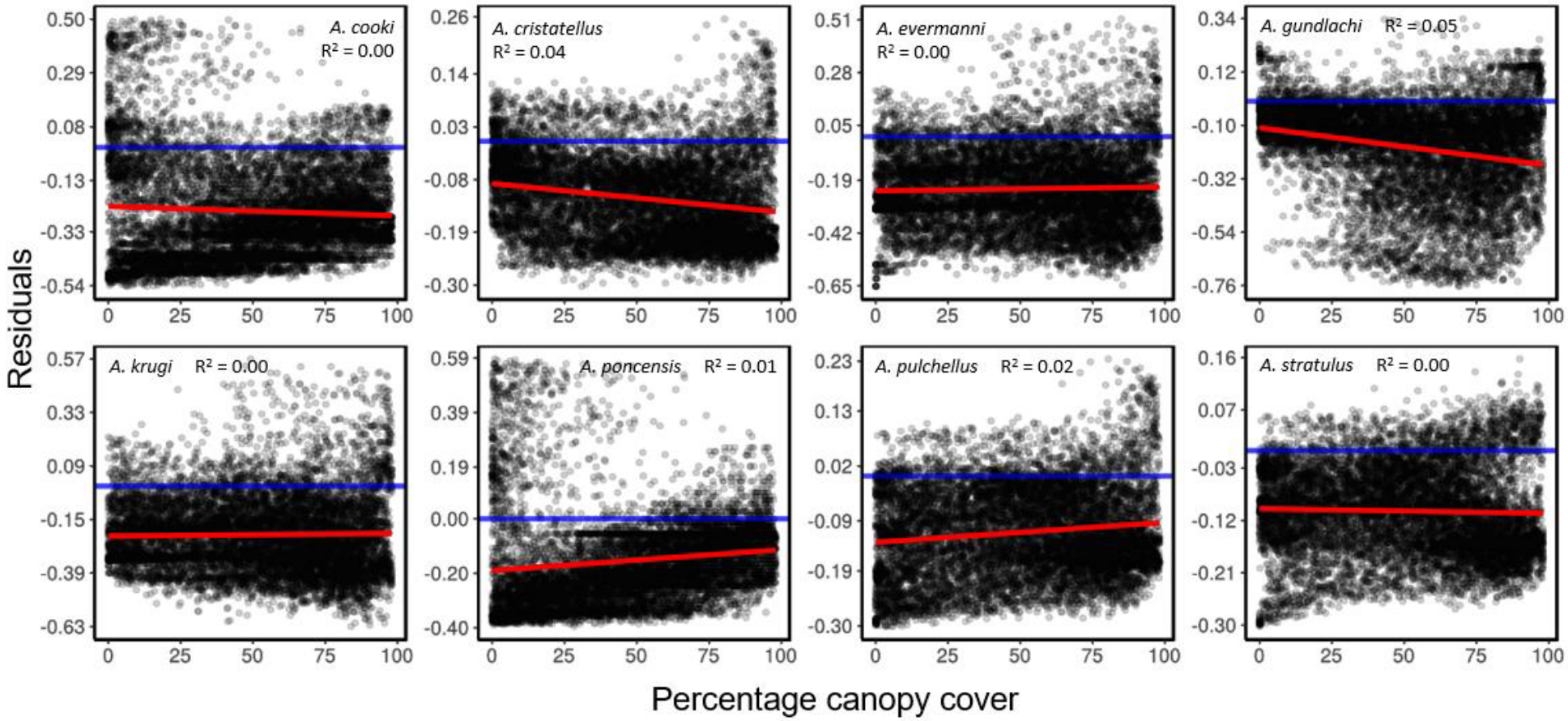


Figure 4-5 Relationships between percentage canopy cover and fundamental niche residuals. Blue line indicates where residuals are zero.

4.4 Discussion

Three key factors are hypothesised to limit species' distributions across broad spatial extents; the distribution of preferred abiotic conditions (e.g. climate), biotic interactions (e.g. interspecific competition, predation) and dispersal limitation (Soberón and Nakamura, 2009). However, for entire faunas, the relative contributions of these factors in limiting species' distributions is generally unknown. To resolve this, I first quantified distributional debt (i.e. where species fail to full their fundamental niches) for *Anolis* lizards on Puerto Rico before testing for the effects of interspecific competition, dispersal limitation and access to preferred habitat type to explain patterns of fundamental niche underfilling. To explicitly test for the effects of interspecific competition I implemented a novel framework integrating mechanistic and correlative niche models—and species' morphological traits—to map areas of distributional debt across the island. Overall, I found substantial areas of distributional debt for 5 of the 8 species studied but uncovered no evidence of either interspecific competition, dispersal limitation or the availability of forested areas as limiting factors in the distribution of anoles across Puerto Rico. My results indicate that either these processes are unimportant in generating the observed patterns of distributional debt, or that our models fail to accurately capture them at this spatial resolution.

Comparing variation in activity time to estimated probability of presence from correlative models (based of geographic occurrences) identified three distinct patterns of distributional debt. First, three species (*A. cristatellus*, *A. stratulus* and *A. pulchellus*) showed little distributional debt with no (or a very weak) relationship between EPP and the fundamental niche, with the upper and lower

qualities of the activity time-EPP relationship tracking each other, mostly in parallel (Figure 4-3). These species are widespread across Puerto Rico (Schwartz and Henderson, 1991) and are found in a broad range of climates. Maxent models were poor at distinguishing between presences and random background in all three species (Table 4-4), as expected for such widespread generalists (Elith et al., 2011). For these species the entirety of Puerto Rico, except for the highest elevations, has high fundamental niche suitability compared to other anoles species on the island, particularly *A. cristatellus* and *A. stratulus*.

Second, three species—*A. cooki*, *A. poncensis* and *A. gundlachi*—displayed substantial distributional debt across Puerto Rico. All of these species have relatively restricted distributions, with *A. cooki* and *A. poncensis* restricted to the arid south-western lowlands and *A. gundlachi* to upland areas (Schwartz and Henderson, 1991). The clear triangular relationship between EPP and activity hours suggest that these distributions, in some areas, reflect fundamental niche constraints. The known occurrences for these species are restricted to conditions in which mechanistic niche models predicted high activity hours, though this pattern is weaker in *A. gundlachi*. This suggests that available activity hours may be too low to obtain viable populations in upland areas for *A. cooki* and *A. poncensis* and in lowland areas for *A. gundlachi*. Thermal physiological adaptation in these species bolsters this interpretation: *A. cooki* and *A. poncensis* have evolved greater heat tolerance (higher T_{opt} and/or CT_{max}), than closely related species, while *A. gundlachi* is adapted to cooler conditions (Gunderson et al., 2018). However, although the distribution of these species is constrained in some areas by fundamental niche limits, the

large areas of distributional debt identified in Figure 4-2 and 3-3 indicate that they still fail to fill the entirety of their fundamental niches in geographical space i.e. their realised distribution is smaller than their potential distribution. The triangularity of the EPP-activity areas relationship demonstrates that these species are regularly absent from areas with substantial scope for activity, indicating realised, rather than fundamental, constraints on their distributions.

Third, two species—*A. evermanni* and *A. krugi*—display negative correlations between EPP and activity hours, a pattern I did not predict. Fundamental niche predictions for both species suggest that mid- to high-elevation areas (the middle of Puerto Rico) are relatively unsuitable compared to lower lying coastal areas (Figure 4-2). However, these species are known to generally occupy mid- to high-elevation areas (Schwartz and Henderson, 1991), further corroborated by my GARN predictions (Figure 4-2). This result suggests that these species tend to occupy relatively unfavourable climate conditions. One possible reason for this discrepancy is that these species can select thermally favourable microhabitats at high elevations, which is known to occur on Hispaniola (Hertz and Huey, 1981; Muñoz et al., 2014). Although *NicheMapR* models an individual organisms' behaviour to maintain preferred temperatures, if microhabitat heterogeneity at finer scales is not captured in the underlying microclimate data, then it may be unable to capture the complexities of behavioural thermoregulation. Consequently, high elevation (i.e. cooler) areas will tend to be predicted as less suitable, reducing the number of predicted activity hours available to the organism. Additionally, these species may also be unable to persist across a broader range of predicted hours than other species. My results here indicate this may be the case – both

species' known observation records (red points, Figure 4-3) span a large range of activity hours (around 110 – 142 hours for *A. evermanni* and 118 – 144 hours or *A. krugi*).

The conspicuous patterns of distributional debt uncovered for *A. cooki*, *A. poncensis* and *A. gundlachi* are indicative of one—or possibly several—processes preventing these species from occupying the entirety of their predicted fundamental niches. While biotic interactions may generate observable distributional debt in some instances (Algar et al., 2013), other factors, such as unmeasured niche axes, dispersal limitation or the spatial distribution of preferred habitat type, can produce similar patterns (Algar et al., 2013; Barve et al., 2011). To test for biotic interactions specifically, I predicted a negative relationship between fundamental niche boundary residuals and ecological similarity of incumbent species, using morphological similarity as a proxy (Algar et al., 2013; Glor and Warren, 2011). I, in fact, uncovered the opposite relationship; for all species except *A. evermanni*—whose relationship was flat—morphological similarity is positively correlated with fundamental niche residuals (Figure 4-4).

The consistent positive correlations between morphological similarity and residual deviance observed here suggests that fine-scale resource partitioning, facilitating species co-occurrence across the island, negates direct interactions leading to competitive exclusion at the scale of our analysis. Our models—while fine resolution in the context of many macroecological studies at 1km—may be too coarse to identify fine-scaled spatial partitioning of resources. For example, nearly all sympatric species of anole across the Greater Antilles differ in structural or thermal microhabitat preference/use (Losos 2009).

Within terrestrial anole ecomorphs (e.g. grass-bush or trunk-ground), species occurring in sympatry are often similar in body size but exploit different thermal microhabitats; one species may exploit sunny patches while another will prefer the shade (Losos 2009). *A. cooki*, for instance, is a trunk-ground anole, ecologically and morphologically similar to the geographically widespread *A. cristatellus*. These two species occur in sympatry in southern Puerto Rico but partition microhabitats, with *A. cooki* favouring hotter, more xeric, microhabitats (Schwartz and Henderson 1991), which is reflected in their thermal performance optima (Gunderson et al. 2018). Early research on these anole species indicated that interspecific competition between them may further strengthen microhabitat partitioning (Huey and Webster, 1976). Rather than promoting outright competitive exclusion—which could result in a negative correlation between morphological similarity and residual deviation—competition between these species may instead strengthen microhabitat resource partitioning, thus promoting co-occurrence. Thus, when viewed at coarse resolutions, sympatry will be observed, rather than exclusion. If resource partitioning is promoting co-occurrence on Puerto Rico, it is possible that the probability of observing a morphologically similar species (to any given focal species) will increase. This is because more species could occur in the same area, increasing the probability of sampling a morphologically similar species (to the focal species). This could ultimately result in high morphological similarity being calculated within a given area when taking the maximum morphological similarity score within a cell, as I did here.

At progressively finer spatial resolutions, it is possible that the predicted negative correlation between fundamental niche residuals and morphological similarity may become apparent. Although interspecific competition has been observed at macroecological scale for anoles on Hispaniola (Algar et al., 2013), total species richness on this island compared to Puerto Rico is substantially higher. If resource partitioning can facilitate co-existence, a limit may be reached when most thermal/structural microhabitats are exploited (i.e. negative correlations could manifest when alpha diversity reaches a certain amount). At this point, species may be competitively excluded from an area. A potentially fruitful area of future research would be to apply this methodological framework to the Hispaniolan anole fauna to test this hypothesis explicitly.

Biotic interactions encompass more than interspecific competition. Parasitism, mutualism or predation may also alter a species' distribution (Losos, 2009; Pringle et al., 2019; Wisz et al., 2013). As I only tested directly for the effects of interspecific competition here, it is possible that these other interactions could result in the observed patterns of distributional debt. For example, predation on anoles is well documented with snakes, birds and spiders regularly preying upon them (Losos 2009). Anole predators have also been shown to influence their communities indirectly, creating a complex interaction between predation and interspecific competition. Recent work by Pringle et al. (2019) showed that the presence of an anole predator could result in structural niche shifts within its prey species, even if the predator rarely consumed those same species. In the presence of an experimentally-introduced ground-dwelling predator (*Leiocephalus carinatus*), *Anolis sagrei* and *Anolis*

smaragdinus were forced into exploiting similar structural microhabitats in a fear-driven response to predation, with *A. sagrei* ultimately outcompeting *A. smaragdinus* (Pringle et al., 2019). Although these results are from relatively small-scale manipulative experiments, they suggest that the spatial distribution of predators could subsequently alter the distribution of structural habitat use, with concomitant changes in species' co-existence through geographic space.

It is unlikely that dispersal limitation or the availability of preferred habitat type across the island is responsible for the distributional debt I observe here (Figure 4-5); percent canopy cover explained almost no residual deviation from the fundamental niche boundary (the highest R^2 across all species was only 0.05 for *A. gundlachi*). Maxent models that include dispersal constraints, as mine did here, may infer low suitability (or probability of presence) in areas well within the fundamental niche, because they are inaccessible because of large distances or dispersal barriers (Algar et al., 2013). If this process was responsible for the triangular relationships I observed, then refitting the CNMs without dispersal cost surfaces should have removed the triangular relationship between activity hours and EPP; it did not (Figure 4-7). However, I did not explicitly include dispersal barriers in my dispersal-cost surfaces, so their effects may have gone undetected, though longer dispersal-cost paths are more likely to encounter barriers and thus their effects may be, partly, implicit in our dispersal-cost surfaces. Furthermore, while dispersal limitation effects on anole ranges have been detected on the island of Hispaniola (Algar et al., 2013; Glor and Warren, 2011), the smaller size of Puerto Rico and lack of extreme climatic barriers relative to larger islands such as Hispaniola or Cuba may make dispersal limitation less likely. My fundamental niche modelling

revealed that much of the island may be highly suitable physiologically for most species (Figure 4-2), suggesting there are limited climatic barriers preventing dispersal. Except at the highest of elevations, models predict similar numbers of activity hours around the entire coastline of Puerto Rico (Figure 4-2) indicating that these areas could provide dispersal pathways. The lack of an effect of land cover could indicate that species use a wide range of habitats, provided sun and shade are available (see also Logan et al. 2013), or that effects of macrohabitat preference are not detectable at the resolution examined here.

By modelling both the fundamental and realised niche of anoles across Puerto Rico, I have revealed, for the first time, large areas of distributional debt for 5 of 8 species studied here. However, clear explanations for the patterns of distributional debt observed remain elusive. While I tested directly for the effects of interspecific competition, dispersal limitation and the availability of preferred habitat, I found that none of these processes could adequately account for these observations. Contrary to my prediction of a negative correlation between distributional debt and morphological similarity as an explanation for debt, I uncovered the opposite; clear positive correlations for 7 of the 8 species studied here. This result indicates that fine-scale resource partitioning, whether in terms of food, structural or thermal niches, facilitates co-occurrence across the island. Further, the relatively low species richness on Puerto Rico—compared to larger islands such as Hispaniola, where interspecific competition has been shown to limit ranges (Algar et al., 2013)—would suggest that there is niche space available for most species to co-exist

without competitive exclusion becoming a dominant force in shaping species ranges at macroecological scales.

Finally, methods to estimate a species' realised niche (via correlative species distribution models e.g. Maxent) are mature but the same cannot be said for mechanistic models such as *NicheMapR*¸ which are still developing. A better understanding of how such models perform, particularly for tropical species inhabiting topographically complex areas, must be considered a research priority going forward. The framework I have introduced here has the potential to be applied more widely—both geographically, taxonomically (including for endotherms)—provided that sufficient physiological, behavioural and ecomorphologicaldata are available to parameterise the mechanistic model and quantify ecological similarity. Currently, such data are likely to be lacking across broad taxonomic and spatial scales. Thus, to effectively test the generality of our methods, it is important that future research not only focus on model development but also field- and lab-based organismal research to provide the fundamental data to effectively parameterise these ever more powerful models.

4.5 Supporting Information

Table 4-1 Replacement climate layers for *NicheMapR's* microclimate sub-model. Here original Climate Research Unit's (CRU) TS version 1.0 and 2.0 climate surfaces (at ~17km^2 resolution) were replaced with alternative data products at ~1km^2 resolution.

Variable	Description	Replacement
ELV	Altitude (m)	NASA MODIS GTOPO30
PRE	Precipitation (mm)	Worldclim v2
WETDAYS	Wet day frequency (days)	N/A*
WND	Wind speed (m/s)	Worldclim v2
TMEAN	Mean temperature (^{o}C)	Worldclim v2
TMIN	Minimum temperature (^{o}C)	Worldclim v2
TMAX	Maximum temperature (^{o}C)	Worldclim v2
DTR	Mean diurnal temperature range (^{o}C)	Worldclim v2
REH	Relative humidity (%)	N/A*
CCMIN	Cloud cover (%)	EarthEnv cloud cover

* These variables had no replacement at ~1km^2 in the WorldClim dataset. Here, the original CRU TS data were used or, in the case of minimum and maximum relative humidity, recalculated from original CRU data using the 'Wetair' and 'VAPRRS' functions within *NicheMapR*.

Table 4-2 Thermal parameters for *NicheMapR* obtained from an extensive literature search. Wherever possible, experimental data were used. Data on emergence and basking temperatures were not available in the literature and have been estimated (see table for details on these parameters).

Parameter	Description	Source(s)
AMASS	Animal mass (g).	(Butler and Losos, 2002; Jenssen et al., 1984)
VTMAX	Voluntary thermal maximum temperature. This is the upper preferred body temperature the organism will permit while foraging (^{o}C). Set to maximum field body temperature recorded in the field across all data sources.	(Blouin-Demers and Nadeau, 2005; Hertz, 1979; Hertz et al., 1993; Rand, 1964; Sinervo et al., 2010)
VTMIN	Voluntary thermal minimum. This is the lower preferred body temperature the organism will permit while foraging (^{o}C). Set to minimum field body temperature recorded in the field across all data sources.	(Blouin-Demers and Nadeau, 2005; Rand, 1964)
TEMERGE	Temperature at which the organism will move to a	N/A

	basking site (ºC). Emerge temperature arbitrarily set at 1c below VTMIN (voluntary thermal minimum; lower body temperature for foraging).	
TBASK	Minimum basking temperature (ºC). Basking temperature arbitrarily set to the temperature at which organism emerges (organism therefore emerges and immediately starts basking until VTMIN is reached, upon which it starts foraging)	N/A
TPREF	Preferred body temperature (ºC). TPref values were taken from the literature for: *A. cooki*, *A. cristatellus, A. gundlachi* and *A. stratulus* (see Clusella-Trullas et al. 2011). The remaining species' T_{Prefs} were estimated by correlating $T_{opt} \sim T_{pref}$ and testing whether the fitted model slope was different than 1.0 and the	(Clusella-Trullas et al., 2011; Hertz et al., 2013; Huey and Webster, 1976; Malhotra and Thorpe, 1993; Rand, 1964)

	intercept was significantly different from zero. I found that neither the slope nor intercept differed from 1.0 and 0, respectively ($p = 0.76$ and $p = 0.79$). I therefore assumed that $T_{pref} = T_{opt}$ and used published Topt data from Gunderson et al. (2018) for the remaining species.	
CTMAX	Critical thermal maximum (^oC). Experimentally derived.	(Gunderson et al., 2018)
CTMIN	Critical thermal minimum (^oC). Empirical CTMin data only available for *A. cristatellus* (13.1 ^oC). To estimate CTMin for the remaining species, I computed the mean elevation each species was observed at from the same occurrence records used to construct MaxEnt models across Puerto Rico. I then fit a linear model of $CT_{Min} \sim$ Altitude ($R^2 = 0.83$, p	(Gunderson et al., 2011; Gunderson and Leal, 2012; Muñoz et al., 2014)

	< 0.001) from the wild-measured species in Table 1 of (Muñoz et al. 2014a)). Using this model I predicted CT_{Min} for the species in our study, given the mean elevation across all observation records.	
SKINWET	Organism's surface area acting as free-water exchanger. Calculated using empirical water loss measurements (mg/hr) from (Hillman and Gorman 1977).	(Hillman and Gorman, 1977)

Table 4-3 Default ectotherm sub-model parameters for NicheMapR v1.1.4. Parameters missing from this table can be found in Table 3-2 (e.g. mass) or the main text (e.g. shade-sheeking allowed) and include empirical morphological and physiological data I wwas able to obtain from extensive literature searches. This version of *NicheMapR* can be downloaded and installed in R using devtools (e.g. devtools::install_github("mrke/nichemapr@v1.1.4))

Parameter	Description
lometry	= 3, Organism shape, 0-5, Determines whether standard or custom shapes/surface area/volume relationships are used: 0=plate, 1=cyl, 2=ellips, 3=lizard (desert iguana), 4=frog (leopard frog), 5=custom (see details)
ABSMAX	0.85, Maximum solar absorptivity, decimal percent
ABSMIN	0.85, Maximum solar absorptivity, decimal percent
dayact	1, Diurnal activity allowed? 1=yes, 0=no
nocturn	0, Nocturnal activity allowed? 1=yes, 0=no
crepus	0, Crepuscular activity allowed? 1=yes, 0=no
burrow	1 Shelter in burrow allowed? 1=yes, 0=no
M_1	.013, Metabolic rate parameter 1 V_O2=M_1*M^M_2*10^(M_3*Tb) based on Eq. 2 from Andrews & Pough 1985. Physiol. Zool. 58:214-231
M_2	0.800, Metabolic rate parameter 2
M_3	0.038, Metabolic rate parameter 3
extref	= 20, % oxygen extraction efficiency, for respiratory water loss

DELTAR	0.1, Temperature difference (Â°C) between expired and inspired air, for computing respiratory water loss
aestdepth	= 10, Depth (soil node #) to which animal retreats if burrowing and aestivating due to desiccation

Table 4-4 Summary statistics for MaxEnt species distribution models. I used *ENMeval* (Muscarella et al., 2014) to balance model complexity and goodness of fit. I selected the 'best' model by sorting on lowest omission rate and then selecting the model with the highest AUC in line with (Galante et al., 2018).

Species	**n**	**Partition Method**	**Regularisation Multiplier**	**Feature Class(es)**	**Mean omission rate**	**Best model mean AUC**	**AICc**	**ΔAIC**
Anolis cooki	6	k-1 ('jackknife')	3.5	LQHP	0.33	0.97	99.17	8.84
Anolis cristatellus	58	Random k-fold	3.0	LQH	0.12	0.58	1116.18	38.51
Anolis cuvieri	8	k-1 ('jackknife')	2.5	H	0.25	0.44	150.81	2.01
Anolis evermanni	21	k-1 ('jackknife')	1.0	LQ	0.14	0.79	368.89	0.43
Anolis gundlachi	24	k-1 ('jackknife')	1.5	LQH	0.16	0.82	486.21	66.75
Anolis krugi	40	Random k-fold	1.0	LQ	0.10	0.80	367.50	1.84
Anolis occultus	4	k-1 ('jackknife')	2.0	L	0.50	0.69	84.80	10.40
Anolis poncensis	8	k-1 ('jackknife')	3.0	LQ	0.13	0.98	112.48	0.98
Anolis pulchellus	48	Random k-fold	3.5	L	0.14	0.58	892.62	0.04
Anolis stratulus	35	Random k-fold	2.5	LQ	0.14	0.57	650.29	0.19

Table 4-5 List of the 18 traits used in this analysis. The traits presented here are a subset of those in Mahler et al. (2010) Table 1.

Trait
Snout-vent length (SVL)
Tail length
Head length
Head width
Head height
Lower jaw length
Femur length
Tibia length
Metatarsal IV length
Lamella number, toe IV
Lamella width, toe IV
Humerus length
Radius length
Metacarpel IV length
Lamella number, foretoe IV
Lamella width, foretoe IV
Pelvis height
Pelvis width

Table 4-6 Euclidean morphological distances between all 10 species of *Anolis* on Puerto Rico.

	A. cooki	*A. cristatellus*	*A. cuvieri*	*A. evermanni*	*A. gundlachi*	*A. krugi*	*A. occultus*	*A. poncensis*	*A. pulchellus*	*A. stratulus*
A. cooki	0	1.880	6.110	2.787	2.296	2.736	9.531	2.662	4.614	2.328
A. cristatellus	1.880	0	7.190	2.235	3.970	4.475	10.218	4.314	6.310	2.018
A. cuvieri	6.110	7.190	0	6.156	6.239	6.546	5.833	5.281	5.831	6.940
A. evermanni	2.787	2.235	6.156	0	4.953	5.116	8.806	4.728	5.976	1.465
A. gundlachi	2.296	3.970	6.239	4.953	0	1.400	10.316	2.391	3.821	4.446
A. krugi	2.736	4.475	6.546	5.116	1.400	0	10.398	2.751	2.754	4.354
A. occultus	9.531	10.218	5.833	8.806	10.316	10.398	0	8.269	9.594	9.549
A. poncensis	2.662	4.314	5.281	4.728	2.391	2.751	8.269	0	4.112	4.436
A. pulchellus	4.614	6.310	5.831	5.976	3.821	2.754	9.594	4.112	0	5.436
A. stratulus	2.328	2.018	6.940	1.465	4.446	4.354	9.549	4.436	5.436	0

Table 4-7 Fundamental niche summary statistics for 8 *Anolis* species across Puerto Rico. Note missing mean and range activity hours for *A. cuvieri* and *A. occultus* due to incomplete physiological data necessary to parameterise NicheMapR for these species.

Species	**Activity Hours (Range)**	**Mean Activity Hours (±SD)**
A. cooki	105–143	134.03 (±6.96)
A. cristatellus	120–144	141.69 (±3.47)
A. cuvieri		
A. evermanni	108–144	137.00 (±5.94)
A. gundlachi	93–144	125.81 (12.99)
A. krugi	110 –144	138.37 (5.13)
A. occultus		
A. poncensis	83–137	121.21 (9.44)
A. pulchellus	94–143	129.35 (8.34)
A. stratulus	125–144	142.39 (2.90)

Table 4-8 ANOVA test of slope differences between upper and lower quantiles (see Fig 3 in main text for plots).

Species	**F**	**DF**	**P**
A. cooki	5758.9	1, 21345	<0.001
A. cristatellus	89.05	1, 21345	<0.001
A. evermanni	301.16	1, 21345	<0.001
A. gundlachi	10815	1, 21345	<0.001
A. krugi	217.44	1, 21345	<0.001
A. poncensis	638.31	1, 21345	<0.001
A. pulchellus	974.27	1, 21345	<0.001
A. stratulus	0.90	1, 21345	0.34

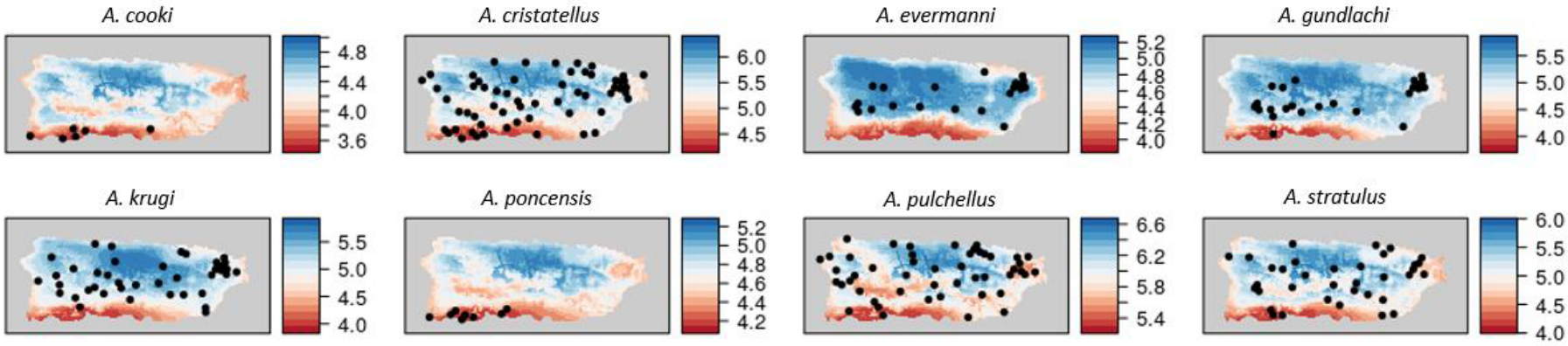


Figure 4-6 Morphological similarity surfaces (MSS). Blue areas indicate locations where morphological similarity is low compared to the focal species. Red areas indicate locations where more morphologically similar species are present (compared to the focal species are present). Higher values indicate greater inferred 'biotic resistance' experienced by the focal species. Black points are observation records used when fitting MaxEnt models.

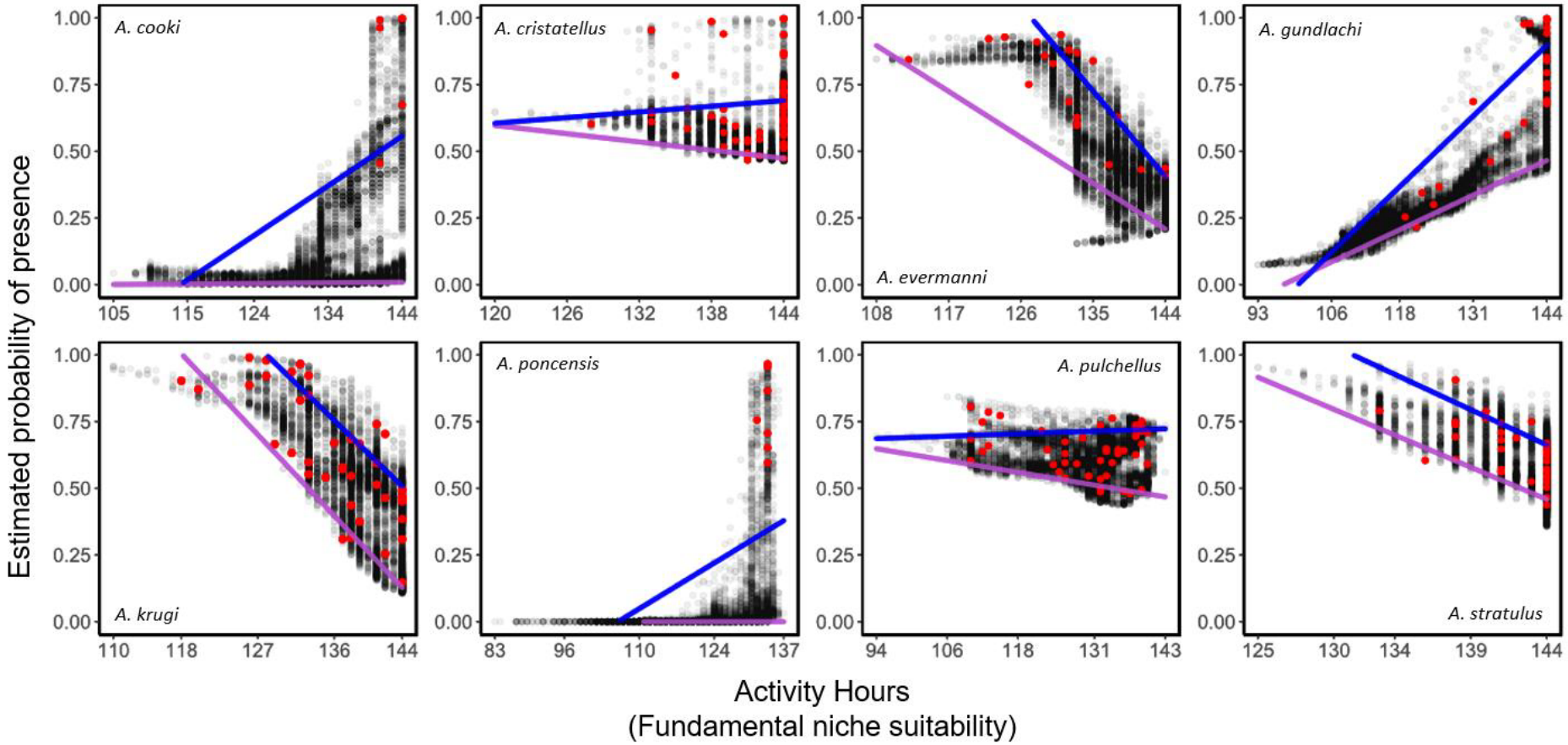


Figure 4-7 Activity hours/estimated probability of presence plots with cost surface (dispersal constraint) removed from MaxEnt models prior to extracting EPP estimates and correlating against activity hours. Note how these plots differ little from those containing a dispersal constraint (main article, Figure 3-3), indicating that dispersal is contributing little to the relationship between EPP and activity hours.

Chapter 5: Testing for macroecological convergence of climate-richness relationships in replicated island radiations

5.1 Introduction

The species richness of individual islands varies in predictable ways within archipelagos and across the globe (Cabral et al., 2014; Kalmar and Currie, 2007; Weigelt and Kreft, 2013), but little is known about species richness patterns within, or across, individual islands and even less about their predictability. For whole islands, differences in species richness among smaller islands largely reflect MacArthur and Wilson (MacArthur and Wilson, 1967, 1963) immigration–extinction dynamics which vary as a function of island isolation and area. On larger islands, diversification and cladogenesis become increasingly important, again as a function of area (Algar and Losos, 2011; Losos and Schluter, 2000; Parent and Crespi, 2006) and isolation (Rosindell and Phillimore, 2011), but also island age and heterogeneity (Borregaard et al., 2016; Matthews et al., 2016; Whittaker et al., 2008). Across broader spatiotemporal extents, climate and climatic instability can also influence inter-island variation in species richness (Kalmar and Currie, 2007; Weigelt et al., 2016).

Although theory and accumulating empirical evidence recognize a role for environmental heterogeneity within islands for species diversification and niche evolution (Algar and Mahler, 2016; Hortal et al., 2009; Stein et al., 2014), the unit of biogeographic focus has, in general, remained the whole

island, with far less consideration of ecological gradients within islands (for example, species richness gradients, but see Steinbauer et al. 2016, Frishkoff et al. 2019). One reason islands have been treated as homogeneous entities is that they are small and 'simplified' compared to mainland systems (Losos and Ricklefs, 2009). However, large islands can harbour considerable environmental heterogeneity and host many of the same processes that combine to produce mainland macroecological patterns (e.g. the latitudinal diversity gradient), including cladogenesis (Kisel and Barraclough, 2010; Losos and Schluter, 2000; Whittaker et al., 2008), anagenesis (Stuessy et al., 2006), local adaptation (Wang et al., 2013), and climatic niche conservatism and radiation (Algar and Mahler, 2016). Species ranges on large islands are also determined by similar processes as those acting on mainland ecosystems including climatic niche limits, dispersal limitations and biotic interactions (Algar et al. 2013, see also Chapter 3 in this thesis). Given that these processes are known to operate within islands, macroecological patterns, like climate–species richness relationships, may also emerge.

Across large spatial extents, species richness peaks in warm, wet areas (e.g. the tropics) and declines towards colder and/or drier areas, typically at higher latitudes and elevations (Field et al., 2009; Hawkins et al., 2003). These broad-scale associations between climate and richness are reasonably consistent through time and space (Boucher-Lalonde et al., 2014; Vázquez-Rivera and Currie, 2015; Willig et al., 2003; Yasuhara et al., 2012), often despite marked differences in clades' evolutionary histories (Hawkins et al., 2012; Latham and Ricklefs, 1993; Qian and Ricklefs, 2004). Across smaller spatial extents, climate is a less consistent predictor of species richness (Field et al., 2009);

along elevational gradients, for example, climate–richness relationships are often complex and taxon-specific (McCain and Grytnes, 2010; Sanders and Rahbek, 2012; Steinbauer et al., 2016). Large islands fall between continental spatial extents and considerably smaller elevational ones but can nonetheless present a broad range of climatic conditions. It is reasonable, therefore, to hypothesise that climate may also contribute towards determining species richness gradients within individual islands with sufficient climatic range.

The replicated nature of islands can provide an opportunity to test predictions when replicated, controlled experiments are not possible, as is often the case for biogeographical and macroecological hypotheses (Gaston and Blackburn, 1999). Evolutionary biologists, who often try to retrospectively infer the processes and drivers that have produced particular phenotypes or clades (Lobkovsky and Koonin, 2012), have long viewed islands as a solution to this inferential barrier, exploiting them as ‘natural laboratories’ that offer replicated natural experiments to test the predictability of evolution (Diamond, 1986; Losos and Ricklefs, 2009). For example, similar stickleback morphs have repeatedly evolved in multiple freshwater lakes (Rundle et al., 2000) and Caribbean *Anolis* lizards have independently evolved into similar sets of ecomorphs on each of the four islands of the Greater Antilles (Losos, 2009; Mahler et al., 2013; Williams, 1972). Both of these examples, in addition to demonstrating the repeatability of evolution, have provided new insights into the workings of natural selection, adaptation, and speciation (Losos, 2009; Rundle et al., 2000). Large heterogeneous islands have similar potential to provide insight into the outcome and workings of ecological processes by testing the repeatability and predictability of ecological patterns. The ability of

ecological models, even phenomenological ones, to make accurate predictions of independent data is key to obtaining and evaluating scientific understanding (Houlahan et al., 2017; Peters, 1991) and predictive performance on new data are especially important when controlled experiments are impossible, as is often the case in macroecology (Blackburn, 2004; Davies and Gray, 2015; H-Acevedo and Currie, 2003).

In this paper, I test for macroecological convergence of climate-richness gradients using the independent radiations of *Anolis* lizards (anoles) on the Greater Antilles as a replicated biogeographical experiment. Anoles have diversified on each of the four Greater Antillean islands (Cuba, Hispaniola, Puerto Rico and Jamaica), radiating into similar sets of ecomorphs on each of the four islands (Losos, 2009; Mahler et al., 2013; Williams, 1972). As such, they provide independent replicates of ecologically convergent faunas that can be used to test the repeatability and predictability of macroecological relationships. I use museum records and species distribution modelling to produce the first maps of species richness within individual islands for this iconic radiation and ask three questions:

1. How does species richness vary within islands?

2. Are species richness gradients within individual islands related to climate?

3. Are climate–richness relationships repeatable and predictable between islands?

5.2 Methods

Study System

I focus on the anole faunas of the four islands of the Greater Antilles (Cuba, Hispaniola, Jamaica and Puerto Rico). These islands vary in size from 9,104km^2 (Puerto Rico) to 109,884 km^2 (Cuba) and cover a combined area in excess of 205,000 km^2. Total island species richness varies from ~6 species on Jamaica to more than 60 on Cuba. Despite covering a small latitudinal extent (approximately 5.5 degrees) the islands are varied topographically and display a wide range of climatic conditions from cool mountainous regions to warm tropical forest. *Anolis* lizards have independently radiated on each island, producing ecologically similar but independent faunas (Losos, 2009). Nearly all species on each island are single-island endemics arising from intra-island cladogenesis (Losos and Schluter, 2000).

Estimating species richness across islands

I modelled species' geographical distributions on each island using occurrence records from a database of previously published observations (n = 5335 georeferenced records representing 94 anole species; (Algar et al., 2013). After filtering to remove species represented by fewer than 6 observation records, I was left with 27 species on Cuba, 32 on Hispaniola, 6 on Jamaica and 9 on Puerto Rico for a total of 72 species across islands. For the remaining species' observation records, I filtered those that were closer than 3km in order to reduce the effects of spatial sampling bias using spThin (Aiello-Lammens et al., 2015). I modelled species' distributions using MaxEnt version 3.4.1k (Phillips et al., 2006) at a ~1km resolution. I included four Worldclim

v2 (Fick and Hijmans, 2017) bioclimatic variables as predictors in my models which are thought to be important to ecotherm macrophysiology (Clusella-Trullas et al., 2011; Deutsch et al., 2008; Kingsolver et al., 2013): mean diurnal temperature range (BIO2), maximum temperature of the warmest month (BIO5), temperature of the coldest month (BIO6) and precipitation of the driest month (BIO14). I also included percentage canopy cover as an additional predictor given the extensive arboreality of *Anolis* across the islands (Losos, 2009). I used ENMEval (Muscarella et al., 2014) to tune regularisation and feature classes for each species to balance model complexity and goodness of fit. For species with fewer than 20 observation records I used k-1 ('jackknife') to partition training and test data and for all other species I used random k-fold partitioning (k=10). I selected the 'best' Maxent model for each species by first sorting on lowest omission rate then selecting the model with the highest AUC, as per recommendations by Galante et al. (2018).

To predict a species' probability of presence using presence-only data, species prevalence is required (Elith et al., 2011). In practice, prevalence is nearly always unknown so models are only able to predict relative suitability. However, probability of presence values are necessary to accurately estimate species richness from stacked distribution models (Calabrese et al., 2014). I estimated prevalence for each species by dividing the number of unique cells each species occurred in by the total number of unique cells occupied by any species. This approach assumes that species with a low number of observations in my data are geographically rarer than species with a greater number of observations which seems reasonable given the extensive sampling of anoles over the preceding decades. Niche models based on climate can

identify those areas where a species can, potentially, occur with some probability, given the climatic conditions (Elith et al., 2011). However, species may not occur in all suitable areas; dispersal limitation, whether because of distance or biogeographic barriers, is known to prevent anoles from filling their potential distributions (Algar et al., 2013; Glor and Warren, 2011). In order to account for the effects of dispersal limitation, I used cost-distance surfaces (Algar et al., 2013; Allouche et al., 2008) as predictors in my distribution models. For each species independently, I summed the overland distances from each location on an island to all known occurrences, using the R package 'gDistance' (van Etten, 2015). I inverted the summed distance surface such that locations near many known occurrences will have high values and those far from any occurrences will have low values. Therefore, my models can constrain a species' predicted distribution to those areas that are both environmentally suitable and accessible. Background locations for each species' model were selected using observations of other *Anolis* species on the island where the focal species was modelled (i.e. target group absences). This approach was chosen over random background points as target-group background points have been shown to improve average performance of MaxEnt models (Phillips et al., 2009; Ranc et al., 2017). Presence and background data points were filtered to remove duplicates in each cell.

To create species richness maps for each island, the clog-log output from each species' distribution model was stacked and summed to generate an expected richness value for each pixel across the landscape (Calabrese et al., 2014; Phillips et al., 2017). I stacked and summed probability of presence estimates

over using a binary threshold value because arbitrarily defined threshold values can have a dramatic effect on model accuracy, especially for species with low prevalence values (Freeman and Moisen, 2008; Nenzén and Araújo, 2011). Estimated species richness therefore represents the average number of species expected to be found within a pixel, given multiple sampling attempts at the locality. As my models do not explicitly include factors like biotic interactions which could further limit ranges, model outputs should still be interpreted as potential species distributions across the landscape (Peterson and Soberón, 2012).

Fitting climate–richness regression models

To fit climate–richness regression models, I estimated species richness in 10km x 10km cells across each island and removed cells with < 50% land area, leaving 1345 cells on Cuba, 950 on Hispaniola, 140 on Jamaica and 111 on Puerto Rico. I used generalised least squares (GLS) regression to model how species richness on each island varied as a function of four climate variables: BIO2, BIO5, BIO6 and BIO14. These four climate variables are known to be important for ectotherm macrophysiology (Clusella-Trullas et al., 2011; Deutsch et al., 2008) and are thought to influence the distribution of lizard species (Buckley et al., 2012). Despite using some of the same environmental variables in my SDMs and regression models, I do not consider this approach circular as each species range was modelled independently. Thus, any correlations between richness and climate that may arise reflect shared biological responses to these climatic variables among species (Algar et al., 2009), rather than an artefact of the modelling procedure.

On each island, following Algar et al., (2009), I fitted regression models that included all possible combinations of my four bioclimatic predictors (plus quadratic terms and first-order interactions), with the constraint that the maximum number of predictors per model was five. I fitted each set of predictors using three different spatially autocorrelated error structures: exponential, spherical and Gaussian. This process resulted in 155 models for each error structure or 465 models in total for each island.

Regression model evaluation and prediction

I identified the model with the lowest Bayesian Information Criterion (BIC) value from the total set of 465 models for each island. I then used this 'best' model to predict richness on the other islands using R's built-in 'predict' function. Extrapolation into novel climatic conditions can reduce model performance (Elith et al., 2010; Mesgaran et al., 2014) so to avoid this, I implemented 'ExDet' (EXtrapolation and DETection; Mesgaran et al. 2014) to quantify the degree of climatic similarity between locations. ExDet provides a measure of climatic similarity with negative values indicating pixels which are dissimilar to the model training set in univariate space and values above 1 indicating dissimilarity in multivariate space. When predicting richness on new islands, I removed cells from the target island which were environmentally dissimilar with both univariate and covariate space (values outside a range of 0 to 1) from the source island, so that models predicted only within analogous climatic conditions.

I evaluated predictive performance by regressing observed richness against predicted richness for each island. To determine predictive accuracy, I tested

whether the intercept of this regression differed from zero and the slope from one. To test predictive precision, I computed r^2. I also calculated a second measure of predictive precision, which I call relative predictive precision rP^2. rP^2 is the ratio of the r^2 of the observed–predicted regression to the observed–fitted r^2 of the 'best' model fitted on the target island. Since it is highly unlikely that predictions would perfectly predict richness on an island when a climate richness relationship fitted on that island still contains scatter, the rP^2 provides a measure of predictive performance relative to the highest r^2 I could reasonably expect observed–predicted regressions to achieve.

5.3 Results

Species richness patterns within islands

Species' distribution models for individual species had area under the curve of the receiver operating characteristic (AUC) values ranging from 0.38 to 0.99, with an overall mean ± s.d. of 0.76 ± 0.17 (Table 5 5 in supporting information). Mean ± s.d. AUC on individual islands were: Cuba (0.72 ± 0.72), Hispaniola (0.85 ± 0.12), Jamaica (0.65 ± 0.15) and Puerto Rico (0.66 ± 0.19; Table 5-1). Species richness varied substantially across each island (Figure 5-1). The range of species richness values within 10km x 10km cells on Cuba was 11.02–14.68, Hispaniola: 5.80–11.82, Jamaica: 2.79–3.95, and Puerto Rico: 3.74–5.09. Examining the richness maps revealed that species richness on Cuba was highest along the majority of its Northern coast. Species richness on Hispaniola was found to be greatest in areas of mid- to high elevation to the south and middle of the island but declined atop the very highest peaks (which exceed 3000 m a.s.l). On both Jamaica and Puerto Rico,

species richness was found to be greater at mid to high elevations (e.g. the Blue Mountains on Jamaica and within the El Yunque national park on the eastern side of Puerto Rico; Figure 5-1).

Table 5-1 Summary statistics for species occurrence data and species distribution models. AUC is Area Under the Receiver Operating Characteristic (ROC) Curve.

Island	**Number of species**	**Occurrence points (Total)**	**Mean occurrence points per species (±s.d.)**	**Mean AUC (±s.d.)**
Cuba	27	765	14.16 (24.16)	0.72 (0.17)
Hispaniola	32	2818	70.45 (133.81)	0.85 (0.13)
Jamaica	6	559	93.16 (54.09)	0.65 (0.15)
Puerto Rico	9	250	25.00 (19.47)	0.66 (0.19)

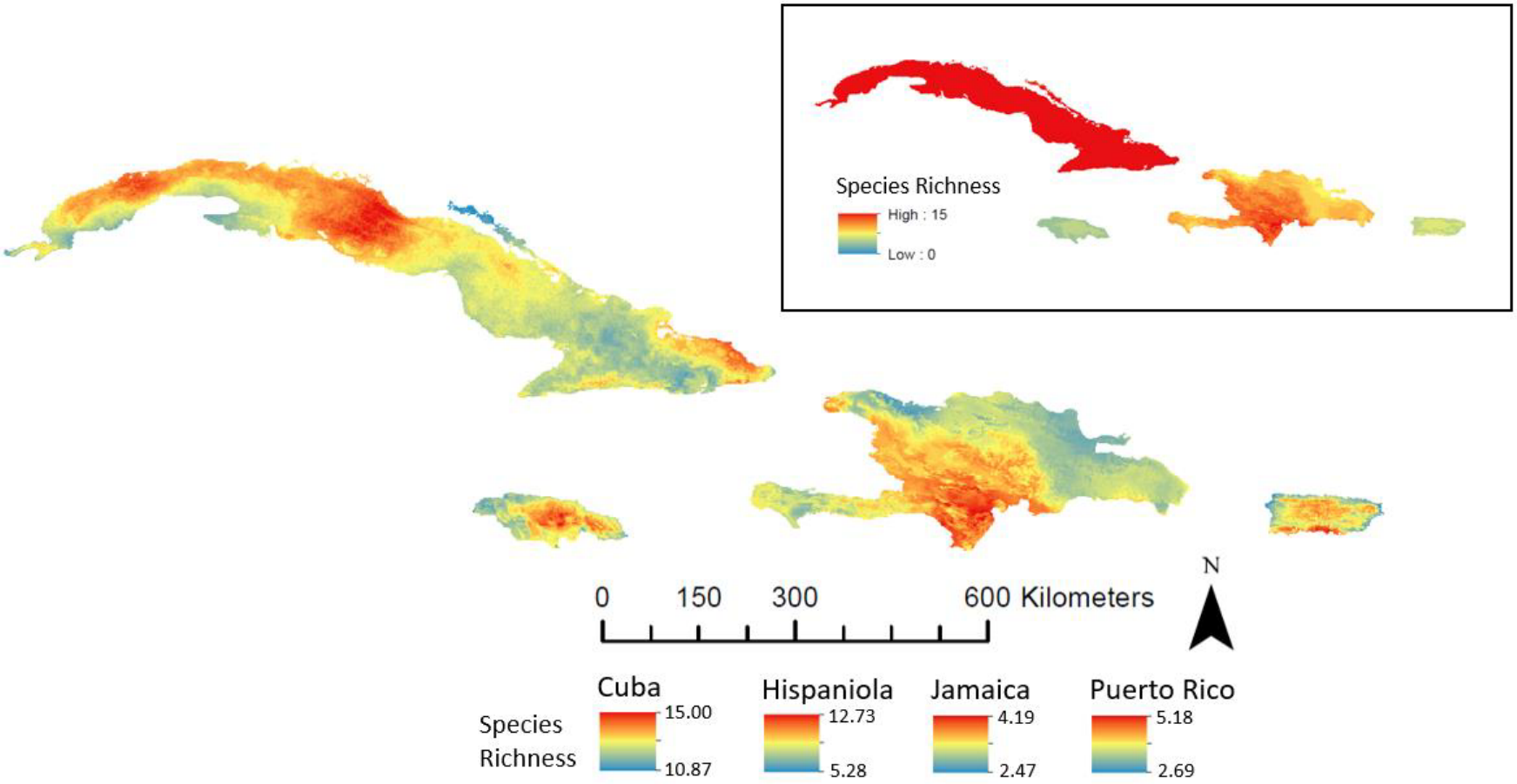


Figure 5-1 Potential species richness for 74 species of *Anolis* lizard across the Greater Antilles at 1x1km resolution. Note that covariates for regression analyses were extracted at 10x10km resolution; 1x1km map provided for improved clarity. Legend scales for the main figure are unique for each island so that intra-island species richness can be more easily discerned. Inset map shows a single scale for potential species richness across all islands.

Fitted regression models

I used constrained all-subsets regression to identify the climate–richness regression model with the lowest BIC on each island (Table 5-2) while accounting for spatial autocorrelation by testing a range of autocorrelated error structures. I evaluated fit of the best models by calculating a pseudo-R2 value by regressing observed richness against fitted richness. Although the 'best' predictors varied across islands (Table 5-2), mean diurnal temperature range (BIO2) was included for all islands. Maximum temperature of the warmest month (BIO5) was present in all 'best' models except for Hispaniola whereas minimum temperature of the coldest month was present in all models except for Puerto Rico (Table 5-3). Fitted models on Hispaniola, Puerto Rico and Jamaica explained between 47-75% of the variation in species richness within each island (based on pseudo-r^2; Table 5-2). Richness was most strongly related to climate on Hispaniola (pseudo-r^2 = 0.75), then Jamaica (pseudo-r^2 = 0.49), and then Puerto Rico (pseudo-r^2 = 0.47). Cuba's fitted model was unique in that climate explained no variation in species richness.

Table 5-2 Summary statistics of the 'best' model for each island (lowest Bayesian Information Criterion value, BIC). ES denotes the error structure associated with the 'best' model (E = Exponential, S = Spherical). N = number of data points in each model, pseudo-r^2 is the r^2 of the observed vs. fitted regression model.

Island	Predictors in best model	ES	BIC	*loglik*	N	Pseudo-r^2
Cuba	BIO2 + BIO5 + BIO6 + BIO14 + $BIO6^2$	E	-510.57	284.10	1345	0.00
Hispaniola	BIO2 + BIO6 + BIO14 + $BIO2^2$ + BIO6:BIO14	E	-47.62	51.11	920	0.75
Jamaica	BIO2 + BIO5 + BIO6 + $BIO2^2$ + BIO2:BIO6	S	-424.26	231.99	140	0.49
Puerto Rico	BIO2 + BIO5 + BIO6 + $BIO14^2$ + BIO2:BIO14	S	-241.21	139.44	111	0.47

BIO2 = Mean Diurnal Range, BIO5 = Max Temp of Warmest month, BIO6 = Min Temperature of Coldest Month, BIO14 = Precipitation of Driest Month

Table 5-3 Environmental predictor coefficients for the 'best' fitting model on each island. Figures in brackets are standard errors.

	Cuba	**Hispaniola**	**Jamaica**	**Puerto Rico**
BIO2	0.61^{***} (0.06)	2.16^{***} (0.16)	3.62^{***} (0.45)	-0.008 (0.049)
BIO5	-0.45^{***} (0.06)		-0.13^{***} (0.03)	-0.06^{***} (0.014)
BIO6	-0.44^{**} (0.14)	0.09^{***} (0.02)	0.32^{***} (0.05)	
BIO14	0.02^{***} (0.00)	0.001 (0.007)		-0.09^{***} (0.009)
$BIO2^2$		-0.12^{***} (0.008)	-0.18^{***} (0.02)	
$BIO6^2$	0.03^{***} (0.00)			
$BIO14^2$				0.0004^{***} (0.00)
BIO2:BIO6			-0.03^{***} (0.006)	
BIO2:BIO14				0.003^{***} (0.00)
BIO6:BIO14		-0.002^{***} (0.00)		
Intercept	21.68^{***} (1.28)	-0.89 (0.87)	-11.34^{***} (2.21)	8.06^{***} (0.68)
N	1,345	920	140	111
LogLik	284.10	51.11	231.99	139.44
BIC	-510.57	-47.62	-424.26	-241.21

BIO2 = Mean Diurnal Range, BIO5 = Max Temp of Warmest month, BIO6 = Min Temperature of Coldest Month, BIO14 = Precipitation of Driest Month

Repeatability and predictability of climate–richness relationships

I tested whether macroecological richness patterns converge in similar environmental conditions by using the 'best' model from each island to predict richness gradients on the other islands. Predictive performance varied across source and target islands (Figure 5-2, Figure 5-3, Table 5-2, Table 5-4). In general, models were unable to predict absolute richness, as most intercepts of the observed–predicted regressions differed noticeably from zero, with the exception of Jamaica predicting to Hispaniola (0.07 ± 2.72), and Puerto Rico predicting to Hispaniola (-1.63 ± 0.77; Table 5-4).

Predictions of richness gradients (based on slope) were variable (Table 5-4, Figure 5-3). Jamaica's best model predicted slopes which did not differ significantly from 1 across all islands (Table 5-4) and, except for Puerto Rico's ftted model, all other slopes differed significantly from 1 (Table 5-4). Predictions between islands were poor when using Cuba's 'best' model to predict to other islands. Predictions for the remaining models either over- or under predicted species richness gradients depending on whether a large island was predicting to a small island (e.g. Cuba predicting to Jamaica or Puerto Rico) or whether a small island was predicting richness on a larger island (e.g. Puerto Rico predicting to Cuba or Hispaniola under-predicts species richness; Figure 5-3). Slopes varied greatly but were rarely close to unity (Figure 5-3). Exceptions to this include fitted model predictions for Hispaniola, Jamaica and Puerto Rico (slopes of 1.39, 1.14 and 0.97, respectively) and Jamaica predicting to Cuba (slope = 1.17 ± 0.33). Precision (which should not be mistaken for accuracy), measured by r^2, varied from 0 to 47%, and rP^2, which

accounts for the fact that even a fitted climate-richness relationship will not have r^2=1.0, ranged from 0 to 100%.

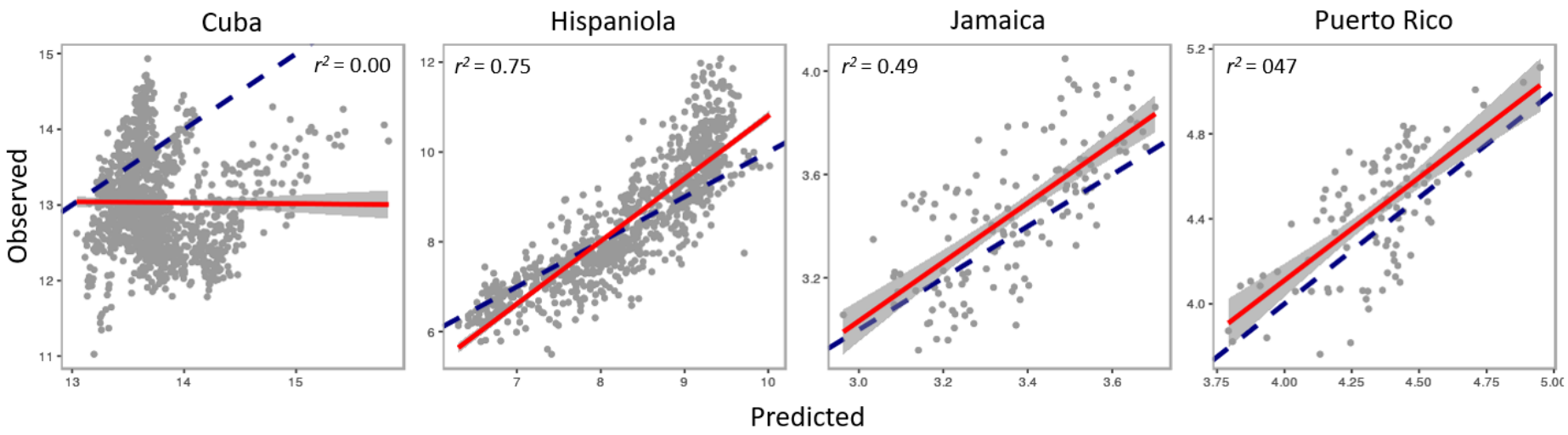


Figure 5-2 Relationships between observed richness and fitted species richness on each island where the fitted values are obtained from the 'best' model for each island (see main text). Blue dashed lines represent a slope of one and intercept of zero, i.e. perfect correlation between fitted and observed species richness.

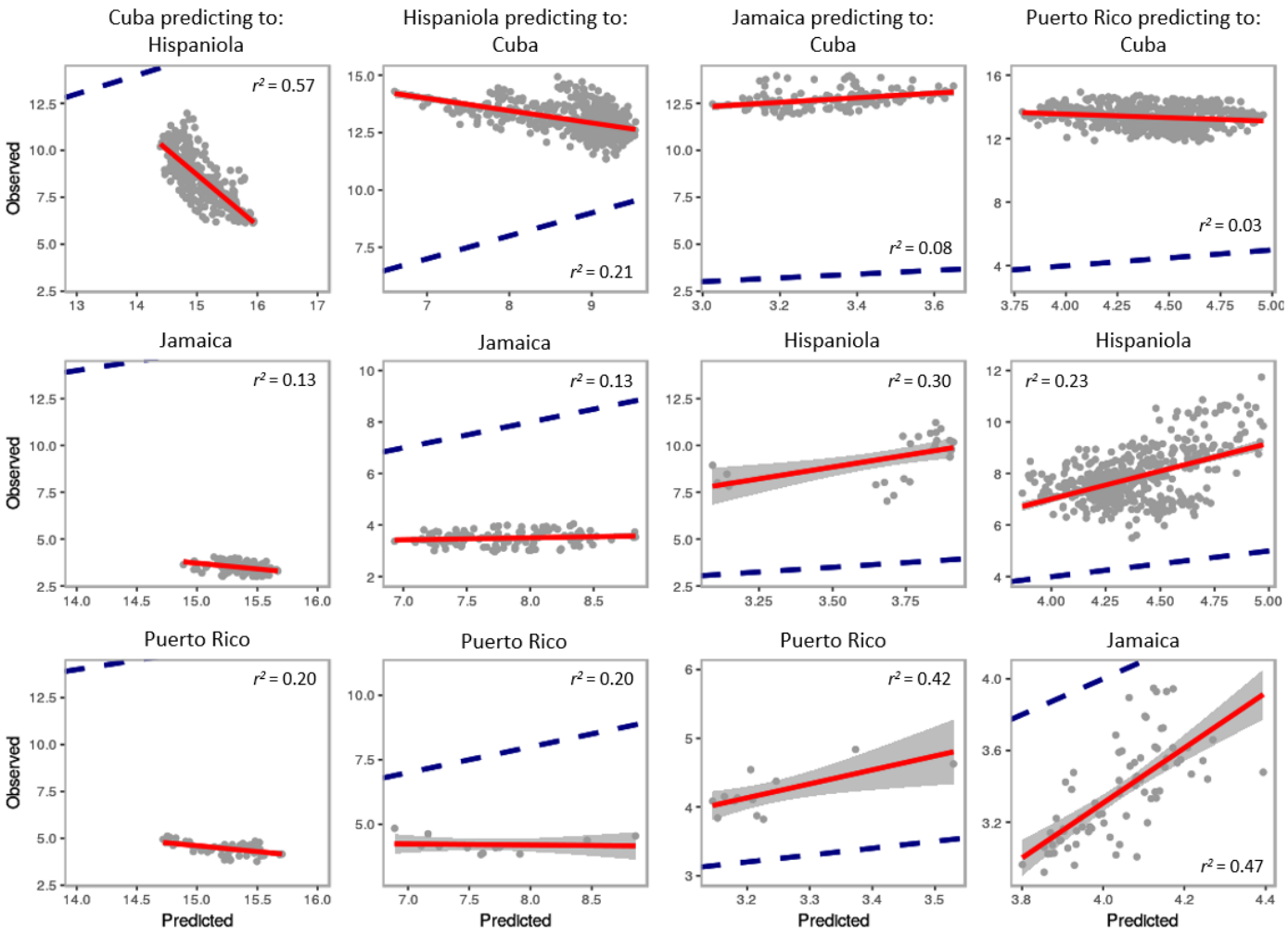


Figure 5-3 Predictions of climate richness relationships on independent islands. The best model for each island was used to predict richness for the other three islands (columns). Red lines are the observed vs. predicted regression line and blue dashed lines represent a slope of one and intercept of zero, i.e. perfect correlation between fitted and observed species richness.

Table 5-4 Summary statistics for model predictions. Relative predictive precision (rP^2) is defined as the ratio of the r^2 of the observed–predicted regression to the observed–fitted r^2 of the 'best' model fitted on the target island. Bold figures indicate slopes which are not significantly different from 1.0. Shaded cells are summary statistics of the observed-predicted (fitted) regressions. Figures in brackets are standard errors.

	Cuba				**Hispaniola**				**Jamaica**				**Puerto Rico**			
	Slope	**Intercept**	***r²***	**rP²**	**Slope**	**Intercept**	***r²***	**rP²**	**Slope**	**Intercept**	***r²***	**rP²**	**Slope**	**Intercept**	***r²***	**rP²**
Cuba	-0.01	12.21	0.00	0.00	-0.53	17.73	0.21	0.28	**1.17**	**8.85**	**0.08**	**0.16**	-0.45	15.34	0.03	0.06
	(0.04)	(0.62)			(0.04)	(0.39)			**(0.33)**	**(1.12)**			(0.10)	(0.45)		
Hispaniola	-2.69	49.12	0.57	0.00	1.39	-3.14	0.75	1.00	**2.51**	**0.07**	**0.30**	**0.61**	2.16	-1.63	0.23	0.49
	(0.14)	(2.12)			(0.02)	(0.22)			**(0.74)**	**(2.72)**			(0.18)	(0.77)		
Jamaica	-0.64	12.30	0.13	0.00	0.08	2.86	0.00	0.00	**1.14**	**-0.39**	**0.49**	**1.00**	1.54	-2.84	0.47	1.00
	(0.15)	(2.30)			(0.06)	(0.44)			**(0.10)**	**(0.33)**			(0.19)	(0.76)		
Puerto Rico	-0.62	13.93	0.20	0.00	-0.04	4.52	-0.09	-0.12	**2.03**	**-2.37**	**0.42**	**0.86**	**0.97**	**0.23**	**0.47**	**1.00**
	(0.16)	(2.51)			(0.18)	(1.39)			**(0.67)**	**(2.18)**			**(0.09)**	**(0.43)**		

5.4 Discussion

Islands provide a valuable opportunity to test macroecological hypotheses by using natural replicates when experimental manipulation and replication are impossible (Blackburn, 2004; Gaston and Blackburn, 1999). In evolutionary biology for example, islands have played a key role in testing the predictability of natural selection (Losos, 2009; Rundle et al., 2000). Although macroecologists, like macroevolutionary biologists, are usually unable to perform large-scale manipulative experiments, macroecology has not exploited islands as replicated natural experiments to the same extent (but see Wollenberg et al. 2014 and Muñoz et al. 2014 for examples with morphological traits). Here, I constructed the first maps of how *Anolis* species richness varies within large Caribbean islands and tested for convergence (i.e. the repeatability and predictability) of climate–richness relationships among islands. Although Greater Antillean anoles are an iconic example of convergent evolution (Losos, 2009), I found that this evolutionary predictability does not extend to macroecological richness gradients. Although richness varied geographically within each island, this variation was island-specific and not predictable using models from other islands, indicating a lack of macroecological convergence of climate–richness relationships.

When estimating species richness from occurrence points and distribution models, a key consideration is whether modelled richness is accurate. Published field-collected data on complete anole communities are surprisingly few given the long history of study of this clade. However, I did find records

of field-observed sympatric richness from three different localities on Cuba: Soroa (11 species; Schettino et al. 2010), Meseta de Cabo Cruz, Granma (15 species; Diaz et al. 1998), and La Tabla, Santiago de Cuba (14 species; Garrido). My models predict similar, but slightly lower, species richness values at these localities: 13.84 (s.d.±0.44) at Soroa, 12.69 (s.d±0.21) at Meseta de Cabo Cruz, and 12.51 (s.d. ±0.12) at La Tabla (see Figure 4-5 in supporting information). These field observations are qualitaitvely in line with my estimates (see Figure 4-5 in supporting information), but suggest my maps may underestimate richness, at least on Cuba. On Hispaniola, a recent investigation of anole communities along elevational gradients (Frishkoff et al., 2019) provided detailed plot-level species richness estimates in the south east of the island which I used to ground-truth my predictions. Using my estimate of species richness on the island (Figure 5-3), I found that mean species richness across the plot localities in Frishkoff et al. (2019) was 8.00 ± 0.97 (n=55). The greatest observed plot-level richness was 7 species (Fig 2a in Frishkoff et al. 2019), indicating that, at least in this part of the island, my richness estimates are reasonably accurate.

The strength of climate–richness gradients varied greatly across islands. Leaving Cuba aside for now, where richness was unrelated to climate, pseudo-r^2 values for the other three islands ranged from 0.47 (Puerto Rico) to 0.75 (Hispaniola). With the exception of Hispaniola, these relationships are weaker than those often observed at broader geographical extents, especially for continental and global gradients (Field et al., 2009; Hawkins et al., 2003). The strength of climate-richness relationships is known to decline with decreasing spatial extent and grain (Field et al., 2009), so the relationships viewed here

are not out of line with previous work as, despite being large for islands, the Greater Antilles are still much smaller than continents. Within the Greater Antilles, island size seems to mediate the strength of within-island climate-richness gradients to some extent. Hispaniola, the largest island, has the strongest relationship while the two small islands (Jamaica and Puerto Rico) both have weaker yet similar-strength relationships. Previous work has shown that repeated lineages of *Anolis* lizards across the Greater Antilles have consistently adapted and evolved to the climatic space within each island (Velasco et al., 2018, 2016), suggesting that I should expect to observe repeated within-island relationships between climate and richness, as I see here.

Cuba – the largest island – displays no relationship between climate and richness; three main factors could be responsible for this result. First, and despite its size, Cuba has the most spatially homogeneous climate conditions of the four Greater Antillean islands (Algar and Mahler, 2016). The lack of climate heterogeneity on Cuba may explain why I found no relationship between climate and species richness. Second, Cuba is the least-sampled island in relation to its size. Given my data, I was only able to parameterise models for 27 of the 60+ species known to occur on the island (Losos, 2009; Schwartz and Henderson, 1991) meaning that I am missing more than half of all species on the island. In addition, Cuba has the smallest median number of occurrence records per species of 5.5 (Hispaniola = 25, Jamaica = 103.5, Puerto Rico = 22.5). In comparison, I modelled all 6 species known to occur on Jamaica and 90% of all species on Puerto Rico. It is possible that with more complete sampling of the anole fauna on Cuba I may have uncovered a

stronger climate-richness relationship. Finally, Cuba is home to many species of “unique” anole (that do not fall into the traditional ecomorph ‘classification’ system) which may not respond to climate in the manner congeners do. For example, water-dwelling, cave-dwelling and rock wall-dwelling species all exist here (see Losos 2009) and could display idiosyncratic responses to climate as little is known of the natural history of many of the unique species on Cuba (Losos, 2009). Even with better sampling, it is possible that climate is generally unimportant in regulating species richness across Cuba.

If the effects of environmental drivers on ecological patterns reflect deterministic, general, processes then models trained in one system should successfully predict richness using new, independent, data (Houlahan et al., 2017). That is, climate–richness models fitted on one island should successfully predict species richness on the other three islands, especially if climate sets a cap on the number of species that can co-occur (e.g. H-Acevedo and Currie 2003). Instead, I found that models were unable to predict absolute species richness on any island, as indicated by non-zero intercepts of the observed–predicted regressions. Specifically, the two larger islands, Cuba and Hispaniola, over-predicted richness on the smaller islands of Jamaica and Puerto Rico, while the smaller islands under-predicted richness on the larger ones. This is perhaps unsurprising given that larger islands contain many more species than smaller ones i.e. they have greater γ-diversity (Losos and Schluter, 2000; Matthews et al., 2016). The lower richness in 10x10km squares (α-diversity) on Puerto Rico and Jamaica must, in part, reflect a limitation of supply as these entire islands have fewer species than are known

to coexist in sympatry at a single site in Cuba (Schettino et al., 2010). However, an increase in species richness at a local scale (α-diversity) is not a necessary consequence of an increase in total island richness (γ-diversity). Given the inextricable link between α-, β-, and γ-diversity (Ulrich et al. 2017), the higher γ-diversity of larger islands could manifest as higher β-diversity, or species turnover, between sites without higher α-diversity. However this was not the case: α-diversity was higher on larger islands, a pattern also observed by Wilson (1961) for Melanesian ant faunas.

My results suggest that there is an interaction between cladogenesis, ecological radiation and local community dynamics, leading to increases in local community richness and γ-diversity on larger islands. This increased supply of potential species on large, topographically complex islands may increase competition (Wilson, 1961), forcing species to exploit new areas of niche space or more finely divide existing resources, leading to ecological radiation (Gavrilets and Vose, 2005; Rundle et al., 2000; Schluter, 1996) and increased coexistence at local scales. Anoles have diversified into distinct ecomorphs to partition arboreal niche space (Losos, 2009; Mahler et al., 2013; Williams, 1972) and most of these ecomorphs are found almost ubiquitously across all four Greater Antillean islands (Wollenberg et al., 2014). However, complete sets of ecomorphs are only found on the larger islands of Hispaniola and Cuba. Trunk anoles are lacking from Jamaica and Puerto Rico and grass-bush anoles from Jamaica (Losos, 2009). Within ecomorphs, coexisting species also differ in size and/or thermal preferences (Schoener, 1970) which may permit increased α-diversity via resource partitioning on larger islands with multiple species in the same ecomorph. Larger islands may also have

unique portions of niche space that are not present on smaller, less complex islands. For example, there are multiple species of 'unique' anoles that fall outside the traditional ecomorph classification, including semi-aquatic species (Leal et al., 2002), chameleon mimics (Losos, 2009) and a cave-dwelling species, *Anolis lucius* (Williams and Hecht, 1955). These unique species are concentrated on the larger islands: Cuba has 14, while Puerto Rico has none (Mahler et al., 2013). These unique types may be more likely to arise on larger islands because they harbour unique combinations of resources and/or because higher population sizes on larger islands may increase sampling of potential mutation space, increasing the likelihood that a unique, yet advantageous, trait may arise (Jasmin and Kassen, 2007; Stevens et al., 2007).

I uncovered little evidence for the convergence of climate-richness gradients across the Greater Antilles, as indicated by observed–predicted slopes which often differed substantially from unity. Across the four islands, richness responded differently to environmental gradients. The only comparison where both slope and intercept were remotely similar to zero and unity, respectively, was for Puerto Rico's prediction of Jamaican richness. Both islands are of similar size and γ-diversity, which likely aided the accuracy and precision of prediction (which was still was not especially high). One possibility which explains prediction failure to large islands is that richness is more predictable on smaller islands for reasons other than the influence of climate. Processes that may affect species richness, but are not necessarily related to climate, like biotic interactions, may be weaker on smaller islands than on larger ones, where greater species richness increases the strength of biotic interactions. For example, Algar et al. (2013) found that one third of Hispaniolan species in

their study were less likely to occur in climatically suitable areas if a morphologically similar species was already present. This suggests an effect of competition on species co-occurrence which could alter climate–richness relationships. Additional evidence on the effects of biotic interactions and their influence on local community assembly across these islands is needed to test this hypothesis.

The lack of convergence in species richness gradients across the four independent radiations of Greater Antillean anoles stands in contrast to two recent studies that found cross-island convergence of geographical trait patterns in these anole faunas. Muñoz et al. (2014) found that different processes generated similar body size declines with increasing elevation in Cuban and Hispaniolan trunk-ground anoles. In a broader analysis, Wollenberg et al. (2014) found convergence of the geographical distribution of anole ecomorphs across the four islands, with a similar decline in body size at higher elevations as that found by Muñoz et al. (2014). Together, these results suggest that geographical relationships between environment and traits known to influence ecological interactions are more predictable than species richness. This makes sense since species richness contains little direct ecological information while traits determine the outcome of interactions between individual organisms and their biotic and abiotic environments (Dawson et al., 2013; McGill et al., 2006).

Overall, my results suggest that, at least within individual islands, climate is a reasonably important factor in shaping patterns of *Anolis* species richness (with the exception of Cuba where climate explained none of the variation in species richness). Despite the reasonably strong within-island relationships

between climate and species richness, when predicting across islands, patterns became idiosyncratic and were neither repeatable or predictable. Size differences between islands and the greater number of “unique” anole species found exclusively on the larger islands likely prevent climate-only models from accurately prediting species richness across islands. A larger sample of size-matched islands would be necessary to test the overall prevalence of climate-richness gradients across multiple large islands.

5.5 Supporting Information

Table 5-5 Summary AUC statistics for MaxEnt species distribution models across Cuba, Hispaniola, Jamaica and Puerto Rico. AUC = Area Under the Receiver Operating Characteristic (ROC) Curve.

Island	**N**	**Mean AUC (±s.d.)**	**Median AUC**	**AUC Range**
Cuba	27	0.88 (0.10)	0.92	0.60 – 0.99
Hispaniola	33	0.91 (0.09)	0.93	0.63 – 0.99
Jamaica	6	0.70 (0.12)	0.66	0.63 – 0.95
Puerto Rico	9	0.75 (0.12)	0.70	0.60 – 0.95

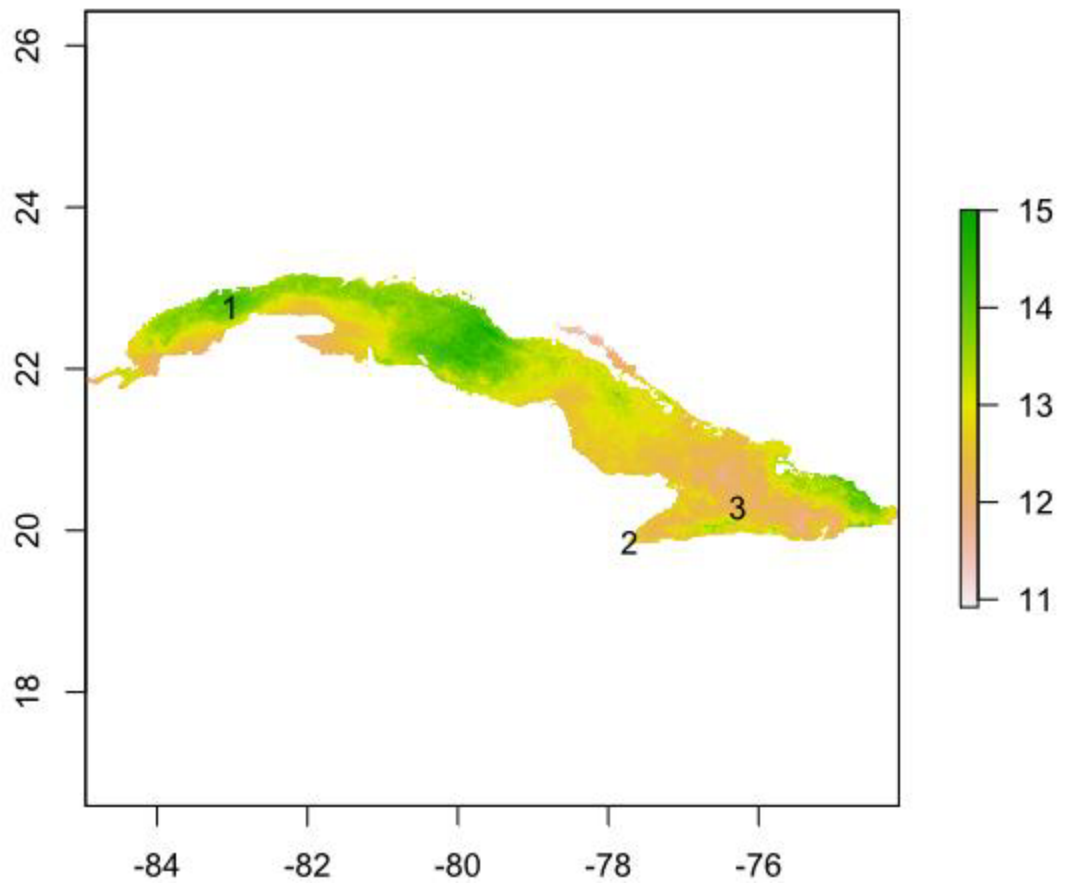


Figure 5-4 Estimated species richness on Cuba. Numbers represent approximate locations of published field observations of sympatric *Anolis* species richness on the island. (1) Soroa; predicted species richness 13.84 (SD ± 0.44). Rodríguez-Schettino et al. (2010) sympatric richness 11 species. (2) Meseta de Cabo Cruz, Granma; predicted species richness 12.69 (SD ± 0.21). Diaz et al. (1998) sympatric richness 15 species (3) La Tabla, Santiago de Cuba; predicted species richness 12.51 (SD ± 0.12) Garrido and Hedges (2001) sympatric richness 14 species. I estimated mean species richness for each location by querying 10 points within the immediate vicinity of each published location above.

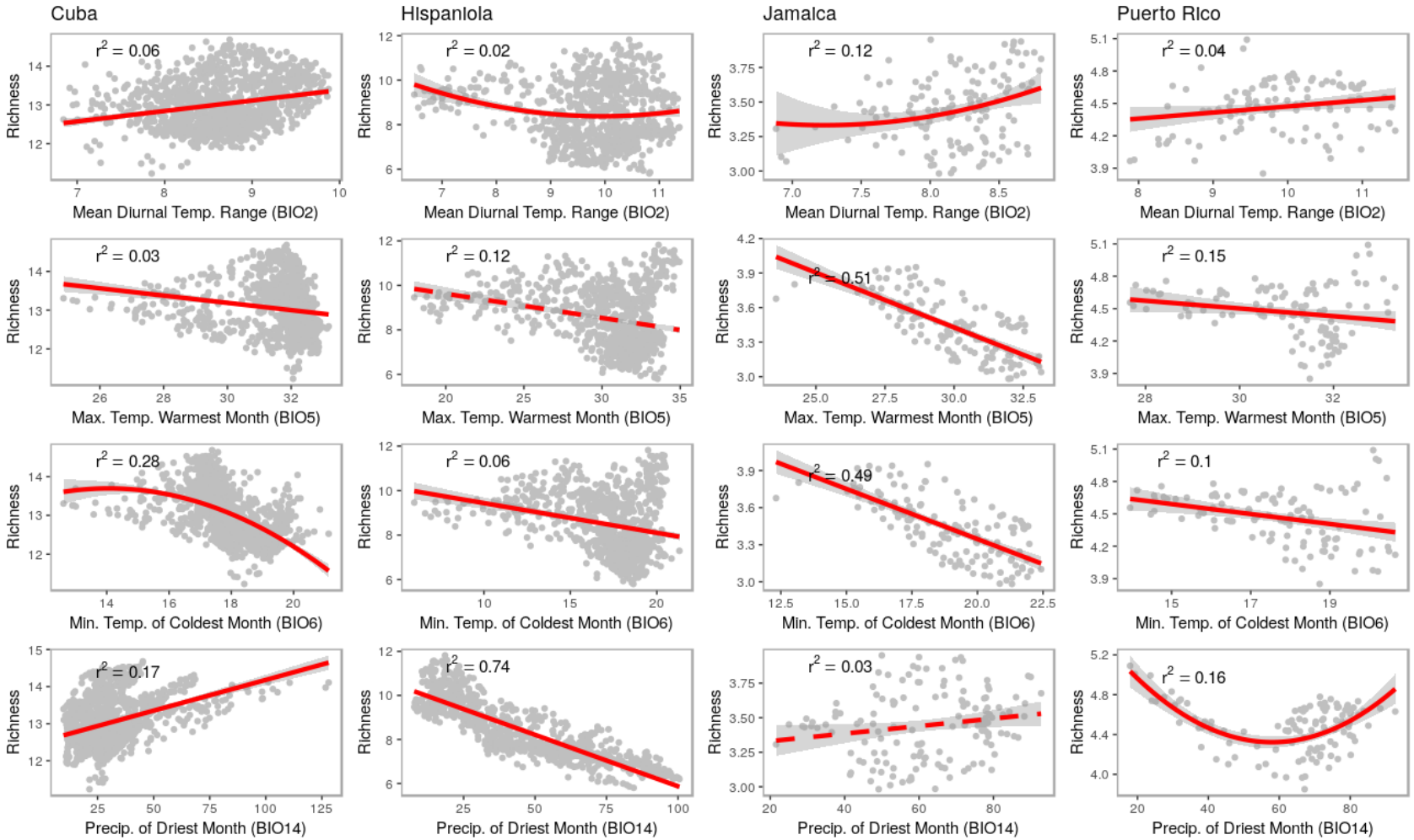


Figure 5-5 Relationships between species richness and climate on each island of the Caribbean. Relationships included in the 'best' model for an island are shown with solid red lines and relationships not included in the 'best' model are shown with dashed red lines. Quadratic relationships are used where the 'best' model for each island included a quadratic term. Each column is an island and each row represents a bioclimatic variable.

Chapter 6: General conclusions and future directions

Understanding the factors which delimit species' ranges and distributions is a long-standing goal in ecology and modelling them accurately is both complex and challenging. Range limits reflect several interacting processes including an individual's physiological response to abiotic conditions, biotic interactions and species' dispersal capabilities across geographic space (Soberón and Nakamura, 2009). This complexity is compounded further under rapid anthropogenic climate change which is predicted to affect all of these processes simultaneously (Chen et al., 2011; Elith et al., 2010; Gilman et al., 2010; Parmesan and Yohe, 2003; Pecl et al., 2017; Sinervo et al., 2010; Sunday et al., 2014, 2010; Urban, 2015; Urban et al., 2013; Wisz et al., 2013). As a discipline, ecology requires robust theory and methods to answer long-standing questions central to the field including the role of climate and biotic interactions in delimiting species ranges and the repeatability and predictability of macroecological patterns to solidify our understanding of causal mechanisms. As a society, we require—now more than ever—robust theory and methods to predict species' distributions in the face of ongoing climate change, land use degradation and human-mediated dispersal of species across the planet.

Appropriate methods tuned to the research question at hand are key to generating more robust predictions of species' ranges. There is no 'one size fits all' approach to modelling species' distributions because different models ultimately have different strengths, weaknesses and quantify different aspects

of a species' niche. With this in mind, I used both correlative and mechanistic species distribution models to address three long-standing questions in the field of ecology:

> **(1)** How does climate alter the spatial distribution of ectotherm activity budgets through time and space?
>
> **(2)** What are the relative contributions of biotic interactions, dispersal and availability of preferred habitat type in limiting species' ranges through geographic space?
>
> (3) Does climate generate repeatable and predictable patterns of biodiversity?

In **Chapter 3**, I used mechanistic distribution modelling to quantify animal activity budgets through time and space to better understand how climate shapes 'time for life' across the globe. I found that prior to the start of the industrial revolution and the onset of mass anthropogenic greenhouse gas emissions, animal activity budgets remained remarkably consistent through time and space. After the industrial revolution and toward the present day, warming has increased the duration of favourable conditions across much of the globe. However, predictions of the effects of future warming on tropical animal activity budget post industrial revolution are dire; the time available to ecothermic organisms is predicted to decline substantially. The high spatial discordance between where most of the planet's biodiversity resides and where conditions are becoming increasing more hostile is a worrying finding. Without substantial mitigation—whether through acclimation, adaption or dispersal—fitness is likely to decline into the future in highly diverse regions

of the globe, ultimately resulting in range contractions and possible extinctions.

Correlative models (e.g. Maxent) are unsuitable for predicting past and future responses to climate as extrapolation violates many of the assumptions of correlative models, potentially generating unreliable predictions (Elith et al., 2010; Fitzpatrick and Hargrove, 2009; Maguire et al., 2015; Urban, 2015; Urban et al., 2013; Veloz et al., 2012). Mechanistic models, however, avoid extrapolation by quantifying suitability from first principles, making them more robust for hind- and forecasting species' response to climate through time (Kearney and Porter, 2009, 2004). Although mechanistic models are more robust than correlative models when fore- and hindcasting species responses to climatic (abiotic) conditions, they are no panacea. Key factors known to limit animal distributions—including the effects of biotic interactions and dispersal—are hard to integrate into such models (but see Lischke et al. 2006, Scheiter and Higgins 2009, Hartig et al. 2012 for mechanistic models accounting for dispersal in plants). This difficulty, however, must not become a permanent barrier; integrating these processes into mechnastic models should be considered a research priority going forward. Increasing empirical evidence shows that climate change is altering the composition of communities across the globe, generating novel assemblages of species and interactions (Gilman et al., 2010; Wisz et al., 2013). Failing to account for processes such as ecological release from native competitors or competition from potentially well-adapted, incumbent, species will ultimately result in less robust preditions of species ranges into the future.

Another avenue of potentially fruitful research would be to investigate whether animals shift the time of day when they are active to mitigate the effects of climate change. In response to increasing temperatures, it is possible that animals may become active at earlier or later times of the day to avoid the highest daytime temperatures. For example, previously diurnal species could shift toward crepuscular or even nocturnal activity patterns. At present, there has been very little research into how climate may change ectotherm behavioural responses across the course of a day (but see Levy et al. 2019 for a discussion on endotherm diel cycles) and thorough investigation of this aspect of climate change may yield very interesting results.

In **Chapter 4** I used mechanistic and correlative niche models to map areas of distributional debt (i.e. where species fail to fill their fundamental niches) for *Anolis* lizards on Puerto Rico. I then tested whether dispersal limitation, access to preferred habitat type or biotic interactions can explain mismatches between realized and fundamental niches across geographic space. I uncovered substantial areas of distributional debt for 5 out of 8 species studied but which could not be explained by biotic interactions, dispersal limitation or access to preferred habitat type. Instead, it is possible that highly localised processes such as resource, structural or thermal niche partitioning between species promotes co-existence of *Anolis* lizards across the island.

The framework I presented here was an effort to quantify multiple processes that are theorised to act upon species to delimit their ranges across geographic space, while also contributing toward alleviating the current methodological shortfalls associated with modelling biotic interactions (Anderson, 2017). Although I found that fine-scaled resource partitioning may facilitate species

co-existance when considering the anole fauna of Puerto Rico, this methodological framework could still be tested in other scenarios in the future. For example, this method could be applied to larger terrestrial organisms who may be incapable of physically partitioning niche space at such fine spatial scales to determine whether the predicted negative correltations between morphological similarity and magnitude of distributional debt manifest at macroecological scales.

Although the combined data requirements for all aspects of the framework are high, they reflect the complex nature of species' distributions and biotic interactions. The paucity of data for many taxa should not automatically be considered a barrier to modelling; rather, increased effort should be placed on gathering the required morphological and behavioural data either by detailed literature searches or via fieldwork. I found that a surprising amount of physiological and morphological data were available in the literature with a concerted effort to find it. For species where data is truly absent, allometric equations could be considered to fill in the gaps, while acknowledging that this will introduce extra error into modelled distributions. I would encourage future researchers to apply this framework to their study systems and would be excited to see whether this approach can be considered a general method to quantify biotic interactions across large geographical extents.

In **Chapter 5** I used correlative SDMs to test for the repeatability and predictability of macroecological patterns within and across large islands. Specifically, I investigated whether climate generates repeatable patterns of species richness within and across islands. Islands are ideal 'natural laboratories' which provide an opportunity to test predictions when replicated,

controlled, experiments are impossible, as is often the case in biogeography and macroecology. I found that within individual islands (except Cuba), climate is an important factor in shaping patterns of *Anolis* species richness. When predicting across islands, however, models were unable to accurately predict species richness. Despite the anole fauna of the Greater Antilles being a classic example of adaptive radiation and subsequent convergent evolution, I found that the convergence of macroecological patterns such as climate-richness gradients are not guaranteed.

I identify two main areas of research to explore further given the results of this chapter. First, it would be valuable to extend the study to other islands across the world. The present study was limited to the largest islands of the Antilles as only these islands contained a sufficiently large anole fauna to test for within-island climate-richness gradient. The smaller islands of the Lesser Antilles often only contain one or two species of anole, limiting the maximum island sample size in this study. Extending this study to other, size-matched, islands across the world would both increase the sample size and allow for a more robust test of the convergence of climate-richness gradients across large islands. Second, targeted fieldwork is necessary to ground-truth predicted richness at key locations across the study extent. In particular, Cuba is relatively undersampled compared to the other islands and the lack of association between climate and richness on Cuba could be one of sample size, rather than a lack of relationship between climate and species richness. Ground truthing along elevational gradients would also be beneficial to test the robustness of models across complex topographical landscapes.

The field of species' distribution modelling has advanced considerably over the past 20 years, facilitating a fantastic amount of useful—and very interesting—research. With the recent arrival of mechanistic distribution models to complement correlative models, ecologists can now quantify all aspects of a species' niche. Over the next few years I forsee an increased use of correlative and mechanistic models in tandem to leverage the strengths of both approaches. While a unified species distribution model which could account for all factors and processes describing a species' distribution would be an exceptionally powerful tool, I think the reality of using and integrating a range of specialist models—designed to quantify different aspect of a species niche—is the most practical and effective way to predict ranges moving forward.

Finally, I caution the macroecological community against the use of correlative SDMs when the focus is to hind– or forecast species distributions through time. This point is particularly important in the context of climate change and conservation management where robust predictive models are essential to sway skeptics, inform meaningful policy and enact change to protect the natural world. The use of models applied in the wrong context could ultimately result in doing more harm than good if future predictions are found to be inaccurate. Although, as I have shown here, climate change will likely be highly detrimental to ectothermic species over the next 80 years, it is nonetheless an exciting time to be working in the field of species distribution modelling.

References

Abouheif, E., Fairbairn, D., 1997. A comparative analysis of allometry for sexual size dimorphism: assessing Rensch's rule. The American Naturalist 149, 540–562.

Aiello-Lammens, M.E., Boria, R.A., Radosavljevic, A., Vilela, B., Anderson, R.P., 2015. spThin: An R package for spatial thinning of species occurrence records for use in ecological niche models. Ecography 38, 541–545.

Algar, A.C., Kharouba, H.M., Young, E.R., Kerr, J.T., 2009. Predicting the future of species diversity: macroecological theory, climate change, and direct tests of alternative forecasting methods. Ecography 32, 22–33.

Algar, A.C., López-Darias, M., 2016. Sex-specific responses of phenotypic diversity to environmental variation. Ecography 39, 715–725.

Algar, A.C., Losos, J.B., 2011. Evolutionary assembly of island faunas reverses the classic island–mainland richness difference in *Anolis* lizards. Journal of Biogeography 38, 1125–1137.

Algar, A.C., Mahler, D.L., 2016. Area, climate heterogeneity, and the response of climate niches to ecological opportunity in island radiations of *Anolis* lizards. Global Ecology and Biogeography 25, 781–791.

Algar, A.C., Mahler, D.L., Glor, R.E., Losos, J.B., 2013. Niche incumbency, dispersal limitation and climate shape geographical distributions in a species-rich island adaptive radiation: Geographical distributions of *Anolis* lizards. Global Ecology and Biogeography 22, 391–402.

Algar, A.C., Morley, K., Boyd, D.S., 2018. Remote sensing restores predictability of ectotherm body temperature in the world's forests. Global Ecology and Biogeography 27, 1412–1425.

Allouche, O., Steinitz, O., Rotem, D., Rosenfeld, A., Kadmon, R., 2008. Incorporating distance constraints into species distribution models. Journal of Applied Ecology 45, 599–609.

Anderson, R.P., 2017. When and how should biotic interactions be considered in models of species niches and distributions? Journal of Biogeography 44, 8–17.

Angilletta, M.J., 2009. Thermal adaptation: a theoretical and empirical synthesis. Oxford University Press, New York.

Araújo, C.B. de, Marcondes-Machado, L.O., Costa, G.C., 2014. The importance of biotic interactions in species distribution models: a test of the Eltonian noise hypothesis using parrots. Journal of Biogeography 41, 513–523.

Araújo, M.B., Ferri-Yáñez, F., Bozinovic, F., Marquet, P.A., Valladares, F., Chown, S.L., 2013. Heat freezes niche evolution. Ecology Letters 16, 1206–1219.

Araújo, M.B., Thuiller, W., Pearson, R.G., 2006. Climate warming and the decline of amphibians and reptiles in Europe. Journal of Biogeography 33, 1712–1728.

Ashton, K.G., Feldman, C.R., 2003. Bergmann's rule in nonavian reptiles: turtles follow it, lizards and snakes reverse it. Evolution 57, 1151–1163.

Barve, N., Barve, V., Jiménez-Valverde, A., Lira-Noriega, A., Maher, S.P., Peterson, A.T., Soberón, J., Villalobos, F., 2011. The crucial role of the accessible area in ecological niche modeling and species distribution modeling. Ecological Modelling 222, 1810–1819.

Bennett, J.M., Calosi, P., Clusella-Trullas, S., Martínez, B., Sunday, J., Algar, A.C., Araújo, M.B., Hawkins, B.A., Keith, S., Kühn, I., Rahbek, C., Rodríguez, L., Singer, A., Villalobos, F., Ángel Olalla-Tárraga, M., Morales-Castilla, I., 2018. GlobTherm, a global database on thermal tolerances for aquatic and terrestrial organisms. Scientific Data 5, 180022.

Berry, J.F., Shine, R., 1980. Sexual size dimorphism and sexual selection in turtles (Order Testudines). Oecologia 44, 185–191.

Beuchat, C.A., 1986. Reproductive influences on the thermoregulatory behavior of a live-bearing lizard. Copeia 1986, 971–979.

Blackburn, T.M., 2004. Method in macroecology. Basic and Applied Ecology 5, 401–412.

Blanckenhorn, W.U., Stillwell, R.C., Young, K.A., Fox, C.W., Ashton, K.G., 2006. When Rensch meets Bergmann: does sexual size dimorphism change systematically with latitude? Evolution 60, 2004–2011.

Blois, J.L., Zarnetske, P.L., Fitzpatrick, M.C., Finnegan, S., 2013. Climate Change and the Past, Present, and Future of Biotic Interactions. Science 341, 499–504.

Blouin-Demers, G., Nadeau, P., 2005. The Cost-Benefit Model of Thermoregulation Does Not Predict Lizard Thermoregulatory Behavior. Ecology 86, 560–566.

Bonebrake, T.C., Deutsch, C.A., 2012. Climate heterogeneity modulates impact of warming on tropical insects. Ecology 93, 449–455.

Borregaard, M.K., Matthews, T.J., Whittaker, R.J., 2016. The general dynamic model: towards a unified theory of island biogeography? Global Ecology and Biogeography 25, 805–816.

Boucher-Lalonde, V., Kerr, J.T., Currie, D.J., 2014. Does climate limit species richness by limiting individual species' ranges? Proceedings of the Royal Society B: Biological Sciences 281.

Breshears, D.D., Cobb, N.S., Rich, P.M., Price, K.P., Allen, C.D., Balice, R.G., Romme, W.H., Kastens, J.H., Floyd, M.L., Belnap, J., Anderson, J.J., Myers, O.B., Meyer, C.W., 2005. Regional vegetation die-off in response to global-change-type drought. PNAS 102, 15144–15148.

Bruno, J.F., Stachowicz, J.J., Bertness, M.D., 2003. Inclusion of facilitation into ecological theory. Trends in Ecology & Evolution 18, 119–125.

Buckley, L.B., Hurlbert, A.H., Jetz, W., 2012. Broad-scale ecological implications of ectothermy and endothermy in changing environments. Global Ecology and Biogeography 21, 873–885.

Buckley, L.B., Jetz, W., 2007. Environmental and historical constraints on global patterns of amphibian richness. Proc Biol Sci 274, 1167–1173.

Buckley, L.B., Kingsolver, J.G., 2012. The demographic impacts of shifts in climate means and extremes on alpine butterflies: Alpine butterfly demography. Functional Ecology 26, 969–977.

Bugmann, H., 2001. A Review of Forest Gap Models. Climatic Change 51, 259–305.

Bulleri, F., Bruno, J.F., Silliman, B.R., Stachowicz, J.J., 2016. Facilitation and the niche: implications for coexistence, range shifts and ecosystem functioning. Functional Ecology 30, 70–78.

Butler, Losos, J.B., 2002. Multivariate sexual dimorphism, sexual selection, and adaptation in Greater Antillean Anolis lizards. Ecological Monographs 72, 541–559.

Butler, M.A., Schoener, T.W., Losos, J.B., 2000. The relationship between sexual size dimorphism and habitat use in Greater Antillean *Anolis* lizards. Evolution 54, 259–272.

Cabral, J.S., Weigelt, P., Kissling, W.D., Kreft, H., 2014. Biogeographic, climatic and spatial drivers differentially affect α-, β- and γ-diversities on oceanic archipelagos. Proc Biol Sci 281.

Calabrese, J.M., Certain, G., Kraan, C., Dormann, C.F., 2014. Stacking species distribution models and adjusting bias by linking them to macroecological models. Global Ecology and Biogeography 23, 99–112.

Campbell, J.A., Frost, D.R., 2016. A new species of *Abronia* (Squamata: Anguidae) from the Sierra Madre del Sur of Oaxaca, Mexico. Journal of Herpetology 50, 149–156.

Cardillo, M., 2002. The life-history basis of latitudinal diversity gradients: how do species traits vary from the poles to the equator? Journal of Animal Ecology 71, 79–87.

Chase, J.M., Leibold, M.A., 2003. Ecological Niches: Linking classical and contemporary approaches. University of Chicago Press.

Chen, I.-C., Hill, J.K., Ohlemüller, R., Roy, D.B., Thomas, C.D., 2011. Rapid Range Shifts of Species Associated with High Levels of Climate Warming. Science 333, 1024–1026.

Chown, S.L., Marais, E., Terblanche, J.S., Klok, C.J., Lighton, J.R.B., Blackburn, T.M., 2007. Scaling of insect metabolic rate is inconsistent with the nutrient supply network model. Functional Ecology 21, 282–290.

Chown, S.L., Sørensen, J.G., Terblanche, J.S., 2011. Water loss in insects: An environmental change perspective. Journal of Insect Physiology, “Cold and Desiccation Tolerance” honoring Karl Erik Zachariassen 57, 1070–1084.

Clusella-Trullas, S., Blackburn, T.M., Chown, S.L., 2011. Climatic predictors of temperature performance curve parameters in ectotherms imply complex responses to climate change. Am. Nat. 177, 738–751.

Cooney, C.R., Seddon, N., Tobias, J.A., 2016. Widespread correlations between climatic niche evolution and species diversification in birds. J Anim Ecol 85, 869–878.

Cooper, N., Freckleton, R.P., Jetz, W., 2011. Phylogenetic conservatism of environmental niches in mammals. Proc Biol Sci 278, 2384–2391.

Cox, R.M., Butler, M.A., John-Alder, H.B., 2007. The evolution of sexual size dimorphism in reptiles. In: Fairbairn, D.J., Blanckenhorn, W.U., Szekely, T. (Eds.), Sex, Size and Gender Roles: Evolutionary Studies of Sexual Size Dimorphism. Oxford University Press, Oxford, pp. 38–49.

Cox, R.M., Skelly, S.L., John-Alder, H.B., 2003. A comparative test of adaptive hypotheses for sexual size dimorphism in lizards. Evolution 57, 1653–1669.

Cruz, F.B., Fitzgerald, L.A., Espinoza, R.E., Schulte, J.A., 2005. The importance of phylogenetic scale in tests of Bergmann’s and Rapoport’s rules: lessons from a clade of South American lizards. Journal of Evolutionary Biology 18, 1559–1574.

Currie, D.J., 1991. Energy and large-scale patterns of animal-species and plant-species richness. The American Naturalist 137, 27–49.

Davies, G.M., Gray, A., 2015. Don’t let spurious accusations of pseudoreplication limit our ability to learn from natural experiments (and other messy kinds of ecological monitoring). Ecology and Evolution 5, 5295–5304.

Dawson, M.N., Algar, A.C., Antonelli, A., Dávalos, L.M., Davis, E., Early, R., Guisan, A., Jansson, R., Lessard, J.-P., Marske, K.A., McGuire, J.L.,

Stigall, A.L., Swenson, N.G., Zimmermann, N.E., Gavin, D.G., 2013. An horizon scan of biogeography. Front Biogeogr 5.

Dayan, T., Simberloff, D., 2005. Ecological and community-wide character displacement: the next generation. Ecology Letters 8, 875–894.

De Lisle, S.P., Rowe, L., 2015. Independent evolution of the sexes promotes amphibian diversification. Proceedings of the Royal Society B: Biological Sciences 282, 20142213.

Deutsch, C.A., Tewksbury, J.J., Huey, R.B., Sheldon, K.S., Ghalambor, C.K., Haak, D.C., Martin, P.R., 2008. Impacts of climate warming on terrestrial ectotherms across latitude. PNAS 105, 6668–6672.

Diamond, J., 1986. Overview: Laboratory experiments, field experiments, and natural experiments. In: Diamond, J., Case, T.J. (Eds.), Community Ecology. Harper & Row, New York., pp. 3–22.

Diamond, S.E., Sorger, D.M., Hulcr, J., Pelini, S.L., Toro, I.D., Hirsch, C., Oberg, E., Dunn, R.R., 2012. Who likes it hot? A global analysis of the climatic, ecological, and evolutionary determinants of warming tolerance in ants. Global Change Biology 18, 448–456.

Diaz, L.M., M.N., N., Garrido, O.H., 1998. Nueva especie de Chamaeleolis (Sauria: Iguanidae) de la Meseta de Cabo Cruz, Granma, Cuba. Avicennia 8/9, 27–34.

Díaz-Cárdenas, B., Ruiz-Sanchez, E., Castro-Felix, P., Castañeda-Gaytán, G., Ruiz-Santana, S., Gadsden, H., 2017. Species delimitation of the blue-spotted spiny lizard within a multilocus, multispecies coalescent framework, results in the recognition of a new *Sceloporus* species. Molecular Phylogenetics and Evolution 111, 185–195.

Diffenbaugh, N.S., Field, C.B., 2013. Changes in Ecologically Critical Terrestrial Climate Conditions. Science 341, 486–492.

Elith, J., Graham*, C.H., Anderson, R.P., Dudík, M., Ferrier, S., Guisan, A., Hijmans, R.J., Huettmann, F., Leathwick, J.R., Lehmann, A., Li, J., Lohmann, L.G., Loiselle, B.A., Manion, G., Moritz, C., Nakamura, M., Nakazawa, Y., Overton, J.M.M., Peterson, A.T., Phillips, S.J., Richardson, K., Scachetti-Pereira, R., Schapire, R.E., Soberón, J., Williams, S., Wisz, M.S., Zimmermann, N.E., 2006. Novel methods

improve prediction of species' distributions from occurrence data. Ecography 29, 129–151.

Elith, J., Kearney, M., Phillips, S., 2010. The art of modelling range-shifting species. Methods in Ecology and Evolution 1, 330–342.

Elith, J., Leathwick, J.R., 2009. Species Distribution Models: Ecological Explanation and Prediction Across Space and Time. Annual Review of Ecology, Evolution, and Systematics 40, 677–697.

Elith, J., Phillips, S.J., Hastie, T., Dudík, M., Chee, Y.E., Yates, C.J., 2011. A statistical explanation of MaxEnt for ecologists. Diversity and Distributions 17, 43–57.

Fairbairn, D.J., 2007. Introduction: the enigma of sexual size dimorphism. In: Fairbairn, D.J., Blanckenhorn, W.U., Szekely, T. (Eds.), Sex, Size and Gender Roles: Evolutionary Studies of Sexual Size Dimorphism. Oxford University Press, Oxford, pp. 1–10.

Feder, M.E., Burggren, W.W., 1992. Environmental Physiology of the Amphibians. University of Chicago Press.

Feldman, A., Sabath, N., Pyron, R.A., Mayrose, I., Meiri, S., 2016. Body sizes and diversification rates of lizards, snakes, amphisbaenians and the tuatara. Global Ecology and Biogeography 25, 187–197.

Fet, V., Hennawy, H.E., Braunwalder, M.E., Cloudsley-Thompson, J.L., 2009. The first observation on scorpion biogeography by Aristotle. Boletín Sociedad Entomológica Aragonesa 147–150.

Fick, S.E., Hijmans, R.J., 2017. WorldClim 2: new 1-km spatial resolution climate surfaces for global land areas. International Journal of Climatology 37, 4302–4315.

Field, R., Hawkins, B.A., Cornell, H.V., Currie, D.J., Diniz-Filho, J.A.F., Guégan, J.-F., Kaufman, D.M., Kerr, J.T., Mittelbach, G.G., Oberdorff, T., O'Brien, E.M., Turner, J.R.G., 2009. Spatial species-richness gradients across scales: a meta-analysis. Journal of Biogeography 36, 132–147.

Fitch, H.S., 1976. Sexual size differences in the mainland anoles. Occasional Papers of the Museum of Natural History, The Univirsity of Kansas 50, 1–21.

Fitch, H.S., 1981. Sexual size differences in reptiles, Misecellan. ed. Kansas Museum of Natural History, Lawrence, Kansas.

Fitch, H.S., Hillis, D.M., 1984. The *Anolis* dewlap: interspecific variability and morphological associations with habitat. Copeia 1984, 315–323.

Fitzpatrick, M.C., Hargrove, W.W., 2009. The projection of species distribution models and the problem of non-analog climate. Biodivers Conserv 18, 2255.

Fois, M., Cuena-Lombraña, A., Fenu, G., Bacchetta, G., 2018. Using species distribution models at local scale to guide the search of poorly known species: Review, methodological issues and future directions. Ecological Modelling 385, 124–132.

Fois, M., Cuena-Lombraña, A., Fenu, G., Cogoni, D., Bacchetta, G., 2016. The reliability of conservation status assessments at regional level: Past, present and future perspectives on Gentiana lutea L. ssp. lutea in Sardinia. Journal for Nature Conservation 33, 1–9.

Freeman, E.A., Moisen, G.G., 2008. A comparison of the performance of threshold criteria for binary classification in terms of predicted prevalence and kappa. Ecological Modelling 217, 48–58.

Friedman, N.R., Remeš, V., 2016. Global geographic patterns of sexual size dimorphism in birds: Support for a latitudinal trend? Ecography 39, 17–25.

Frieler, K., Lange, S., Piontek, F., Reyer, C.P.O., Schewe, J., Warszawski, L., Zhao, F., Chini, L., Denvil, S., Emanuel, K., Geiger, T., Halladay, K., Hurtt, G., Mengel, M., Murakami, D., Ostberg, S., Popp, A., Riva, R., Stevanovic, M., Suzuki, T., Volkholz, J., Burke, E., Ciais, P., Ebi, K., Eddy, T.D., Elliott, J., Galbraith, E., Gosling, S.N., Hattermann, F., Hickler, T., Hinkel, J., Hof, C., Huber, V., Jägermeyr, J., Krysanova, V., Marcé, R., Müller Schmied, H., Mouratiadou, I., Pierson, D., Tittensor, D.P., Vautard, R., Vliet, M. van, Biber, M.F., Betts, R.A., Bodirsky, B.L., Deryng, D., Frolking, S., Jones, C.D., Lotze, H.K., Lotze-Campen, H., Sahajpal, R., Thonicke, K., Tian, H., Yamagata, Y., 2017. Assessing the impacts of 1.5 °C global warming – simulation

protocol of the Inter-Sectoral Impact Model Intercomparison Project (ISIMIP2b). Geoscientific Model Development 10, 4321–4345.

Friend, A.D., Stevens, A.K., Knox, R.G., Cannell, M.G.R., 1997. A process-based, terrestrial biosphere model of ecosystem dynamics (Hybrid v3.0). Ecological Modelling 95, 249–287.

Frishkoff, L.O., Gabot, E., Sandler, G., Marte, C., Mahler, D.L., 2019. Elevation shapes the reassembly of Anthropocene lizard communities. Nature Ecology & Evolution 1.

Galante, P.J., Alade, B., Muscarella, R., Jansa, S.A., Goodman, S.M., Anderson, R.P., 2018. The challenge of modeling niches and distributions for data-poor species: a comprehensive approach to model complexity. Ecography 41, 726–736.

Garrido, O.H., Hedges, S.B., 2001. A New Anole from the Northern Slope of the Sierra Maestra in Eastern Cuba (Squamata: Iguanidae). Journal of Herpetology 35, 378–383.

Gaston, K.J., Blackburn, T.M., 1999. A Critique for Macroecology. Oikos 84, 353–368.

Gates, D.M., 1980. Biophysical Ecology, Springer advanced texts in life sciences. Springer-Verlag.

Gavrilets, S., Vose, A., 2005. Dynamic patterns of adaptive radiation. PNAS 102, 18040–18045.

Gilman, S.E., Urban, M.C., Tewksbury, J., Gilchrist, G.W., Holt, R.D., 2010. A framework for community interactions under climate change. Trends Ecol. Evol. (Amst.) 25, 325–331.

Glor, R.E., Warren, D., 2011. Testing Ecological Explanations for Biogeographic Boundaries. Evolution 65, 673–683.

Gottscho, A.D., Wood, D.A., Vandergast, A.G., Lemos-Espinal, J., Gatesy, J., Reeder, T.W., 2017. Lineage diversification of fringe-toed lizards (Phrynosomatidae: *Uma notata* complex) in the Colorado Desert: delimiting species in the presence of gene flow. Molecular Phylogenetics and Evolution 106, 103–117.

Grant, B.W., Dunham, A.E., 1988. Thermally Imposed Time Constraints on the Activity of the Desert Lizard Sceloporus Merriami. Ecology 69, 167–176.

Grummer, J.A., Bryson, R.W., 2014. A new species of bunchgrass lizard (Squamata: Phrynosomatidae) from the southern sky islands of the Sierra Madre Occidental, Mexico. Zootaxa 3790, 439–450.

Guisan, A., Zimmermann, N.E., 2000. Predictive habitat distribution models in ecology. Ecological Modelling 135, 147–186.

Gunderson, A.R., Leal, M., 2012. Geographic variation in vulnerability to climate warming in a tropical Caribbean lizard. Functional Ecology 26, 783–793.

Gunderson, A.R., Leal, M., 2015. Patterns of Thermal Constraint on Ectotherm Activity. The American Naturalist 185, 653–664.

Gunderson, A.R., Mahler, D.L., Leal, M., 2018. Thermal niche evolution across replicated *Anolis* lizard adaptive radiations. Proceedings of the Royal Society B: Biological Sciences 285, 20172241.

Gunderson, A.R., Siegel, J., Leal, M., 2011. Tests of the contribution of acclimation to geographic variation in water loss rates of the West Indian lizard *Anolis cristatellus*. J. Comp. Physiol. B, Biochem. Syst. Environ. Physiol. 181, 965–972.

Gunderson, A.R., Stillman, J.H., 2015. Plasticity in thermal tolerance has limited potential to buffer ectotherms from global warming. Proc. Biol. Sci. 282, 20150401.

Gutiérrez, E.E., Boria, R.A., Anderson, R.P., 2014. Can biotic interactions cause allopatry? Niche models, competition, and distributions of South American mouse opossums. Ecography 37, 741–753.

H-Acevedo, D., Currie, D.J., 2003. Does Climate Determine Broad-Scale Patterns of Species Richness? A Test of the Causal Link by Natural Experiment. Global Ecology and Biogeography 12, 461–473.

Hansen, M.C., Potapov, V.P., Moore, R., Hancher, M., Turubanova, S.A., Tyukavina, A., Thau, D., Stehman, V.S., Goetz, S.J., Loveland, T.R., Kommareddy, A., Egorov, A., Chini, L., Justice, C.O., Townshend,

J.R.G., 2013. High-resolution global maps of 21st-century forest cover change. Science 342, 850–853.

Harmon, L.J., Weir, J.T., Brock, C.D., Glor, R.E., Challenger, W., 2008. geiger: analysis of evolutionary diversification. Bioinformatics 24, 129–131.

Harris, I., Jones, P.D., Osborn, T.J., Lister, D.H., 2014. Updated high-resolution grids of monthly climatic observations – the CRU TS3.10 Dataset. International Journal of Climatology 34, 623–642.

Hartig, F., Dyke, J., Hickler, T., Higgins, S.I., O'Hara, R.B., Scheiter, S., Huth, A., 2012. Connecting dynamic vegetation models to data – an inverse perspective. Journal of Biogeography 39, 2240–2252.

Hawkins, B.A., Field, R., Cornell, H.V., Currie, D.J., Guégan, J.-F., Kaufman, D.M., Kerr, J.T., Mittelbach, G.G., Oberdorff, T., O'Brien, E.M., Porter, E.E., Turner, J.R.G., 2003. Energy, Water, and Broad-Scale Geographic Patterns of Species Richness. Ecology 84, 3105–3117.

Hawkins, B.A., Leroy, B., Rodríguez, M., Singer, A., Vilela, B., Villalobos, F., Wang, X., Zelený, D., 2017. Structural bias in aggregated species-level variables driven by repeated species co-occurrences: a pervasive problem in community and assemblage data. Journal of Biogeography 44, 1199–1211.

Hawkins, B.A., McCain, C.M., Davies, T.J., Buckley, L.B., Anacker, B.L., Cornell, H.V., Damschen, E.I., Grytnes, J.-A., Harrison, S., Holt, R.D., Kraft, N.J.B., Stephens, P.R., 2012. Different evolutionary histories underlie congruent species richness gradients of birds and mammals. Journal of Biogeography 39, 825–841.

Haxeltine, A., Prentice, I.C., 1996. A General Model for the Light-Use Efficiency of Primary Production. Functional Ecology 10, 551–561.

Hedrick, V.A., Temeles, E.J., 1989. The evolution of sexual dimorphism in animals: hypotheses and tests. Trends in Ecology and Evolution 4, 136–138.

Herrel, A., Spithoven, L., Van Damme, R., DE Vree, F., 1999. Sexual dimorphism of head size in *Gallotia galloti*: testing the niche

divergence hypothesis by functional analyses. Functional Ecology 13, 289–297.

Hertz, P.E., 1979. Sensitivity to high temperatures in three west Indian grass anoles (sauria, iguanidae), with a review of heat sensitivity in the genus Anolis. Comparative Biochemistry and Physiology Part A: Physiology 63, 217–222.

Hertz, P.E., Arima, Y., Harrison, A., Huey, R.B., Losos, J.B., Glor, R.E., 2013. Asynchronous evolution of physiology and morphology in Anolis lizards. Evolution 67, 2101–2113.

Hertz, P.E., Huey, R.B., 1981. Compensation for Altitudinal Changes in the Thermal Environment by Some *Anolis* Lizards on Hispaniola. Ecology 62, 515–521.

Hertz, P.E., Huey, R.B., Stevenson, R.D., 1993. Evaluating temperature regulation by field-active ectotherms: the fallacy of the inappropriate question. Am. Nat. 142, 796–818.

Hijmans, R.J., Cameron, S.E., Parra, J.L., Jones, P.G., Jarvis, A., 2005. Very high resolution interpolated climate surfaces for global land areas. International Journal of Climatology 25, 1965–1978.

Hijmans, R.J., Phillips, S., Leathwick, J., Elith, J., 2016. dismo: Species Distribution Modeling.

Hillman, S.S., Gorman, G.C., 1977. Water loss, desiccation tolerance, and survival under desiccating conditions in 11 species of Caribbean Anolis. Oecologia 29, 105–116.

Holt, R.D., 2009. Bringing the Hutchinsonian niche into the 21st century: Ecological and evolutionary perspectives. PNAS 106, 19659–19665.

Hortal, J., Triantis, K.A., Meiri, S., Thébault, E., Sfenthourakis, S., 2009. Island species richness increases with habitat diversity. Am. Nat. 174, E205-217.

Houlahan, J.E., McKinney, S.T., Anderson, T.M., McGill, B.J., 2017. The priority of prediction in ecological understanding. Oikos 126, 1–7.

Huey, R.B., Deutsch Curtis A., Tewksbury Joshua J., Vitt Laurie J., Hertz Paul E., Álvarez Pérez Héctor J., Garland Theodore, 2009. Why tropical

forest lizards are vulnerable to climate warming. Proceedings of the Royal Society B: Biological Sciences 276, 1939–1948.

Huey, R.B., Webster, T.P., 1976. Thermal Biology of *Anolis* Lizards in a Complex Fauna: The Christatellus Group on Puerto Rico. Ecology 57, 985–994.

Hutchinson, G.E., 1957. Concluding Remarks. Cold Spring Harb Symp Quant Biol 22, 415–427.

Jasmin, J.-N., Kassen, R., 2007. Evolution of a single niche specialist in variable environments. Proc Biol Sci 274, 2761–2767.

Jayatilaka, P., Narendra, A., Reid, S.F., Cooper, P., Zeil, J., 2011. Different effects of temperature on foraging activity schedules in sympatric Myrmecia ants. Journal of Experimental Biology 214, 2730–2738.

Jenssen, T.A., Marcellini, D.L., Pague, C.A., Jenssen, L.A., 1984. Competitive Interference between the Puerto Rican Lizards, *Anolis cooki* and *A. cristatellus*. Copeia 1984, 853–862.

Jezkova, T., Wiens, J.J., 2016. Rates of change in climatic niches in plant and animal populations are much slower than projected climate change. Proceedings of the Royal Society B: Biological Sciences 283, 20162104.

Kaky, E., Gilbert, F., 2016. Using species distribution models to assess the importance of Egypt's protected areas for the conservation of medicinal plants. Journal of Arid Environments 135, 140–146.

Kalmar, A., Currie, D.J., 2007. A unified model of avian species richness on islands and continents. Ecology 88, 1309–1321.

Karger, D.N., Conrad, O., Böhner, J., Kawohl, T., Kreft, H., Soria-Auza, R.W., Zimmermann, N.E., Linder, H.P., Kessler, M., 2017. Climatologies at high resolution for the earth's land surface areas. Scientific Data 4, 170122.

Kearney, M., Phillips, B.L., Tracy, C.R., Christian, K.A., Betts, G., Porter, W.P., 2008. Modelling species distributions without using species distributions: the cane toad in Australia under current and future climates. Ecography 31, 423–434.

Kearney, M., Porter, W., 2009. Mechanistic niche modelling: combining physiological and spatial data to predict species' ranges. Ecology Letters 12, 334–350.

Kearney, M., Porter, W.P., 2004. Mapping the fundamental niche: Physiology, climate and the distribution of a nocturnal lizard. Ecology 85, 3119–3131.

Kearney, M.R., Porter, W.P., 2017. NicheMapR – an R package for biophysical modelling: the microclimate model. Ecography 40, 664–674.

Kearney, M.R., Porter, W.P., 2020. NicheMapR – an R package for biophysical modelling: the ectotherm and Dynamic Energy Budget models. Ecography 43, 85–96.

Kearney, M.R., Simpson, S.J., Raubenheimer, D., Kooijman, S.A.L.M., 2013. Balancing heat, water and nutrients under environmental change: A thermodynamic niche framework. Functional Ecology 27, 950–966.

Kingsolver, J.G., Diamond, S.E., Buckley, L.B., 2013. Heat stress and the fitness consequences of climate change for terrestrial ectotherms. Functional Ecology 27, 1415–1423.

Kisel, Y., Barraclough, T.G., 2010. Speciation has a spatial scale that depends on levels of gene flow. Am. Nat. 175, 316–334.

Kissling, W.D., Dormann, C.F., Groeneveld, J., Hickler, T., Kühn, I., McInerny, G.J., Montoya, J.M., Römermann, C., Schiffers, K., Schurr, F.M., Singer, A., Svenning, J.-C., Zimmermann, N.E., O'Hara, R.B., 2012. Towards novel approaches to modelling biotic interactions in multispecies assemblages at large spatial extents. Journal of Biogeography 39, 2163–2178.

Koenker, R., 2017. quantreg: Quantile Regression.

Köhler, G., Townsend, J.H., Peterson, C.B.., 2016. Taxonomic revision of the *Norops tropidonotus* complex (Squamata, Dactyloidae), with the resurrection of *N. spilorhipis* (Alvarez del Toro and Smith, 1956) and the description of two new species. Mesoamerican Herpetology 3, 8–41.

Köhler, G., Vargas, J., Lotzkat, S., 2014. Two new species of the *Norops pachypus* complex (Squamata , Dactyloidae) from Costa Rica. Mesoamerican Herpetology 1, 254–280.

Köhler, J.J., Poe, S., Ryan, M.J., K, Öhler, G., 2015. *Anolis marsupialis* Taylor 1956, a valid species from southern Pacific Costa Rica (Reptilia, Squamata, Dactyloidae). Zootaxa 3915, 111–122.

Kottek, M., Grieser, J., Beck, C., Rudolf, B., Rubel, F., 2006. World Map of the Köppen-Geiger climate classification updated. Meteorologische Zeitschrift 15, 259–263.

Lara-Tufiño, J.D., Nieto-Montes De Oca, A., Ramírez-Bautista, A., Gray, L.N., 2016. Resurrection of *Anolis ustus* Cope, 1864 from synonymy with *Anolis sericeus* Hallowell, 1856 (Squamata, Dactyloidae). ZooKeys 619, 147–162.

Latham, R.E., Ricklefs, Robert E., 1993. Continental comparisons of temperate-zone tree species diversity. In: Ricklefs, R.E., Schluter, D. (Eds.), Species Diversity in Ecological Communities: Historical and Geographical Perspectives. University of Chicago Press.

Lawson, A.M., Weir, J.T., 2014. Latitudinal gradients in climatic-niche evolution accelerate trait evolution at high latitudes. Ecology Letters 17, 1427–1436.

Leal, M., Knox, A.K., Losos, J.B., 2002. Lack of Convergence in Aquatic *Anolis* Lizards. Evolution 56, 785–791.

Leibold, M.A., 1995. The Niche Concept Revisited: Mechanistic Models and Community Context. Ecology 76, 1371–1382.

Lenoir, J., Svenning, J.-C., 2015. Climate-related range shifts – a global multidimensional synthesis and new research directions. Ecography 38, 15–28.

Levy, O., Dayan, T., Porter, W.P., Kronfeld-Schor, N., 2019. Time and ecological resilience: can diurnal animals compensate for climate change by shifting to nocturnal activity? Ecological Monographs 89, e01334.

Lischke, H., Zimmermann, N.E., Bolliger, J., Rickebusch, S., Löffler, T.J., 2006. TreeMig: A forest-landscape model for simulating spatio-

temporal patterns from stand to landscape scale. Ecological Modelling, Pattern and Processes of Dynamic Mosaic Landscapes -- Modelling, Simulation, and Implications 199, 409–420.

Lobkovsky, A.E., Koonin, E.V., 2012. Replaying the Tape of Life: Quantification of the Predictability of Evolution. Front Genet 3.

Logan, M.L., Huynh, R.K., Precious, R.A., Calsbeek, R.G., 2013. The impact of climate change measured at relevant spatial scales: New hope for tropical lizards. Global Change Biology 19, 3093–3102.

Lopez-Darias, M., Vanhooydonck, B., Cornette, R., Herrel, A., 2014. Sex-specific differences in ecomorphological relationships in lizards of the genus *Gallotia*. Functional Ecology 29, 506–514.

Losos, J.B., 2009. Lizards in an Evolutionary Tree: Ecology and Adaptive Radiation of Anoles. University of California Press, Berkeley.

Losos, J.B., Ricklefs, R.E., 2009. Adaptation and diversification on islands. Nature 457, 830–836.

Losos, J.B., Schluter, D., 2000. Analysis of an evolutionary species–area relationship. Nature 408, 847–850.

Lovich, J.E., Gibbons, J.W., 1992. A review of techniques for quantifying sexual size dimorphism. Growth, Development, and Aging 56, 269–81.

MacArthur, R.H., 1972. Geographical ecology: patterns in the distribution of species. Harper & Row, New York.

MacArthur, R.H., Wilson, E.O., 1963. An Equilibrium Theory of Insular Zoogeography. Evolution 17, 373–387.

MacArthur, R.H., Wilson, E.O., 1967. The theory of island biogeography, Landmarks in Biology Series. Princeton University Press.

Machado, G., Buzatto, B.A., Garcia-Hernandez, S., Macias-Ordonez, R., 2016. Macroecology of sexual selection: a predictive conceptual framework for large-scale variation in reproductive traits. American Naturalist 188, S8–S27.

Macías-Ordóñez, R., Machado, G., Macedo, R.H., 2013. Macroecology of sexual selection: large-scale influence of climate on sexually selected traits. In: Sexual Selection: Perspectives and Models from the Neotropics. Academic Press, pp. 1–32.

Maguire, K.C., Nieto-Lugilde, D., Fitzpatrick, M.C., Williams, J.W., Blois, J.L., 2015. Modeling Species and Community Responses to Past, Present, and Future Episodes of Climatic and Ecological Change. Annual Review of Ecology, Evolution, and Systematics 46, 343–368.

Mahler, D.L., Ingram, T., Revell, L.J., Losos, J.B., 2013. Exceptional Convergence on the Macroevolutionary Landscape in Island Lizard Radiations. Science 341, 292–295.

Mahler, D.L., Revell, L.J., Glor, R.E., Losos, J.B., 2010. Ecological opportunity and the rate of morphological evolution in the diversification of greater Antillean anoles. Evolution 64, 2731–2745.

Malhotra, A., Thorpe, R.S., 1993. An experimental field study of a eurytopic anole, Anolis oculatus. Journal of Zoology 229, 163–170.

Matthews, T.J., Guilhaumon, F., Triantis, K.A., Borregaard, M.K., Whittaker, R.J., 2016. On the form of species–area relationships in habitat islands and true islands. Global Ecology and Biogeography 25, 847–858.

McCain, C.M., Grytnes, J.-A., 2010. Elevational gradients in species richness. In: Encylcopedia of Life Sciences (ELS). John Wiley & Sons Ltd, Chichester.

McGill, B.J., Enquist, B.J., Weiher, E., Westoby, M., 2006. Rebuilding community ecology from functional traits. Trends in Ecology & Evolution 21, 178–185.

Meiri, S., 2008. Evolution and ecology of lizard body sizes. Global Ecology and Biogeography 17, 724–734.

Meiri, S., 2018. Traits of lizards of the world: Variation around a successful evolutionary design. Global Ecology and Biogeography.

Meiri, S., Bauer, A.M., Chirio, L., Colli, G.R., Das, I., Doan, T.M., Feldman, A., Herrera, F.-C., Novosolov, M., Pafilis, P., Pincheira-Donoso, D., Powney, G., Torres-Carvajal, O., Uetz, P., Van Damme, R., 2013. Are lizards feeling the heat? A tale of ecology and evolution under two temperatures. Global Ecology and Biogeography 22, 834–845.

Meiri, S., Brown, J.H., Sibly, R.M., 2012. The ecology of lizard reproductive output. Global Ecology and Biogeography 21, 592–602.

Meiri, S., Kadison, A.E., Novosolov, M., Pafilis, P., Foufopoulos, J., Itescu, Y., Raia, P., Pincheira-Donoso, D., 2014. The number of competitor species is unlinked to sexual dimorphism. The Journal of Animal Ecology 83, 1302–1312.

Meiri, S., Thomas, G.H., 2007. The geography of body size – challenges of the interspecific approach. Global Ecology and Biogeography 16, 689–693.

Mena, J.L., Vázquez-Domínguez, E., 2005. Species turnover on elevational gradients in small rodents. Global Ecology and Biogeography 14, 539–547.

Mesgaran, M.B., Cousens, R.D., Webber, B.L., 2014. Here be dragons: a tool for quantifying novelty due to covariate range and correlation change when projecting species distribution models. Diversity and Distributions 20, 1147–1159.

Mesquita, D.O., Costa, G.C., Colli, G.R., Costa, T.B., Shepard, D.B., Vitt, L.J., Pianka, E.R., 2016. Life-history patterns of lizards of the world. The American Naturalist 187, 689–705.

Montanucci, R.R., 2015. A taxonomic revision of the *Phrynosoma douglasii* species complex (Squamata: Phrynosomatidae). Zootaxa 4015, 1–177.

Morales, N.S., Fernández, I.C., Baca-González, V., 2017. MaxEnt's parameter configuration and small samples: are we paying attention to recommendations? A systematic review. PeerJ 5, e3093.

Muñoz, M.M., Stimola, M.A., Algar, A.C., Conover, A., Rodriguez, A.J., Landestoy, M.A., Bakken, G.S., Losos, J.B., 2014. Evolutionary stasis and lability in thermal physiology in a group of tropical lizards. Proc Biol Sci 281.

Muscarella, R., Galante, P.J., Soley-Guardia, M., Boria, R.A., Kass, J.M., Uriarte, M., Anderson, R.P., 2014. ENMeval: An R package for conducting spatially independent evaluations and estimating optimal model complexity for Maxent ecological niche models. Methods in Ecology and Evolution 5, 1198–1205.

Neilson, R.P., 1995. A model for predicting continental-scale vegetation distribution and water balance. Ecological Applications 5, 362–385.

Nenzén, H.K., Araújo, M.B., 2011. Choice of threshold alters projections of species range shifts under climate change. Ecological Modelling 222, 3346–3354.

New, M., Hulme, M., Jones, P., 1999. Representing Twentieth-Century Space–Time Climate Variability. Part I: Development of a 1961–90 Mean Monthly Terrestrial Climatology. Journal of Climate 12, 829–856.

New, M., Lister, D., Hulme, M., Makin, I., 2002. A high-resolution data set of surface climate over global land areas. Climate Research 21, 1–25.

Nogués-Bravo, D., Rodríguez-Sánchez, F., Orsini, L., Boer, E. de, Jansson, R., Morlon, H., Fordham, D.A., Jackson, S.T., 2018. Cracking the Code of Biodiversity Responses to Past Climate Change. Trends in Ecology & Evolution 33, 765–776.

Olalla-Tarraga, M.A., Rodriguez, M.A., Hawkins, B.A., 2006. Broad-scale patterns of body size in squamate reptiles of Europe and North America. Journal of Biogeography 33, 781–793.

Pacala, S.W., Roughgarden, J., 1985. Population Experiments with the *Anolis* Lizards of St. Maarten and St. Eustatius. Ecology 66, 129–141.

Pacifici, M., Foden, W.B., Visconti, P., Watson, J.E.M., Butchart, S.H.M., Kovacs, K.M., Scheffers, B.R., Hole, D.G., Martin, T.G., Akçakaya, H.R., Corlett, R.T., Huntley, B., Bickford, D., Carr, J.A., Hoffmann, A.A., Midgley, G.F., Pearce-Kelly, P., Pearson, R.G., Williams, S.E., Willis, S.G., Young, B., Rondinini, C., 2015. Assessing species vulnerability to climate change. Nature Climate Change 5, 215–224.

Parent, C.E., Crespi, B.J., 2006. Sequential Colonization and Diversification of Galapagos Endemic Land Snail Genus Bulimulus (gastropoda, Stylommatophora). Evolution 60, 2311–2328.

Parmesan, C., 2006. Ecological and Evolutionary Responses to Recent Climate Change. Annual Review of Ecology, Evolution, and Systematics 37, 637–669.

Parmesan, C., Yohe, G., 2003. A globally coherent fingerprint of climate change impacts across natural systems. Nature 421, 37–42.

Pearse, W.D., Barbosa, A.M., Fritz, S.A., Keith, S.A., Harmon, L.J., Harte, J., Silvestro, D., Xiao, X., Davies, T.J., 2018. Building up biogeography: Pattern to process. Journal of Biogeography 45, 1223–1230.

Pearson, R.G., Dawson, T.P., 2003. Predicting the impacts of climate change on the distribution of species: are bioclimate envelope models useful? Global Ecology and Biogeography 12, 361–371.

Pecl, G.T., Araújo, M.B., Bell, J.D., Blanchard, J., Bonebrake, T.C., Chen, I.-C., Clark, T.D., Colwell, R.K., Danielsen, F., Evengård, B., Falconi, L., Ferrier, S., Frusher, S., Garcia, R.A., Griffis, R.B., Hobday, A.J., Janion-Scheepers, C., Jarzyna, M.A., Jennings, S., Lenoir, J., Linnetved, H.I., Martin, V.Y., McCormack, P.C., McDonald, J., Mitchell, N.J., Mustonen, T., Pandolfi, J.M., Pettorelli, N., Popova, E., Robinson, S.A., Scheffers, B.R., Shaw, J.D., Sorte, C.J.B., Strugnell, J.M., Sunday, J.M., Tuanmu, M.-N., Vergés, A., Villanueva, C., Wernberg, T., Wapstra, E., Williams, S.E., 2017. Biodiversity redistribution under climate change: Impacts on ecosystems and human well-being. Science 355.

Peel, M.C., Finlayson, B.L., Mcmahon, T.A., 2007. Updated world map of the Köppen-Geiger climate classification. Hydrology and Earth System Sciences Discussions 11, 1633–1644.

Peters, R.H., 1991. A Critique for Ecology. Cambridge University Press.

Peterson, A.T., Soberón, J., 2012. Species Distribution Modeling and Ecological Niche Modeling: Getting the Concepts Right. Natureza & Conservação 10, 102–107.

Phillips, S.J., Anderson, R.P., Dudík, M., Schapire, R.E., Blair, M.E., 2017. Opening the black box: an open-source release of Maxent. Ecography 40, 887–893.

Phillips, S.J., Anderson, R.P., Schapire, R.E., 2006. Maximum entropy modeling of species geographic distributions. Ecological Modelling 190, 231–259.

Phillips, S.J., Dudík, M., Elith, J., Graham, C.H., Lehmann, A., Leathwick, J., Ferrier, S., 2009. Sample selection bias and presence-only distribution

models: implications for background and pseudo-absence data. Ecological Applications 19, 181–197.

Phillips, S.J., Elith, J., 2013. On estimating probability of presence from use–availability or presence–background data. Ecology 94, 1409–1419.

Pianka, E.R., Vitt, L.J., 2003. Lizards: Windows to the Evolution of Diversity. University of California Press, Berkeley and Los Angeles.

Pietsch, T.W., 2005. Dimorphism, parasitism, and sex revisited: modes of reproduction among deep-sea ceratioid anglerfishes (Teleostei: Lophiiformes). Ichthyological Research 52, 207–236.

Pincheira-Donoso, D., Hodgson, D.J., Stipala, J., Tregenza, T., 2009. A phylogenetic analysis of sex-specific evolution of ecological morphology in Liolaemus lizards. Ecological Research 24, 1223–1231.

Pincheira-Donoso, D., Hunt, J., 2017. Fecundity selection theory: concepts and evidence. Biological Reviews 92, 341–356.

Pincheira-Donoso, D., Meiri, S., 2013. An intercontinental analysis of climate-driven body size clines in reptiles: no support for patterns, no signals of processes. Evolutionary Biology 40, 562–578.

Pincheira-Donoso, D., Tregenza, T., 2011. Fecundity selection and the evolution of reproductive output and sex-specific body size in the Liolaemus lizard adaptive radiation. Evolutionary Biology 38, 197–207.

Pincheira-Donoso, D., Tregenza, T., Butlin, R.K., Hodgson, D.J., 2018. Sexes and species as rival units of niche saturation during community assembly. Global Ecology and Biogeography 27, 593–603.

Poe, S., Ryan, M.J., 2017. Description of two new species similar to *Anolis insignis* (Squamata: Iguanidae) and resurrection of *Anolis (Diaphoranolis) brooksi*. Amphibian & Reptile Conservation ll, 1–16.

Poloczanska, E.S., Brown, C.J., Sydeman, W.J., Kiessling, W., Schoeman, D.S., Moore, P.J., Brander, K., Bruno, J.F., Buckley, L.B., Burrows, M.T., Duarte, C.M., Halpern, B.S., Holding, J., Kappel, C.V., O'Connor, M.I., Pandolfi, J.M., Parmesan, C., Schwing, F., Thompson, S.A., Richardson, A.J., 2013. Global imprint of climate change on marine life. Nature Climate Change 3, 919–925.

Porter, W.P., Gates, D.M., 1969. Thermodynamic Equilibria of Animals with Environment. Ecological Monographs 39, 227–244.

Porter, W.P., Mitchell, J.W., 2006. Method and system for calculating the spatial-temporal effects of climate and other environmental conditions on animals.

Pringle, R.M., Kartzinel, T.R., Palmer, T.M., Thurman, T.J., Fox-Dobbs, K., Xu, C.C.Y., Hutchinson, M.C., Coverdale, T.C., Daskin, J.H., Evangelista, D.A., Gotanda, K.M., Veld, N.A.M. in 't, Wegener, J.E., Kolbe, J.J., Schoener, T.W., Spiller, D.A., Losos, J.B., Barrett, R.D.H., 2019. Predator-induced collapse of niche structure and species coexistence. Nature 570, 58.

Pulliam, H.R., 2000. On the relationship between niche and distribution. Ecology Letters 3, 349–361.

Qian, H., Ricklefs, R.E., 2004. Geographical distribution and ecological conservatism of disjunct genera of vascular plants in eastern Asia and eastern North America. Journal of Ecology 92, 253–265.

Ranc, N., Santini, L., Rondinini, C., Boitani, L., Poitevin, F., Angerbjörn, A., Maiorano, L., 2017. Performance tradeoffs in target-group bias correction for species distribution models. Ecography 40, 1076–1087.

Rand, A.S., 1964. Ecological Distribution in Anoline Lizards of Puerto Rico. Ecology 45, 745–752.

Revell, L.J., 2012. phytools: an R package for phylogenetic comparative biology (and other things). Methods in Ecology and Evolution 3, 217–223.

Rodríguez-Schettino, L., Losos, J.B., Hertz, P.E., De Queiroz, K., Chamizo, A.R., Leal, M., Rivalta, V., 2010. The anoles of Soroa: aspects of their ecological relationships. Breviora 520, 1–22.

Rohr, J.R., Civitello, D.J., Cohen, J.M., Roznik, E.A., Sinervo, B., Dell, A.I., 2018. The complex drivers of thermal acclimation and breadth in ectotherms. Ecology Letters 21, 1425–1439.

Roll, U., Feldman, A., Novosolov, M., Allison, A., Bauer, A.M., Bernard, R., Böhm, M., Castro-Herrera, F., Chirio, L., Collen, B., Colli, G.R., Dabool, L., Das, I., Doan, T.M., Grismer, L.L., Hoogmoed, M., Itescu,

Y., Kraus, F., LeBreton, M., Lewin, A., Martins, M., Maza, E., Meirte, D., Nagy, Z.T., Nogueira, C. de C., Pauwels, O.S.G., Pincheira-Donoso, D., Powney, G.D., Sindaco, R., Tallowin, O.J.S., Torres-Carvajal, O., Trape, J.-F., Vidan, E., Uetz, P., Wagner, P., Wang, Y., Orme, C.D.L., Grenyer, R., Meiri, S., 2017. The global distribution of tetrapods reveals a need for targeted reptile conservation. Nature Ecology & Evolution 1, 1677.

Rolland, J., Silvestro, D., Schluter, D., Guisan, A., Broennimann, O., Salamin, N., 2018. The impact of endothermy on the climatic niche evolution and the distribution of vertebrate diversity. Nat Ecol Evol 2, 459–464.

Rosindell, J., Phillimore, A.B., 2011. A unified model of island biogeography sheds light on the zone of radiation. Ecology Letters 14, 552–560.

Rundle, H.D., Nagel, L., Wenrick Boughman, J., Schluter, D., 2000. Natural selection and parallel speciation in sympatric sticklebacks. Science 287, 306–308.

Sanders, N.J., Rahbek, C., 2012. The patterns and causes of elevational diversity gradients. Ecography 35, 1–3.

Saupe, E.E., Barve, N., Owens, H.L., Cooper, J.C., Hosner, P.A., Peterson, A.T., 2018. Reconstructing Ecological Niche Evolution When Niches Are Incompletely Characterized. Syst. Biol. 67, 428–438.

Scharf, I., Meiri, S., 2013. Sexual dimorphism of heads and abdomens: different approaches to ‘being large’ in female and male lizards. Biological Journal of the Linnean Society 110, 665–673.

Scheffers, B.R., Evans Theodore A., Williams Stephen E., Edwards David P., 2014. Microhabitats in the tropics buffer temperature in a globally coherent manner. Biology Letters 10, 20140819.

Scheiter, S., Higgins, S.I., 2009. Impacts of climate change on the vegetation of Africa: an adaptive dynamic vegetation modelling approach. Global Change Biology 15, 2224–2246.

Scheller, R.M., Domingo, J.B., Sturtevant, B.R., Williams, J.S., Rudy, A., Gustafson, E.J., Mladenoff, D.J., 2007. Design, development, and application of LANDIS-II, a spatial landscape simulation model with

flexible temporal and spatial resolution. Ecological Modelling 201, 409–419.

Schettino, L.R., Losos, J.B., Hertz, P.E., Queiroz, K. de, Chamizo, A.R., Leal, M., González, V.R., 2010. The Anoles of Soroa: Aspects of Their Ecological Relationships. brvo 454, 1–22.

Schluter, D., 1996. Ecological Causes of Adaptive Radiation. The American Naturalist 148, S40–S64.

Schoener, T.W., 1970. Nonsynchronous spatial overlap of lizards in patchy habitats. Ecology 51, 408–418.

Schoener, T.W., 1977. Competition and the niche. In: Gans, C., Tinkle, D. (Eds.), Biology of the Reptilia, Volume 7: Ecology and Behaviour A. Academic Press, London, UK, pp. 35–136.

Schwartz, A., Henderson, R.W., 1991. Amphibians and Reptiles of the West Indies: Descriptions, Distributions, and Natural History. University of Florida Press.

Schwarz, R., Meiri, S., 2017. The fast-slow life-history continuum in insular lizards: a comparison between species with invariant and variable clutch sizes. Journal of Biogeography 44, 2808–2815.

Schwarzkopf, L., Shine, R., 1991. Thermal biology of reproduction in viviparous skinks, *Eulamprus tympanum*: why do gravid females bask more? Oecologia 88, 562–569.

Sears, M.W., Angilletta, M.J., 2004. Body size clines in *Sceloporus* lizards: proximate mechanisms and demographic constraints. Integrative and Comparative Biology 44, 433–42.

Sears, M.W., Angilletta, M.J., Schuler, M.S., Borchert, J., Dilliplane, K.F., Stegman, M., Rusch, T.W., Mitchell, W.A., 2016. Configuration of the thermal landscape determines thermoregulatory performance of ectotherms. PNAS 113, 10595–10600.

Sexton, J.P., McIntyre, P.J., Angert, A.L., Rice, K.J., 2009. Evolution and Ecology of Species Range Limits. Annual Review of Ecology, Evolution, and Systematics 40, 415–436.

Shine, R., 1978. Sexual size dimorphism and male combat in snakes. Oecologia 33, 269–277.

Shine, R., 1988. The evolution of large body size in females: a critique of Darwin's "fecundity advantage" model. The American Naturalist 131, 124–131.

Shine, R., 1989. Ecological causes for the evolution of sexual dimorphism: a review of the evidence. Quarterly Review of Biology 64, 419–461.

Shine, R., 1994. Sexual size dimorphism in snakes revisited. Copeia 1994, 326–346.

Sinclair, B.J., Marshall, K.E., Sewell, M.A., Levesque, D.L., Willett, C.S., Slotsbo, S., Dong, Y., Harley, C.D.G., Marshall, D.J., Helmuth, B.S., Huey, R.B., 2016. Can we predict ectotherm responses to climate change using thermal performance curves and body temperatures? Ecology Letters 19, 1372–1385.

Sinervo, B., Mendez-de-la-Cruz, F., Miles, D.B., Heulin, B., Bastiaans, E., Villagran-Santa Cruz, M., Lara-Resendiz, R., Martinez-Mendez, N., Calderon-Espinosa, M.L., Meza-Lazaro, R.N., Gadsden, H., Avila, L.J., Morando, M., De la Riva, I.J., Sepulveda, P.V., Rocha, C.F.D., Ibarguengoytia, N., Puntriano, C.A., Massot, M., Lepetz, V., Oksanen, T.A., Chapple, D.G., Bauer, A.M., Branch, W.R., Clobert, J., Sites, J.W., 2010. Erosion of Lizard Diversity by Climate Change and Altered Thermal Niches. Science 328, 894–899.

Slater, G.J., Harmon, L.J., Alfaro, M.E., 2012. Integrating Fossils with Molecular Phylogenies Improves Inference of Trait Evolution. Evolution 66, 3931–3944.

Slatkin, M., 1984. Ecological causes of sexual dimorphism. Evolution 38, 622–630.

Soberón, J., 2007. Grinnellian and Eltonian niches and geographic distributions of species. Ecology Letters 10, 1115–1123.

Soberón, J., Nakamura, M., 2009. Niches and distributional areas: Concepts, methods, and assumptions. PNAS 106, 19644–19650.

Soga, M., Gaston, K.J., 2018. Shifting baseline syndrome: causes, consequences, and implications. Frontiers in Ecology and the Environment 16, 222–230.

Solano-Zavaleta, I., de Oca, A.N.-M., Campbell, J.A., 2016. A New species of Mesaspis (Squamata: Anguidae) from the High Cuchumatanes of Guatemala. Journal of Herpetology 50, 327–336.

Stamps, J.A., 1983. Sexual selection, sexual dimorphism and territoriality. In: Pianka, T.W., E.R...Schoener (Ed.), Lizard Ecology: Studies of a Model Organism. Harvard University Press, Cambridge, MA., pp. 169–204.

Stein, A., Gerstner, K., Kreft, H., 2014. Environmental heterogeneity as a universal driver of species richness across taxa, biomes and spatial scales. Ecology Letters 17, 866–880.

Steinbauer, M.J., Field, R., Grytnes, J.-A., Trigas, P., Ah-Peng, C., Attorre, F., Birks, H.J.B., Borges, P.A.V., Cardoso, P., Chou, C.-H., Sanctis, M.D., Sequeira, M.M. de, Duarte, M.C., Elias, R.B., Fernández-Palacios, J.M., Gabriel, R., Gereau, R.E., Gillespie, R.G., Greimler, J., Harter, D.E.V., Huang, T.-J., Irl, S.D.H., Jeanmonod, D., Jentsch, A., Jump, A.S., Kueffer, C., Nogué, S., Otto, R., Price, J., Romeiras, M.M., Strasberg, D., Stuessy, T., Svenning, J.-C., Vetaas, O.R., Beierkuhnlein, C., 2016. Topography-driven isolation, speciation and a global increase of endemism with elevation. Global Ecology and Biogeography 25, 1097–1107.

Stevens, M.H.H., Sanchez, M., Lee, J., Finkel, S.E., 2007. Diversification rates increase with population size and resource concentration in an unstructured habitat. Genetics 177, 2243–2250.

Stillwell, R.C., Morse, G.E., Fox, C.W., 2007. Geographic variation in body size and sexual size dimorphism of a seed-feeding beetle. The American Naturalist 170, 358–369.

Storz, J.F., Balasingh, J., Bhat, H.R., Nathan, P.T., Doss, D.P.S., Prakash, a. A., Kunz, T.H., 2001. Clinal variation in body size and sexual dimorphism in an Indian fruit bat, *Cynopterus sphinx* (Chiroptera: Pteropodidae). Biological Journal of the Linnean Society 72, 17–31.

Stralberg, D., Jongsomjit, D., Howell, C.A., Snyder, M.A., Alexander, J.D., Wiens, J.A., Root, T.L., 2009. Re-Shuffling of Species with Climate

Disruption: A No-Analog Future for California Birds? PLOS ONE 4, e6825.

Stuessy, T.F., Jakubowsky, G., Gómez, R.S., Pfosser, M., Schlüter, P.M., Fer, T., Sun, B.-Y., Kato, H., 2006. Anagenetic evolution in island plants. Journal of Biogeography 33, 1259–1265.

Sunday, J.M., Bates, A.E., Kearney, M.R., Colwell, R.K., Dulvy, N.K., Longino, J.T., Huey, R.B., 2014. Thermal-safety margins and the necessity of thermoregulatory behavior across latitude and elevation. Proceedings of the National Academy of Sciences 111, 5610–5615.

Sunday, J.M., Bates Amanda E., Dulvy Nicholas K., 2010. Global analysis of thermal tolerance and latitude in ectotherms. Proceedings of the Royal Society B: Biological Sciences 278, 1823–1830.

Thorat, L., Nath, B.B., 2018. Insects With Survival Kits for Desiccation Tolerance Under Extreme Water Deficits. Frontiers in Physiology 9.

Title, P.O., Bemmels, J.B., 2018. ENVIREM: an expanded set of bioclimatic and topographic variables increases flexibility and improves performance of ecological niche modeling. Ecography 41, 291–307.

Title, P.O., Burns, K.J., 2015. Rates of climatic niche evolution are correlated with species richness in a large and ecologically diverse radiation of songbirds. Ecology Letters 18, 433–440.

Tonini, J.F.R., Beard, K.H., Ferreira, R.B., Jetz, W., Pyron, R.A., 2016. Fully-sampled phylogenies of squamates reveal evolutionary patterns in threat status. Biological Conservation 204, 23–31.

Tracy, C.R., 1982. Biophysical modelling in reptilian physiology band ecology. In: Physiology C: Physiological Ecology. Academic Press, London, pp. 275–321.

Triantafyllou, G., Tsonis, A., 1994. Assessing the ability of the Köppen System to delineate the general world pattern of climates. Geophysical Research Letters 21, 2809–2812.

Tuff, K.T., Tuff, T., Davies, K.F., 2016. A framework for integrating thermal biology into fragmentation research. Ecology Letters 19, 361–374.

Urban, M.C., 2015. Accelerating extinction risk from climate change. Science 348, 571–573.

Urban, M.C., Zarnetske, P.L., Skelly, D.K., 2013. Moving forward: dispersal and species interactions determine biotic responses to climate change. Annals of the New York Academy of Sciences 1297, 44–60.

van Etten, J., 2015. gdistance: Distances and Routes on Geographical Grids.

Vázquez-Rivera, H., Currie, D.J., 2015. Contemporaneous climate directly controls broad-scale patterns of woody plant diversity: a test by a natural experiment over 14,000 years. Global Ecology and Biogeography 24, 97–106.

Velasco, J.A., Martínez-Meyer, E., Flores-Villela, O., García, A., Algar, A.C., Köhler, G., Daza, J.M., 2016. Climatic niche attributes and diversification in Anolis lizards. Journal of Biogeography 43, 134–144.

Velasco, J.A., Villalobos, F., Diniz-Filho, J.A.F., Algar, A.C., Flores-Villela, O., KÖhler, G., Poe, S., Martinez-Meyer, E., 2018. Climatic and evolutionary factors shaping geographical gradients of species richness in *Anolis* lizards. Biological Journal of the Linnean Society 123, 615–627.

Veloz, S.D., Williams, J.W., Blois, J.L., He, F., Otto-Bliesner, B., Liu, Z., 2012. No-analog climates and shifting realized niches during the late quaternary: implications for 21st-century predictions by species distribution models. Global Change Biology 18, 1698–1713.

Wang, I.J., Glor, R.E., Losos, J.B., 2013. Quantifying the roles of ecology and geography in spatial genetic divergence. Ecology Letters 16, 175–182.

Warren, D.L., Cardillo, M., Rosauer, D.F., Bolnick, D.I., 2014. Mistaking geography for biology: Inferring processes from species distributions. Trends in Ecology and Evolution 29, 572–580.

Warren, D.L., Glor, R.E., Turelli, M., 2008. Environmental Niche Equivalency Versus Conservatism: Quantitative Approaches to Niche Evolution. Evolution 62, 2868–2883.

Weigelt, P., Kreft, H., 2013. Quantifying island isolation – insights from global patterns of insular plant species richness. Ecography 36, 417–429.

Weigelt, P., Steinbauer, M.J., Cabral, J.S., Kreft, H., 2016. Late Quaternary climate change shapes island biodiversity. Nature 532, 99–102.

Whittaker, R.J., Triantis, K.A., Ladle, R.J., 2008. A general dynamic theory of oceanic island biogeography. Journal of Biogeography 35, 977–994.

Wiens, J.J., 2011. The niche, biogeography and species interactions. Philos Trans R Soc Lond B Biol Sci 366, 2336–2350.

Wiens, J.J., Ackerly, D.D., Allen, A.P., Anacker, B.L., Buckley, L.B., Cornell, H.V., Damschen, E.I., Jonathan Davies, T., Grytnes, J.-A., Harrison, S.P., Hawkins, B.A., Holt, R.D., McCain, C.M., Stephens, P.R., 2010. Niche conservatism as an emerging principle in ecology and conservation biology. Ecol. Lett. 13, 1310–1324.

Williams, E.E., 1965. The species of Hispaniolan green anoles (Sauria, Iguanidae). Breviora 227, 1–16.

Williams, E.E., 1972. The Origin of Faunas. Evolution of lizard congeners in a complex island fauna: a trial analysis. In: Dobzhansky T., Hecht, M.K., Steere W.C. (Eds.), Evolutionary Biology. Springer, Boston, MA.

Williams, E.E., Hecht, M.K., 1955. “Sunglasses” in Two Anoline Lizards from Cuba. Science 122, 691–692.

Williams, J.W., Jackson, S.T., 2007. Novel climates, no-analog communities, and ecological surprises. Frontiers in Ecology and the Environment 5, 475–482.

Williams, S.E., Shoo, L.P., Isaac, J.L., Hoffmann, A.A., Langham, G., 2008. Towards an Integrated Framework for Assessing the Vulnerability of Species to Climate Change. PLOS Biology 6, e325.

Willig, M.R., Kaufman, D.M., Stevens, R.D., 2003. Latitudinal Gradients of Biodiversity: Pattern, Process, Scale, and Synthesis. Annual Review of Ecology, Evolution, and Systematics 34, 273–309.

Wilson, E.O., 1961. The Nature of the Taxon Cycle in the Melanesian Ant Fauna. The American Naturalist 95, 169–193.

Wisz, M.S., Pottier, J., Kissling, W.D., Pellissier, L., Lenoir, J., Damgaard, C.F., Dormann, C.F., Forchhammer, M.C., Grytnes, J.-A., Guisan, A., Heikkinen, R.K., Høye, T.T., Kühn, I., Luoto, M., Maiorano, L., Nilsson, M.-C., Normand, S., Öckinger, E., Schmidt, N.M., Termansen, M., Timmermann, A., Wardle, D.A., Aastrup, P., Svenning, J.-C., 2013. The role of biotic interactions in shaping

distributions and realised assemblages of species: implications for species distribution modelling. Biological Reviews 88, 15–30.

Wollenberg, K.C., Veith, M., Lötters, S., 2014. Expanding the understanding of local community assembly in adaptive radiations. Ecol Evol 4, 174–185.

Yasuhara, M., Hunt, G., Dowsett, H.J., Robinson, M.M., Stoll, D.K., 2012. Latitudinal species diversity gradient of marine zooplankton for the last three million years. Ecol. Lett. 15, 1174–1179.

Appendix 1: A biogeographic reversal in sexual size dimorphism along a continental temperature gradient

AUTHORS

Simon Tarr

School of Geography, University of Nottingham, Nottingham, NG7 2RD, UK

simon.tarr@nottingham.ac.uk

Orcid ID: 0000-0001-8464-1240

Shai Meiri

Department of Zoology, Tel-Aviv University, Tel-Aviv, 69978, Israel

uncshai@post.tau.ac.il

Orcid ID: 0000-0003-3839-6330

James J. Hicks

School of Geography, University of Nottingham, Nottingham, NG7 2RD, UK

james.hicks@nottingham.ac.uk

Orcid ID: 0000-0001-5154-5615

Adam C. Algar (Corresponding Author)

School of Geography, University of Nottingham, Nottingham, NG7 2RD, UK

adam.algar@nottingham.ac.uk

Orcid ID: 0000-0001-8095-0097

KEYWORDS

Body size, sexual size dimorphism, sexual selection

ACKNOWLEDGEMENTS

Thanks to Daniel Pincheira-Donoso and Andrew MacColl for thoughts on the early stages of this work. The University of Nottingham's Biogeography, Ecology and Evolution Research group supplied valuable feedback on an earlier draft.

1.1 Abstract

The magnitude and direction of sexual size dimorphism (SSD) varies greatly across the animal kingdom, reflecting differential selection pressures on the reproductive and/or ecological roles of males and females. If the selection pressures and constraints imposed on body size change along environmental gradients, then SSD will vary geographically in a predictable way. Here, we uncover a biogeographical reversal in SSD of lizards from Central and North America: in warm, low latitude environments, males are larger than females, but at colder, high latitudes, females are larger than males. Comparisons to expectations under a Brownian motion model of SSD evolution indicate that this pattern reflects differences in the evolutionary rates and/or trajectories of sex-specific body sizes. The SSD gradient we found is strongly related to mean annual temperature, but is independent of species richness and body size differences among species within grid cells, suggesting that the biogeography of SSD reflects gradients in sexual and/or fecundity selection, rather than intersexual niche divergence to minimize intraspecific competition. We demonstrate that the SSD gradient is driven by stronger variation in male size than in female size and is independent of clutch mass. This suggests that gradients in sexual selection and male-male competition, rather than fecundity selection to maximize reproductive output by females in seasonal environments, are predominantly responsible for the gradient.

1.3 Introduction

Within animal species, similarly-sized males and females are the exception, not the norm (Fairbairn, 2007). The direction and magnitude of this sexual size dimorphism (SSD) vary greatly across the animal kingdom; in vertebrates alone, females are larger than males (female-biased SSD) in some taxa and males are larger than females in others (male-biased SSD). For example, some female deep-sea anglerfishes (Lophiiformes) are six times larger than their conspecific males (Pietsch, 2005), while male northern elephant seals (Mirounga angustirostris) are three times larger than females (Fairbairn, 2007). SSD also varies geographically in a range of taxa, including lizards (Algar and López-Darias, 2016; Cox et al., 2007, 2003), bats (Storz et al., 2001), and beetles (Stillwell et al., 2007). However, these geographical patterns are not ubiquitous. For example, Cardillo (2002) found no latitudinal trend in SSD of birds, while Blanckenhorn et al. (2006) found latitudinally structured variation in SSD for two-thirds of 96 species from a variety of taxa. Friedman and Remeš's (2016) global study of over 2000 bird species identified a weak tendency for female-biased or low male-biased SSD at high latitudes, with considerable variation across the globe in environment–SSD relationships. Together, these results hint at emergent geographical patterns in SSD, but with considerable variability among taxa and regions, highlighting how much we still do not know about how SSD varies with environmental conditions, and what processes underlie these patterns (Machado et al., 2016).

SSD arises from differing selection pressures related to the reproductive and/or ecological roles of males and females (Fairbairn, 2007). It may be generated and maintained by selection on resource use and survival (viability

selection), or selection on reproductive output (Berry and Shine, 1980; Cox et al., 2003; Fitch, 1976; Fitch and Hillis, 1984; Hedrick and Temeles, 1989; Pincheira-Donoso and Hunt, 2017; Shine, 1994, 1978; Stamps, 1983). The niche divergence hypothesis posits that, when interspecific competitors are few, intraspecific competition between males and females generates disruptive selection between males and females, producing sexual size dimorphism in either direction (Dayan and Simberloff, 2005; Meiri et al., 2014; Pincheira-Donoso et al., 2018, 2009; Schoener, 1977; Shine, 1989; Slatkin, 1984). Alternatively, selection on reproductive success may take the form of fecundity or sexual selection. Fecundity selection acts on females to maximize reproductive output, via larger clutches and/or offspring, in contrast to sexual selection which acts on mating success and viability selection which acts on survival (Pincheira-Donoso and Hunt, 2017). As larger females can produce larger clutches and/or hatchlings (Meiri et al., 2012; Schwarz and Meiri, 2017), strong fecundity selection could favour increases in female size, possibly leading to female-biased SSD (Pincheira-Donoso and Hunt, 2017; Pincheira-Donoso and Tregenza, 2011; Shine, 1988). Sexual selection may act via male–male competition for mates and/or territories which favours large males, increasing male-biased SSD (Cox et al., 2007, 2003; Stamps, 1983).

Fecundity, viability, and sexual selection could all produce gradients in SSD if the strength of selection varies geographically. When the breeding season is short, fecundity selection should favour larger clutches and/or offspring to maximize reproductive output during the limited reproductive season (Pincheira-Donoso and Tregenza, 2011; Shine, 1988). As larger females can produce larger clutches and/or hatchlings (Meiri et al., 2012), selection for

increased clutch mass should lead to increased female-biased SSD in seasonal environments. The strength of sexual selection via male–male competition may also vary with climate and may depend on female reproductive strategies. If females in aseasonal environments lay many clutches throughout the year (Meiri et al., 2012; Mesquita et al., 2016), then sexual selection in males may be stronger as there are greater benefits to long-term control of high-quality territories or mates than if reproduction occurs in a short burst (Machado et al., 2016). Strong fecundity selection for large females and/or weak sexual selection for large males in seasonal environments predict a gradient in SSD from male-biased SSD to female-biased SSD as seasonality increases. We refer to this as the ‘reproductive selection hypothesis’.

The niche divergence hypothesis, which relies on disruptive selection between males and females, also predicts geographical variation in SSD, but as a function of the strength of intraspecific versus interspecific competition in an area, rather than climate directly. Specifically, when the number of competitor species is high, SSD will be low as there is limited opportunity of inter-sexual divergence as resources are already exploited by competitors; alternatively, when interspecific competitors are few, there is opportunity for male and female body sizes to diverge to reduce intraspecific competition (Schoener 1977, Slatkin 1984, Shine 1989, Dayan and Simberloff 2005, Pincheira-Donoso et al. 2009, c.f. Meiri et al. 2014) The niche divergence hypothesis predicts a negative correlation between the magnitude of SSD, regardless of whether males or females are larger, and the number of co-occurring competitor species. There is conflicting evidence for the niche divergence hypothesis. For example, Pincheira-Donoso et al. (2018) found the predicted

negative relationship in local assemblages of South American Liolaemus lizards, but Meiri et al. (2014) found no such relationship on islands worldwide, suggesting that the signal of niche divergence on SSD is scale-dependent (De Lisle and Rowe, 2015). It could also be that the number of co-occurring species is a poor proxy for competitive environment (Meiri et al., 2014). Thus, we also test whether absolute SSD relates to the spacing between adjacent species in body-size space. When species are more similar in size, there should be less potential for size divergence among the sexes (Supplementary material Appendix 1 Fig. A1).

We test for a biogeographical gradient in sexual size dimorphism for lizards across Central and North America, from southern Panama to the northern limit of lizards' ranges in southern Canada. We test predictions of the reproductive selection hypotheses by evaluating the relationships between SSD, male and female size, clutch size and climate. We test the niche divergence hypothesis by examining the relationship between the magnitude of SSD, species richness, and species packing (spacing of neighbours in body size space). To address the potential scale dependence of the SSD–species richness relationship, we carry out our tests at three different sampling grains, with the expectation that patterns should emerge most strongly at finer grain sizes, that may better reflect the existence of sympatric competing species. At large grain sizes, estimates of species richness may not reflect sympatry at local scales and thus may not accurately capture the number of competing species. This may especially be a problem in mountainous areas, which have high beta-diversity (Mena and Vázquez-Domínguez, 2005). To account for this, we test whether the slope of the SSD–richness relationship is shallower in

mountainous areas. We focus on lizards because their SSD ranges from female- to male-biased (Cox et al., 2007; Fitch, 1981) and their ecology and life history is strongly linked to temperature (Meiri et al., 2013; Pianka and Vitt, 2003). Furthermore, males of many lizard species compete for mates and territories (Stamps, 1983), their morphology (including size) has been linked to resource use, competition intensity, clutch size and reproductive output (Butler et al., 2000; Losos, 2009; Meiri, 2008; Meiri et al., 2012; Mesquita et al., 2016), they display a strong species richness gradient in North America (Currie, 1991; Olalla-Tarraga et al., 2006; Roll et al., 2017).

1.4 Methods

Species Data

We quantified presence-absence and species richness (SR) in 50km x 50km, 100km x 100km and 200km×200km grid cells across North and Central America using the Global Assessment of Reptile Distributions range maps (Roll et al., 2017) for all 606 lizard species inhabiting this region. We excluded cells with less than 50% land area, leaving 3521, 928 and 246 cells, respectively, for subsequent analysis. We used the maximum recorded snout¬–vent length (SVL) of males and females as our measure of body size for each sex from Meiri (2018). Male and female body size data were available for 446 species. We used male and female SVL to calculate sexual size dimorphism (SSD) for each species, following Cox et al. (2003):

$$SSD = \begin{cases} \dfrac{SVL_f}{SVL_m} - 1, & \text{if } SVL_f \geq SVL_m \\ -\left(\dfrac{SVL_m}{SVL_f} - 1\right), & \text{if } SVL_m > SVL_f \end{cases}$$

where SVLf and SVLm are female and male SVL respectively. Sexual size dimorphism is positive when females are larger than males, negative when males are larger than females, and zero when the sexes are the same size. This measure of SSD is symmetric around zero, does not asymptote, and contains information on direction, giving it desirable properties as a measure of SSD (Lovich and Gibbons, 1992). To test the niche divergence hypothesis, we calculated the absolute value of SSD for each species and found the average in each grid cell. Absolute SSD measures the magnitude of SSD in a grid cell, regardless of its direction (i.e. whether SSD is male- or female-biased). We

also calculated a measure of species packing by computing the mean ratio of SVL between adjacent species in SVL space (henceforth 'SVL spacing') using the mean of maximum male and female SVL for each species (see Fig. A1). We obtained clutch mass estimates for 135 species from Meiri's (2018) database by multiplying clutch size by the mass of neonates/hatchlings (derived from their SVL using conversion equations from Feldman et al. 2016). We log-transformed clutch mass to help meet subsequent regression assumptions (see below) and calculated the mean log clutch mass in each grid cell.

Climate and Elevation Data

We used the 30 arc-second WorldClim dataset (Hijmans et al., 2005) to quantify climatic variation across North and Central America. For each grid cell we extracted the average mean annual temperature, temperature seasonality, mean annual precipitation, and precipitation seasonality. Temperature seasonality is the standard deviation of mean monthly temperatures ('BIO4' in Hijmans et al. 2005). Precipitation seasonality is the coefficient of variation of monthly precipitation ('BIO15' in Hijmans et al. 2005). The duration of conditions favourable for reproduction is likely correlated with mean climatic conditions (Machado et al., 2016; Meiri et al., 2012), for example the annual growing degrees days (sum of temperatures above 5ºC) variable from the ENVIREM dataset (Title and Bemmels, 2018) had a Pearson's correlation of 0.99 with mean annual temperature in 100km x 100km grid cells. We used the global 30 arc-second elevation dataset available from Worldclim to calculate elevational range within each grid cell.

Regression Analyses

We fit a series of weighted regression models to test our hypotheses' predictions. For all regressions, grid cells were used as the unit of analysis. To test the niche divergence hypothesis, we first regressed mean absolute SSD against the species richness of each grid cell. Next, we fit a model that included an interaction between species richness and elevation range within cells to determine whether the slope of the mean absolute SSD–species richness relationship was greater in areas with small elevational ranges. We repeated the above using SVL spacing, rather than species richness. To test the reproductive selection hypotheses, we fit regression models relating mean SSD, mean clutch size, and mean male and female size to each climate variable. We also tested if mean SSD was related to mean clutch mass across grid cells. As mean annual temperature and mean annual precipitation were the only variables that showed a relationship with any of our dependent variables (see Results), we also fit multiple regressions with these two variables and their interaction as predictors. Mean annual precipitation and SVL spacing were log-transformed to help meet regression assumptions. In all regressions, we weighted data points by the inverse standard error of the response variable in the relevant grid cell. This accounts for variability in mean SSD (or mean SVL or mean log clutch mass) within a cell by assigning lower weights to grid cells where means were less certain. Regressions were limited to grid cells with at least two species with SSD data to allow standard errors to be calculated, leaving 925 (100km x 100km), 3516 (50km x 50km), and 245 (200km x 200km) grid cells for SSD and SVL analyses and 874, 3353, and 236 grid cells for clutch mass analyses.

Randomisation Tests

We tested the significance of regression relationships using an evolutionarily-informed randomisation (Warren et al., 2014), that accounts for spatial and phylogenetic non-independence. Analyses that apply trait data across species' ranges are sensitive to spurious patterns and inflated Type I error rates, even when spatial regression methods are used, because of the spatial cohesiveness of species' ranges (Hawkins et al., 2017). Type I errors can also arise because of difference in species richness among grid cells, as areas with greater species richness, even when community assembly is random, tend to approach the modal value (e.g. if most species are small, areas with high richness are constrained to have low mean body sizes, but low richness grid cells can contain large or small average body sizes (Meiri and Thomas, 2007). Null models that maintain range size and cohesiveness and species richness by randomly shuffling trait values can alleviate these problems by identifying relationships that are stronger (or not) than expected due to sampling effects alone. However, they do not consider phylogenetic non-independence. This can be important because species that occur closely in space are also likely to be closely related and thus may share similar trait values (Warren et al., 2014). To account for this problem, we simulated Brownian motion of SSD along the lizard phylogeny and used the modelled SSD values at the tree's tips to recompute geographical patterns in mean SSD, thereby generating a null distribution against which to compare the observed relationships (Warren et al., 2014). This approach maintains the spatial autocorrelation of SSD data that arises from range cohesion and ranges that span multiple cells, while accounting for sampling effects due to species richness differences among

cells and for phylogenetic non-independence. We repeated this process for male SVL, female SVL, and log clutch mass for regressions where these were the dependent variables

To carry out our randomisation tests, we simulated Brownian motion of SSD (or SVL or log clutch mass) along Tonini et al.'s (2016) consensus phylogenetic tree. Nineteen species in our dataset were absent from the tree. We grafted these species on to the phylogeny as a sister to their closest relative in the tree at a random location along their terminal branch, or randomly within their shallowest clade affiliation, based on descriptions in the literature (Campbell and Frost, 2016; Díaz-Cárdenas et al., 2017; Gottscho et al., 2017; Grummer and Bryson, 2014; Köhler et al., 2016, 2014, 2015; Lara-Tufiño et al., 2016; Montanucci, 2015; Poe and Ryan, 2017; Solano-Zavaleta et al., 2016). A full list of placements is given in Supplementary material Appendix 1 Table A1. We used the fitContinuous function in Geiger v2.0.6 (Harmon et al., 2008) to estimate the mean SSD (or SVL or log clutch mass) at the phylogeny's root and the rate parameter ($\sigma 2$; Supplementary material Appendix 1 Table A2). We next used the fastBM function in phytools v0.6-44 (Revell, 2012) to simulate Brownian motion using these parameters, assigned the simulated values to our species and recomputed the response variable across our cells. We next refit the regression to obtain t-values for the slope. We repeated this 1000 times and computed a two-tailed P-value for the observed relationship. We simulated log clutch mass, rather than clutch mass because simulating clutch mass produced many negative values which could then not be log-transformed (which itself suggests that the observed

distribution of clutch mass is not simply a result of Brownian motion evolution).

1.5 Results

SSD varied greatly across lizard species (Supplementary material Appendix 1 Fig. A2), from -0.76 (male-biased) in Ctenosaura clarki (male SVL: 250mm, female SVL: 142mm) to 0.52 (female-biased) in Phrynosoma hernandesi (male SVL: 82mm, female SVL: 125mm). SSD was female-biased in 178 species and male-biased in 251 species. The sexes were of similar size (within 1%) in 34 species.

We found a clear geographical gradient in mean SSD from female-biased SSD in high latitude, colder areas and male-biased SSD in warm, low latitude regions (Fig. A1). However, there were exceptions. For example, mean SSD was male-biased at the high-latitude limit of lizards' ranges in one part of the central USA. Qualitatively, mean SSD flipped from male-biased to female-biased around 31° latitude, and mean annual temperature of approximately 15°C. As for previous work on lizard body size in North America that did not consider sex, we did not find a clear latitudinal gradients in mean male or female SVL (Olalla-Tarraga et al., 2006); geographical patterns of body size for males and females were qualitatively similar (Fig. A2).

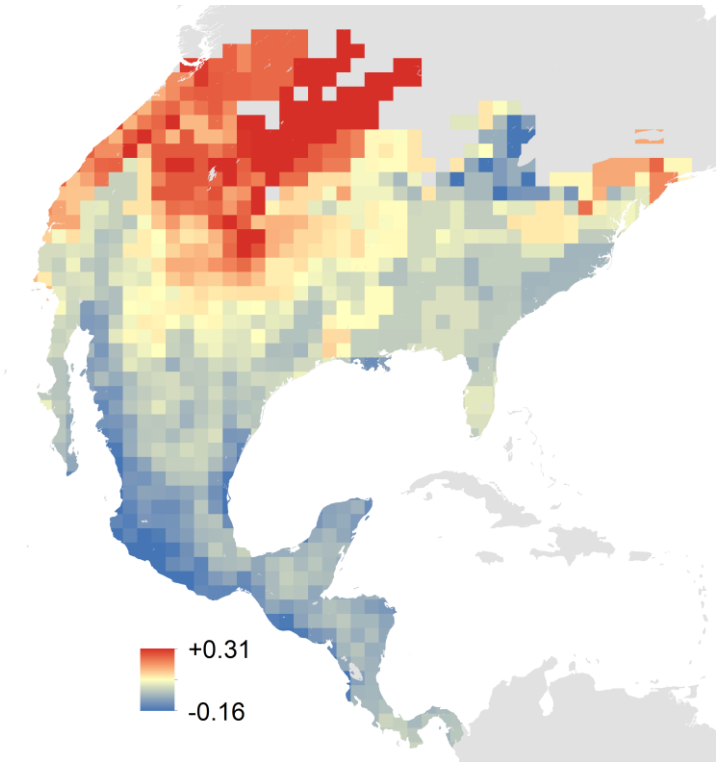


Figure 1 Geographical patterns in mean sexual size dimorphism of lizards in 100km x 100km cells across Central and North America (Mollweide projection). Sexual size dimorphism is positive (red) when females are larger than males and negative (blue) when males are larger than females.

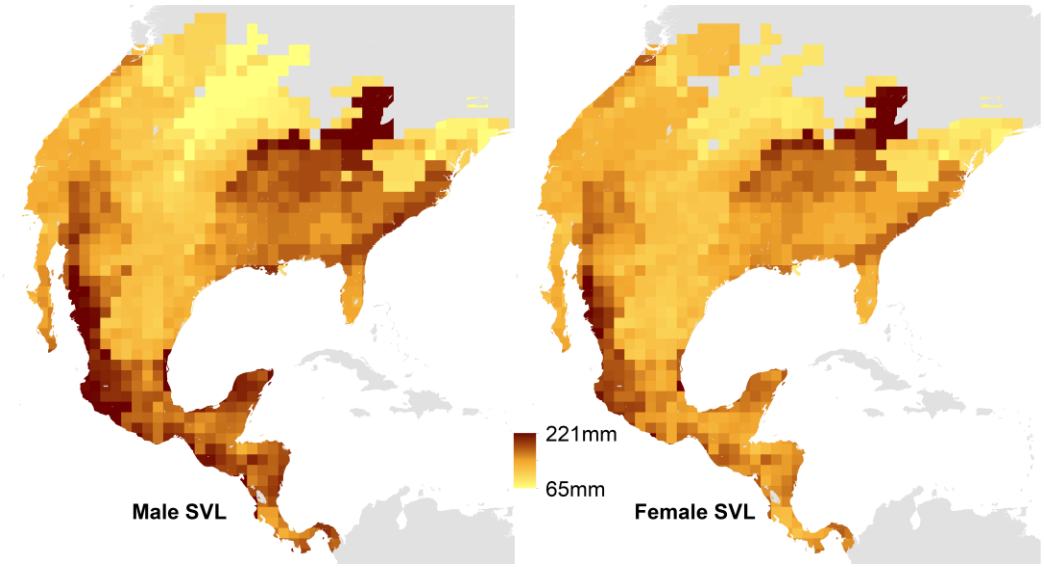


Figure 2 Geographical patterns of mean body size (snout-vent length; SVL in mm) of male (left) and female (right) lizards in 100km x 100km grid cells across Central and North America (Mollweide projection). Colour scales are identical in both panels.

Mean SSD was negatively related to mean annual temperature, based on our randomization test (P=0.03; Fig 3; Supplementary material Appendix 1 Table A3). Mean annual temperature explained 51% of the variance in mean SSD across North America (though this includes potential effects of space and phylogeny). Mean SSD was not significantly related to any of the other climate variables we tested (Fig 3; Supplementary material Appendix 1 Table A3), nor was it related log-transformed clutch mass (Fig. 3; Supplementary material Appendix 1 Table A3). We found no interaction effect on mean SSD between mean annual temperature and mean annual precipitation (Supplementary material Appendix 1 Table A4). These results were consistent at all grain sizes (Supplementary material Appendix 1 Tables A3-A4). The completeness of our SSD data (proportion of species in a grid cell with SSD

data) varied between 0.66 and 1.0 (median=0.95), with the most complete data in north-eastern North America (Supplementary material Appendix 1 Fig. A3). However, this variation in sampling is not responsible for the relationship between mean SSD and mean annual temperature, as the relationship remains even after accounting for the proportion of species with SSD data in grid cell, using partial regression (Supplementary material Appendix 1 Fig. A3).

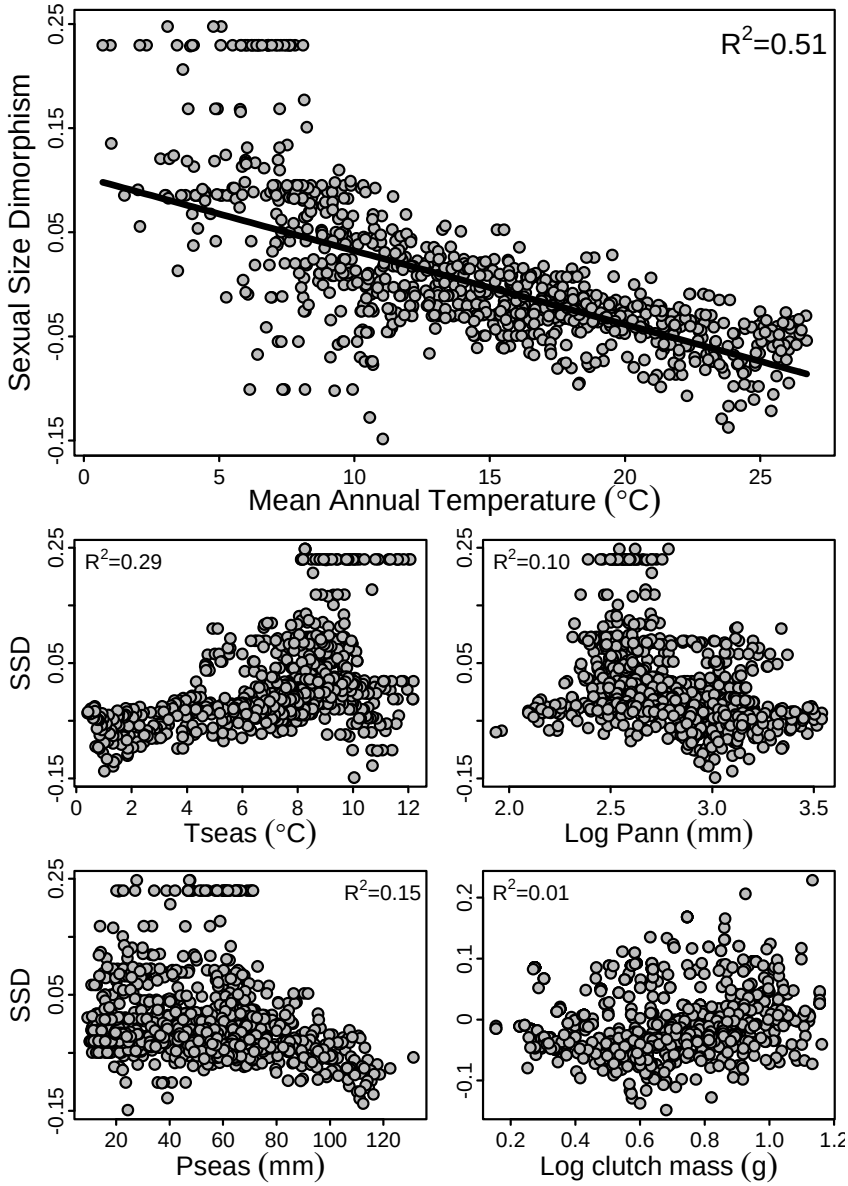


Figure 3 Relationships between sexual size dimorphism (SSD) and climate for lizards in 100km x 100km grid cells across North and Central America. Only the SSD–mean annual temperature relationship was significant (P=0.03; black regression line) relative to the expectation under a Brownian motion evolution of SSD. When SSD is positive, females are larger than males; when it is negative, males are larger than females. T_{seas} is temperature seasonality, Pann is mean annual precipitation, and Pseas is precipitation seasonality.

Female mean SVL was not significantly related to any of the climate variables after accounting for space and phylogeny via randomisation, regardless of grain size (Fig. 4; Supplementary material Appendix 1 Table A3). In contrast, male mean SVL was greater in warmer areas, with mean annual temperature explaining 59% of the variance in male mean SVL (P=0.01; Fig. 4; Supplementary material Appendix 1 Table A3). This relationship held in 50km x 50km and 200km x 200km grid cells (Supplementary material Appendix 1 Table A3). Log clutch mass was related to mean annual precipitation, not temperature, with heavier clutches in drier, areas (P=0.04; Supplementary material Appendix 1 Table A3 and Fig. A4). This relationship was similar across grain sizes (Supplementary material Appendix 1 Tables A3). We found no relationship between mean log clutch mass and mean annual temperature in a multiple regression, either as a main effect or interaction (Supplementary material Appendix 1 Tables A4).

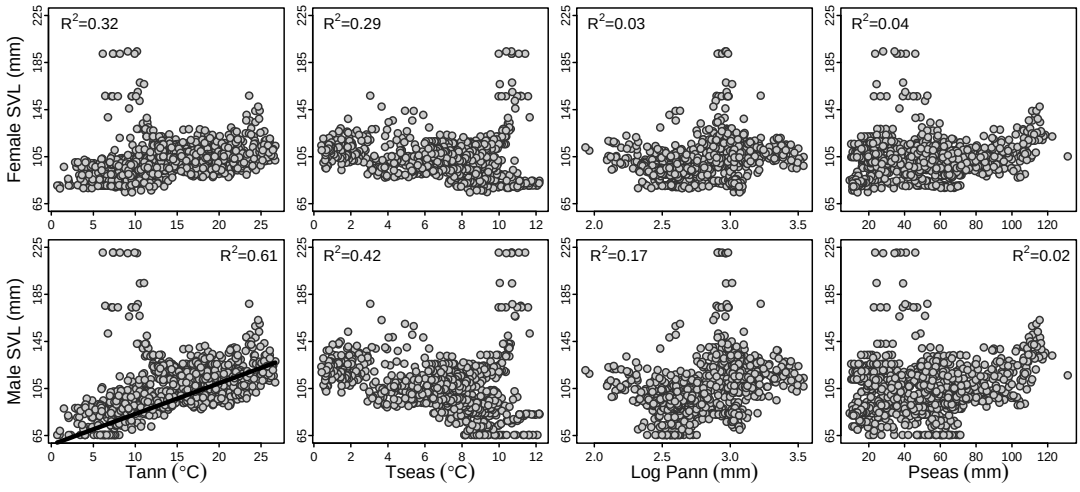


Figure 4 Relationships between sex-specific mean body size (snout–vent length; SVL) and climate for lizards in 100km x 100km grid cells across North and Central America. The relationship between male SVL and mean annual temperature (black line) had P=0.01 relative to the expectation under Brownian motion evolution. Tann

is mean annual temperature, T_{seas} is temperature seasonality, P_{ann} is mean annual precipitation and Pseas is precipitation seasonality.

We found no relationship between mean absolute SSD, i.e. the magnitude of SSD regardless of direction, and species richness at any spatial resolution ($P>0.6$, and $R2<0.08$ for all; Fig. 5). We also found no interaction effect of species richness and elevation range on mean absolute SSD ($P>0.6$ for all grain sizes, Supplementary material Appendix 1 Table A5). Mean absolute SSD was unrelated to the SVL spacing of species in all grid cell sizes ($P>0.9$ for all; see Fig. 5 for results at 100km x 100km). We found no interaction effect between SVL spacing and elevation range at any resolution ($P>0.35$ for all; Supplementary material Appendix 1 Table A6).

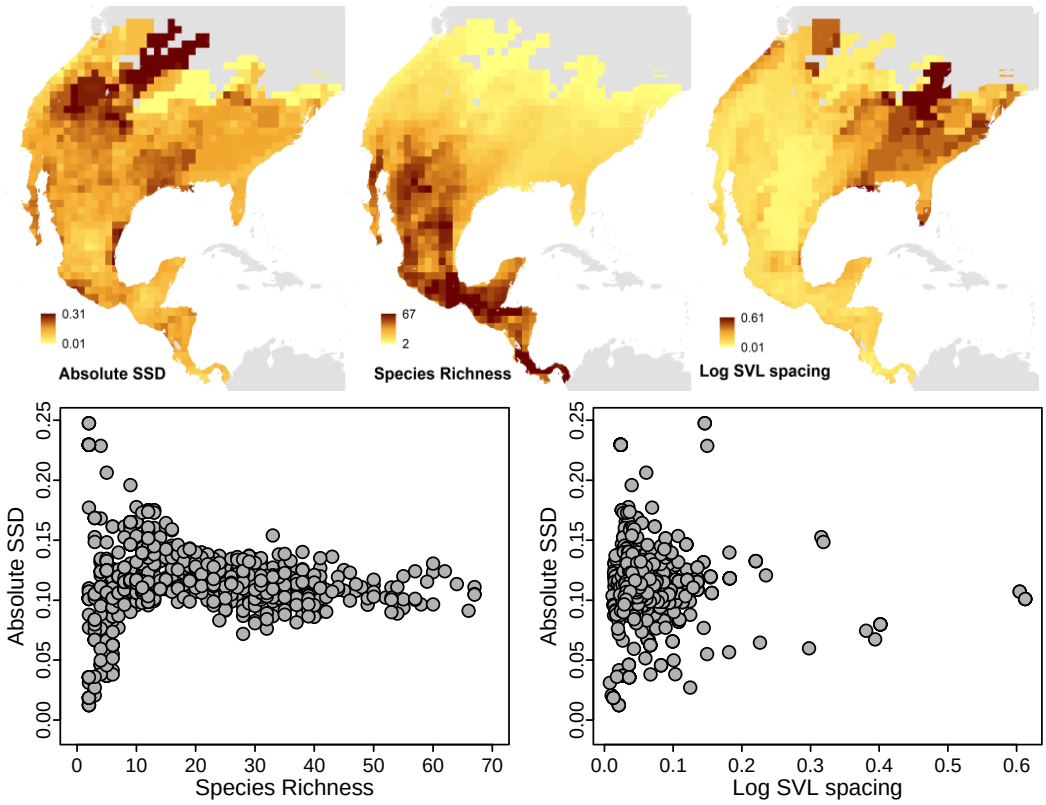


Figure 5 Geographical gradients in the magnitude of sexual size dimorphism, regardless of direction (absolute SSD), species richness, and SVL (snout–vent length) spacing (mean body size ratio of adjacently-sized species) of lizards in 100km x 100km grid cells across Central and North America (Mollweide projection). Absolute SSD ignores the direction of sexual size dimorphism (whether males or females are larger). SVL spacing is shown on a log scale. Absolute SSD was not significantly related to species richness (P=0.79) or log SVL spacing (P=0.99).

1.6 Discussion

We found a continental-scale gradient in lizard sexual size dimorphism that included a switch from female-biased SSD in cold environments to male-biased SSD in warm ones. This gradient was related to mean annual temperature, which also reflects the potential length of breeding season in reptiles and other taxa (Machado et al., 2016; Meiri et al., 2013). This biogeographical pattern cannot be explained as a by-product of Brownian motion evolution, the cohesive structure of species' ranges, or sampling effects due to species richness differences. It thus likely reflects differences in the evolutionary rate and/or trajectory of male and female size differences along the continental temperature gradient that are consistent with differential selection on reproductive success of males and females.

The switch from male-biased SSD to female-biased SSD at mid-latitudes in North America is similar to the global pattern in birds, which also have female-biased SSD, or low male-biased SSD, at high latitudes (Friedman and Remeš, 2016). However, the lizard and bird SSD gradients are not identical. In particular, Friedman and Remeš (2016) found only a very weak global association between climate (including mean annual temperature) and avian SSD,. The strength of this relationship varied by biogeographic realm, but was weak, or non-existent, within the Nearctic and Neotropics. However, Friedman and Remeš (2016) did not analyse these realms together, as we did; the greater female-bias in bird SSD in the Nearctic relative to the Neotropics is roughly collinear with the continental temperature gradient. Of course, other differences between lizards and birds could be responsible for differences in how SSD relates to temperature. Thermoregulatory strategy—ectothermy

versus endothermy—is a tempting hypothesis, but differences could also arise from flight capacity, dispersal ability, migratory behaviour, diet variation, microhabitat use, mating system and so on.

The lizard SSD gradient we observed is consistent with the reproductive selection hypothesis, suggesting continental scale variation in climate does exert pressure on traits related to reproduction (Machado et al., 2016; Macías-Ordóñez et al., 2013). However, our findings are not entirely clear on the relative roles of female fecundity selection and male sexual selection. Fecundity selection imposed by a short reproductive season in seasonal environments should favour larger reproductive output within a limited time frame (Pincheira-Donoso and Tregenza, 2011; Shine, 1988). As larger females can produce larger clutches and/or offspring (Meiri et al., 2012), shorter breeding seasons should thus select for larger females, leading to female-biased SSD in cold, seasonal environments, as observed. However, other lines of evidence suggest the fecundity selection is not the complete story. First, female body size varied little in response to the continental temperature gradient. Second, clutch mass varied with mean annual precipitation, but it was unrelated to temperature, the latter being a stronger predictor of SSD. As such, clutch mass and SSD were not correlated, as we would expect if selection for greater clutch mass was producing female-biased SSD. SSD and clutch mass could be decoupled for several reasons. In particular, females can achieve larger clutches by increasing the size of their abdominal cavity with little increase in their snout-vent length (Scharf and Meiri, 2013), which then wouldn't affect SVL-based measures of SSD. An increase in species exhibiting viviparity in cold environments (Meiri et al., 2013; Scharf and

Meiri, 2013), which also leads to less frequent clutches, could have also contributed to the SSD gradient. The lack of relationship between SSD and clutch mass suggests that female-biased SSD can arise for reasons other than, or in addition to, fecundity selection (Pincheira-Donoso and Hunt, 2017).

The SSD gradient predominantly reflects variation in male size rather than in female size. SSD and male SVL both varied with mean annual temperature, while female SVL did not, though the relationship between male SVL and temperature was much weaker than that of SSD. Still, while our findings must be interpreted cautiously, males tended to be smaller in cooler, more seasonal areas, contradicting Olalla-Tarraga et al.'s (2006) analysis of body size variation (ignoring sex) in North American lizards. However, our analysis included Mexico and Central America, where male lizards, on average, tend to be large, whereas Olalla-Tarraga's et al.'s (2006) only included the USA and Canada. The patterns we observe in the USA are similar to theirs. While female size closely tracked the male pattern, there was insufficient variation in female SVL through space to recover a significant relationship with temperature. Greater variation in males than females is common in studies of sexual dimorphism and is consistent with, if not entirely indicative of, Rensch's rule, which states that when males are larger than females, SSD increases with body size and when females are larger, SSD decreases with body size (Abouheif and Fairbairn, 1997; Blanckenhorn et al., 2006).

The gradient in SSD and male size is consistent with stronger sexual selection, via male-male competition, in warmer environments that lack a prolonged cold season. We found no relationship with precipitation seasonality, suggesting differences between dry and wet seasons are less important than

temperature variation for sexual size dimorphism; this could be because lizards, in general (though there are exceptions), are able to effectively exploit dry environments (Roll et al., 2017). Sexual selection may act directly on male size, if larger males are able to control higher quality territories or access to females. It could also act indirectly, via traits like head size; larger heads increase bite force and combat success in lizards (Herrel et al., 1999; Lopez-Darias et al., 2014; Scharf and Meiri, 2013). Sexual selection on males could be higher in warm, aseasonal environments because the abundance and continual access to resources lessens the relative strength of viability selection or because when resources and reproductive opportunities are available year round, there may be greater total benefit for males that can control high-quality territories and access to mates (Machado et al., 2016). Female lizards tend to have more clutches, spread through the year, in warm, aseasonal, environments (Mesquita et al., 2016), which fits with this hypothesis and suggests that gradients in male sexual selection are not decoupled from female fecundity selection.

Overall, while the patterns of SSD and male size we uncovered are consistent with the reproductive selection hypothesis, especially a gradient in sexual selection, the evidence is indirect and other processes could produce the same pattern. Inverse Bergmann's clines (smaller body size in cold environments), like that observed here for males, are far from ubiquitous in lizards, but nor are they rare (Ashton and Feldman, 2003; Cruz et al., 2005; Muñoz et al., 2014; Olalla-Tarraga et al., 2006; Pincheira-Donoso and Meiri, 2013). Hypotheses have been proposed to explain these clines based on thermoregulatory requirements, via heating and cooling rates, and resource availability (Ashton

and Feldman, 2003; Sears and Angilletta, 2004). Gradients in SSD along temperature gradients could arise if these pressures exert stronger selection on males, or males exhibit greater responses to selection. For example, in some species, gravid females thermoregulate more precisely (Beuchat, 1986) and may maintain different body temperatures than males (Berry and Shine, 1980; Beuchat, 1986; Schwarzkopf and Shine, 1991), which could alter body size gradients as females would operate under different temperatures than males. Another hypothesis, which we propose, is that fecundity selection for larger female size and reproductive output could oppose viability selection for smaller size in cold and seasonal environments, leading to a flatter gradient in female size and an increase in female-biased SSD as males become smaller in cold places. Data on proxies of sexual selection across temperature gradients, such as territoriality, head size, mating system, or—best of all— direct measures of sexual and fecundity selection in the field, are needed to test hypotheses for the biogeographical pattern we have identified here.

The continental mean SSD gradient in lizards was not linked to species richness, at least at the coarse grain size examined here. The niche divergence hypothesis proposes that selection favours size divergence between males and females to limit intraspecific competition for similar resources (Meiri et al., 2014; Pincheira-Donoso et al., 2009; Schoener, 1977; Shine, 1989; Slatkin, 1984). Past findings for this hypothesis are mixed across taxa, including lizards: Schoener (1977) found evidence consistent with this pattern for *Anolis* lizards on small Caribbean islands, but a more recent geographically and taxonomically comprehensive analysis did not find lower SSD on species-rich islands (Meiri et al., 2014). Our results are consistent with Meiri et al.'s (2014)

findings. Instead of a negative correlation between SSD and species richness, we found a funnel-shaped relationship between absolute SSD and species richness, which is consistent with the expected sampling effects of species richness on SSD. When richness is low, mean SSD can be either high or low, but as richness increases, SSD is increasingly constrained to be closer to the mean. Thus, we found no evidence of a negative relationship between SSD and richness. Pincheira-Donoso et al. (2018) found a relationship between SSD and richness in local assemblages of Liolaemus lizards. They suggested that the mixed evidence for the niche divergence hypothesis reflects differences in spatial and ecological scales, where effects of competition on inter-sexual niche divergence will only appear at local scales (also see De Lisle and Rowe 2015). It is thus possible that the species richness of large grid cells, as used here, does not accurately reflect the number of competitors that a species interacts with. This may especially be true in mountainous areas with large environmental gradients and high species turnover. However, our results suggest that the SSD–richness relationship it not stronger in flatter areas where we would expect grid cell richness to better reflect local richness. This suggests either that intersexual niche divergence is not constrained by interspecific competitors, that its effects are not strong enough to leave a signature at macroecological scales, that range maps are too coarse to capture richness patterns accurately, or that species richness is a poor proxy for the ecological opportunities available for intersexual niche divergence (Meiri et al., 2014). Related to this final point, we found no relationship between SVL spacing, i.e. species packing, and mean absolute SSD. If interspecific competition was constraining SSD, as posited by the niche divergence

hypotheses, then SSD should have been lower when species in a grid cell are more similarly sized, but it was not. Our findings suggest that, while competitive processes may be important at local scales, or within guilds, selection on reproductive success is a more likely explanation for broader, continental scale SSD gradients than competition-driven niche divergence.

Classically, studies of macroecological variation in body size across broad geographical extents have ignored sex. Our finding that the direction of SSD switches from larger males to larger females along a temperature gradient stresses the importance of considering sex in macroecological investigations of body size and other traits as the sexes respond differently to the selection pressures imposed along climate gradients. The switch from male-biased SSD to female-biased SSD at mid-latitudes is more than reminiscent of the pattern found in birds worldwide (Friedman and Remeš, 2016), hinting at a general pattern across major taxonomic boundaries. The biogeographical reversal from female-biased SSD in the north to male-biased SSD in the south opens up new avenues to understand how environment affects the origin and maintenance of sexual size dimorphism, the evolutionary processes that underlie it, and the geographical distribution of body size.

1.7 References

Please refer to the main references section starting at page 143.

1.8 Supporting Information

Table A1 Placement of species missing from phylogeny.

Species	Comment	Reference
Abronia cuetzpali	Most closely related to *oaxaca* and *mixteca*, most similar to *mixteca* according to Campbell et al. so add as sister to *mixteca*	Campbell, J.A., et al. 2016. A new species of *Abronia* (Squamata: Anguidae) from the Sierra Madre del Sur of Oaxaca, Mexico. Journal of Herpetology 50: 149-156.
Anolis alocomyos & Anolis leditzigorum	Both formerly part of *tropidolepis*, make a random clade with *tropidolepis*	Köhler, G., et al. 2014. Two new species of the *Norops pachypus* complex (Squamata, Dactyloidae) from Costa Rica. Mesoamerican Herpetology 1: 254–280.
Anolis brooksi & Anolis kathydayae	Part of a clade with *microtus* and *ginaelisae* so make a random clade with these & *brooksi* & *kathydayae*, based on Poe & Ryan.	Poe S, Ryan M.J. 2017. Description of two new species similar to *Anolis insignis* (Squamata: Iguanidae) and resurrection of *Anolis* (*Diaphoranolis*) *brooksi*. Amphibian & Reptile Conservation 11: 1–16.
Anolis marsupialis	Part of a clade with *aquaticus* and *woodi* so make a random clade with these	Köhler, J.J., et al. 2015. *Anolis marsupialis* Taylor 1956, a valid species from southern Pacific Costa Rica (Reptilia, Squamata, Dactyloidae). Zootaxa 3915111–122
Anolis mccraniei, Anolis spilorhipis, & Anolis wilsoni	Formerly part of *tropidonotus*, so split *tropidonotus* into a random clade	Köhler, G., et al. 2016. Taxonomic revision of the *Norops tropidonotus* complex (Squamata, Dactyloidae), with the resurrection of *N. spilorhipis* (Alvarez del Toro and Smith, 1956) and the description of two new species. Mesoamerican Herpetology 3: 8–41
Anolis ustus	Was synonym of *sericeus* but elevated to species so placed as sister to *sericeus*	Lara-Tufiño J.D., et al. 2016. Resurrection of *Anolis ustus* Cope, 1864 from synonymy with *Anolis sericeus* Hallowell, 1856 (Squamata, Dactyloidae). ZooKeys 619: 147–162.
Aspidoscelis costatus	synonym of *sackii* so add as sister to *sackii*	Reptile Database
Mesaspis cuchumatanus	most similar to *moreletii*, so add as sister thereof	Solano-Zavaleta, I., et al. 2016. A new species of *Mesaspis* (Squamata: Anguidae) from the high Cuchumatanes of Guatemala. Journal of Herpetology 50: 327-336
Phrynosoma bauri	Allied to *brevirostris*, add to clade with *hernandesi*, *brevirostris* and *diminutum*	Montanucci, R.R. 2015. A taxonomic revision of the *Phrynosoma douglasii* species complex (Squamata: Phrynosomatidae). Zootaxa 4015: 1–177
Phrynosoma brevirostris	Distinct from *hernandesi*, add to clade with *hernandesi*, *brevirostris* and *diminutum*	Montanucci, R.R. 2015. A taxonomic revision of the *Phrynosoma douglasii* species complex (Squamata: Phrynosomatidae). Zootaxa 4015: 1–177

Phrynosoma diminutum	allied to *brevirostris*, add to clade with *hernandesi*, *brevirostris* and *diminutum*	Montanucci, R.R. 2015. A taxonomic revision of the *Phrynosoma douglasii* species complex (Squamata: Phrynosomatidae). Zootaxa 4015: 1–177
Sceloporus brownorum	in *scalaris* group, but topology of Tonini et al. tree doesn't match Grummer et al. tree, so add next to *scalaris* rather than restructure the whole clade's topology	Grummer, J.A., et al. 2014. A new species of bunchgrass lizard (Squamata: Phrynosomatidae) from the southern sky islands of the Sierra Madre Occidental, Mexico. Zootaxa 3790: 439–450
Sceloporus gadsdeni	Split from *cyanostictus*, so add as a sister to this species	Díaz-Cárdenas, B., et al. 2017. Species delimitation of the blue-spotted spiny lizard within a multilocus, multispecies coalescent framework, results in the recognition of a new *Sceloporus* species. Molecular Phylogenetics and Evolution 111: 185-195
Sceloporus oberon	Paraphyletic with *minor* and *ornatus* which are sisters in tree so randomly add to this clade.	Díaz-Cárdenas, B., et al. 2017. Species delimitation of the blue-spotted spiny lizard within a multilocus, multispecies coalescent framework, results in the recognition of a new *Sceloporus* species. Molecular Phylogenetics and Evolution 111: 185-195
Uma cowlesi	According to Gottscho et al., *rufopunctata* is a hybrid between *cowlesi* and *notata*. *rufopunctata* is in the Tonini et al tree though, so add as sister to *rufopunctata*	Gottscho, A.D., et al. 2016. Lineage diversification of fringe-toed lizards (Phrynosomatidae: *Uma notata* complex) in the Colorado Desert: delimiting species in the presence of gene flow. Molecular Phylogenetics and Evolution 106: 103-117

Table A2 Parameters for Brownian motion simulations for randomisation tests.

Variable	Mean at root	σ^2
Sexual size dimorphism	-0.008	0.0017
Log Clutch mass	0.274	0.005
Male snout-vent length	111.8	92.4
Female snout-vent length	109.2	72.4

Table A3 Univariate regression results relating sexual size dimorphism, clutch mass, male and female size, and climate in grid cells of different grain sizes. Significance was determined based on the distribution of test statistics expected under Brownian motion evolution of the response variable. All P-values are two-tailed. Sexual size dimorphism is positive when females are larger. SVL is snout-vent length. Mean annual precipitation was log-transformed mean annual precipitation. P-values less than 0.05 are in bold.

	Response Variables											
	Sexual Size Dimorphism			Log Clutch Mass			Female SVL			Male SVL		
Predictor Variable	slope	P	r^2	slope	P	r^2	slope	P	r^2	slope	P	r^2
100km x 100km												
Mean annual temperature	**-0.007**	**0.03**	0.51	0.005	0.83	0.01	1.17	0.14	0.32	**2.61**	**0.01**	0.61
Temperature seasonality	1×10^{-4}	0.22	0.29	-1×10^{-5}	0.98	1×10^{-4}	-0.02	0.19	0.29	-0.05	0.08	0.42
Annual Precipitation	-0.06	0.58	0.10	**-0.59**	**0.04**	0.46	7.33	0.80	0.03	34.1	0.43	0.17
Precipitation seasonality	-8×10^{-4}	0.36	0.15	0.003	0.59	0.12	0.10	0.73	0.04	0.11	0.83	0.02
Log clutch mass	0.02	0.90	0.01	-	-	-	-	-	-	-	-	-
50km x 50km												
Mean annual temperature	**-0.007**	**0.03**	0.59	0.004	0.84	0.01	1.28	0.11	0.33	**2.6**	**0.01**	0.59
Temperature seasonality	1×10^{-4}	0.18	0.31	4×10^{-5}	0.96	0.01	-0.03	0.19	0.27	-0.05	0.05	0.42
Annual precipitation	-0.06	0.55	0.11	-0.55	0.05	0.42	9.9	0.74	0.05	29.5	0.46	0.16
Precipitation seasonality	-8×10^{-4}	0.38	0.16	0.003	0.60	0.12	0.11	0.71	0.05	0.16	0.74	0.03
Log clutch mass	-0.02	0.88	0.01	-	-	-	-	-	-	-	-	-
200km x 200km												
Mean annual temperature	-0.007	0.05	0.51	0.007	0.76	0.04	0.98	0.25	0.26	**2.5**	**0.03**	0.56
Temperature seasonality	1×10^{-4}	0.32	0.28	-1×10^{-5}	0.90	0.02	-0.02	0.33	0.25	-0.05	0.11	0.44
Annual precipitation	-0.05	0.64	0.07	**-0.6**	**0.04**	0.43	3.9	0.90	0.01	34.1	0.40	0.17
Precipitation seasonality	-8×10^{-4}	0.48	0.15	0.003	0.65	0.11	0.09	0.81	0.03	0.02	0.98	0.00
Log clutch mass	-0.03	0.87	0.02	-	-	-	-	-	-	-	-	-

Table A4 Multiple regression results relating sexual size dimorphism, clutch mass, and male and female size to mean annual temperature and annual precipitation in 100km x 100km cells. Significance was determined based on the distribution of test statistics expected under Brownian motion evolution of the response variable. All P-values are two-tailed. Sexual size dimorphism is positive when females are larger. SVL is snout-vent length. The interaction is between mean annual temperature and annual precipitation. P-values less than 0.05 are in bold.

	Response Variables											
	Sexual Size Dimorphism			Log Clutch Mass			Female SVL			Male SVL		
Predictor Variable	slope	P	r^2	slope	P	r^2	slope	P	r^2	slope	P	r^2
100km x 100km												
Mean annual temperature	**-0.007**	**0.03**	0.51	0.005	0.83	0.01	1.17	0.14	0.32	**2.61**	**0.01**	0.61
Temperature seasonality	1×10^{-4}	0.22	0.29	-1×10^{-5}	0.98	1×10^{-4}	-0.02	0.19	0.29	-0.05	0.08	0.42
Annual Precipitation	-0.06	0.58	0.10	**-0.59**	**0.04**	0.46	7.33	0.80	0.03	34.1	0.43	0.17
Precipitation seasonality	-8×10^{-4}	0.36	0.15	0.003	0.59	0.12	0.10	0.73	0.04	0.11	0.83	0.02
Log clutch mass	0.02	0.90	0.01	-	-	-	-	-	-	-	-	-
50km x 50km												
Mean annual temperature	**-0.007**	**0.03**	0.59	0.004	0.84	0.01	1.28	0.11	0.33	**2.6**	**0.01**	0.59
Temperature seasonality	1×10^{-4}	0.18	0.31	4×10^{-5}	0.96	0.01	-0.03	0.19	0.27	-0.05	0.05	0.42
Annual precipitation	-0.06	0.55	0.11	-0.55	0.05	0.42	9.9	0.74	0.05	29.5	0.46	0.16
Precipitation seasonality	-8×10^{-4}	0.38	0.16	0.003	0.60	0.12	0.11	0.71	0.05	0.16	0.74	0.03
Log clutch mass	-0.02	0.88	0.01	-	-	-	-	-	-	-	-	-
200km x 200km												
Mean annual temperature	-0.007	0.05	0.51	0.007	0.76	0.04	0.98	0.25	0.26	**2.5**	**0.03**	0.56
Temperature seasonality	1×10^{-4}	0.32	0.28	-1×10^{-5}	0.90	0.02	-0.02	0.33	0.25	-0.05	0.11	0.44
Annual precipitation	-0.05	0.64	0.07	**-0.6**	**0.04**	0.43	3.9	0.90	0.01	34.1	0.40	0.17
Precipitation seasonality	-8×10^{-4}	0.48	0.15	0.003	0.65	0.11	0.09	0.81	0.03	0.02	0.98	0.00
Log clutch mass	-0.03	0.87	0.02	-	-	-	-	-	-	-	-	-

Table A5 Multiple regression results relating the magnitude of sexual dimorphism, regardless of direction, to species richness, elevation range, and their interaction in cells of different sizes. Significance was determined based on the distribution of test statistics expected under Brownian motion evolution of the response variable. All P-values are two-tailed.

	Response Variables						
	Species Richness		Elevation Range		Interaction		
Cell size	slope	P	slope	P	slope	P	R^2
100km x 100km	9×10^{-4}	0.70	7×10^{-6}	0.75	-3×10^{-7}	0.63	0.05
200km x 200km	6×10^{-4}	0.77	9×10^{-6}	0.70	-2×10^{-8}	0.66	0.06
50km x 50km	1×10^{-3}	0.59	5×10^{-6}	0.83	-4×10^{-7}	0.61	0.09

Table A6 Multiple regression results relating the magnitude of sexual dimorphism, regardless of direction, to SVL spacing, elevation range, and their interaction in cells of different sizes. Significance was determined based on the distribution of test statistics expected under Brownian motion evolution of the response variable. All P-values are two-tailed. SVL spacing was log transformed to meet regression assumptions.

	Response Variables						
	Mean SVL spacing		Elevation Range		Interaction		
Cell size	slope	P	slope	P	slope	P	R^2
100km x 100km	0.09	0.72	7×10^{-6}	0.53	-8×10^{-5}	0.39	0.02
200km x 200km	0.06	0.86	4×10^{-6}	0.76	3×10^{-7}	1.0	0.03
50km x 50km	0.10	0.75	8×10^{-6}	0.30	-1×10^{-4}	0.36	0.02

$$\bar{S} = \frac{1}{N-1}\sum_{i=1}^{N-1} s_i$$

$\bar{S}$ = mean trait spacing
s_i = SVL ratio between adjacent species in trait space
N = species richness

$$s_i = \frac{\overline{SVL_{i+1}}}{\overline{SVL_i}}$$

s_i = SVL ratio between adjacent species in trait space
$\overline{SVL_i}$ = mean snout-vent length of the i smallest species
$\overline{SVL_{i+1}}$ = mean snout-vent length of the i+1 smallest species

$$\overline{SVL} = \frac{SVL_m + SVL_f}{2}$$

$\overline{SVL}$ = species' mean snout-vent length
SVL_m = max male snout-vent length
SVL_m = max female snout-vent length

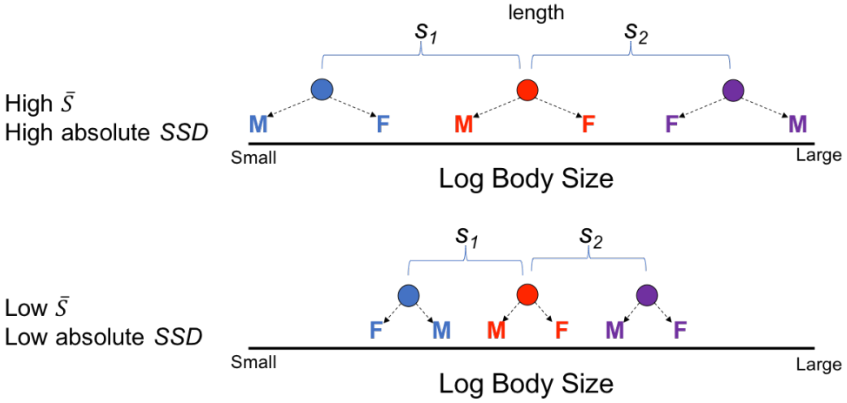


Figure A1 Body size spacing and absolute sexual size dimorphism (absolute *SSD*) under the niche divergence hypothesis. When mean body size spacing ($\bar{S}$) is high (middle panel), selection will favour high absolute *SSD* to reduce intraspecific competition. When $\bar{S}$ is low (bottom panel), absolute *SSD* is lower because interspecific competition constrains intraspecific sexual divergence. Circles indicate species' means and M and F indicate males and females, respectively. Top panel shows equations for mean trait spacing, snout-vent length (SVL) ratio among adjacent species in trait space, and the mean SVL for a species.

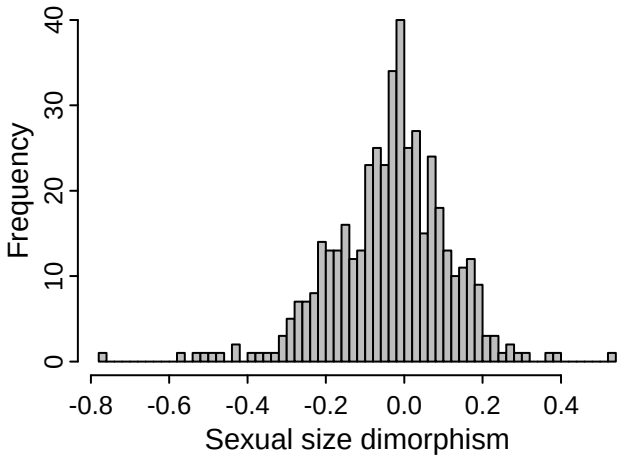


Figure A2 Distribution of sexual size dimorphism (SSD) for 446 species of lizard from North and Central America. Positive values indicate female-biased SSD and negative values male-biased SSD.

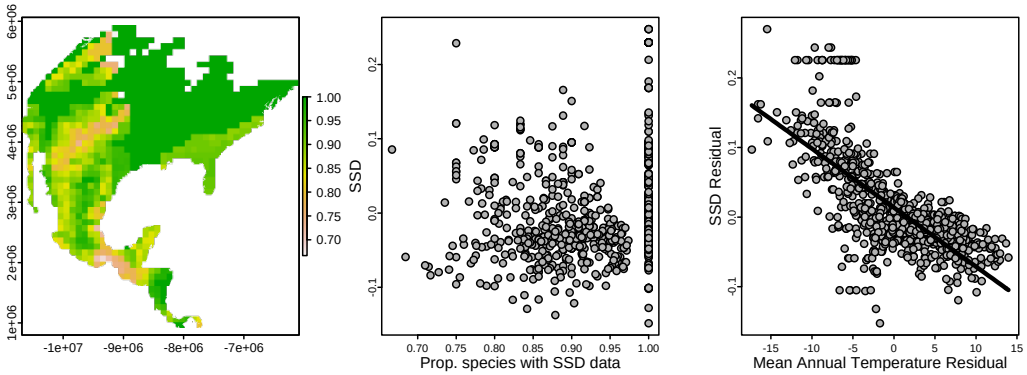


Figure A3 Variation in the proportion of species with sexual size dimorphism (SSD) data in each grid cell and its effect on the mean SSD~mean annual temperature relationship. The left panel shows the proportion of species in each grid cell with SSD data, the middle panel shows the relationship between mean SSD and the proportion of species with SSD data in each grid cell, and the right panel shows the partial regression plot of mean SSD on mean annual temperature, after accounting for the completeness of SSD data within grid cells. Specifically, in the right panel, the y-axis is the residuals from a regression of mean SSD on the proportion of species in a grid cell with SSD data and the x-axis is the residuals from a regression of mean annual temperature on the proportion of species in a grid cell with SSD data.

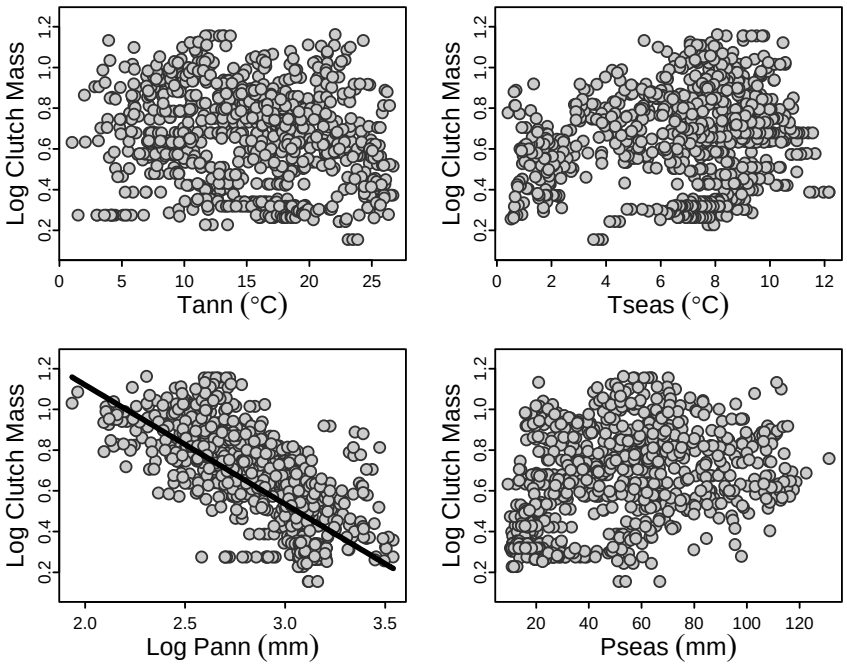


Figure A4 Relationships between mean log clutch mass and climate for lizards in 100km x 100km grid cells across North and Central America. Only the relationship with mean annual precipitation was significant (black line) relative to the expectation under Brownian motion evolution. T_{ann} is mean annual temperature, T_{seas} is temperature seasonality, P_{ann} is mean annual precipitation and Pseas is precipitation seasonality.

Table A7 List of species with range map, sexual size dimorphism (SSD) and clutch size data used in for analyses.

Species	range.map	SSD	clutch.size
Abronia anzuetoi	1	1	0
Abronia aurita	1	1	1
Abronia boqerti	1	1	0
Abronia campbelli	1	0	0
Abronia chiszari	1	1	0
Abronia cuetzpali	1	1	0
Abronia deppii	1	1	1
Abronia fimbriata	1	1	0
Abronia frosti	1	1	0
Abronia fuscolabialis	1	0	0
Abronia qaiophantasma	1	1	0
Abronia qraminea	1	1	0
Abronia leurolepis	1	0	0
Abronia lythrochila	1	0	0
Abronia martindelcampoi	1	0	0
Abronia matudai	1	1	0
Abronia meledona	1	1	1
Abronia mitchelli	1	0	0
Abronia mixteca	1	0	0
Abronia montecristoi	1	0	0
Abronia oaxacae	1	0	0
Abronia ochoterenai	1	1	1
Abronia ornelasi	1	1	0
Abronia ramirezi	1	0	0
Abronia reidi	1	0	0
Abronia salvadorensis	1	0	0
Abronia smithi	1	1	0
Abronia taeniata	1	0	0
Abronia vasconcelosii	1	1	0
Ameiva ameiva	1	1	0
Anadia ocellata	1	1	0
Anadia vittata	1	0	0
Anelytropsis papillosus	1	0	0
Anniella alexanderae	1	0	0
Anniella campi	1	0	0
Anniella qeronimensis	1	1	1
Anniella qrinnelli	1	0	0
Anniella pulchra	1	0	1
Anniella stebbinsi	1	0	0
Anolis allisoni	1	1	0
Anolis alocomyos	1	1	0
Anolis altae	1	1	0
Anolis alvarezdeltoroi	1	1	0
Anolis amplisquamosus	1	1	0
Anolis anchicayae	1	0	0
Anolis anisolepis	1	1	0
Anolis apletophallus	1	1	0
Anolis aquaticus	1	1	0
Anolis auratus	1	1	0
Anolis barkeri	1	1	1
Anolis beckeri	1	1	0
Anolis benedikti	1	1	0
Anolis binotatus	1	0	0
Anolis biporcatus	1	1	0
Anolis boulenqerianus	1	1	0
Anolis brooksi	1	1	0
Anolis campbelli	1	1	0
Anolis capito	1	1	0
Anolis carlliebi	1	1	0
Anolis carolinensis	1	1	1
Anolis carpenteri	1	1	1

Anolis casildae	1	1	0
Anolis charlesmyersi	1	1	0
Anolis chloris	1	1	0
Anolis cobanensis	1	1	0
Anolis compressicauda	1	1	0
Anolis conspersus	1	1	0
Anolis crassulus	1	1	0
Anolis cristifer	1	0	0
Anolis cryptolimifrons	1	1	0
Anolis cupreus	1	1	0
Anolis cuprinus	1	1	0
Anolis cusuco	1	1	0
Anolis cymbops	1	1	0
Anolis damulus	1	1	0
Anolis datzorum	1	1	0
Anolis dollfusianus	1	1	0
Anolis duellmani	1	1	0
Anolis dunni	1	1	0
Anolis elcopeensis	1	1	0
Anolis fortunensis	1	1	0
Anolis frenatus	1	1	0
Anolis fungosus	1	0	0
Anolis fuscoauratus	1	1	0
Anolis gadovii	1	1	0
Anolis gaigei	1	1	0
Anolis ginaelisae	1	1	0
Anolis granuliceps	1	1	0
Anolis gruuo	1	1	0
Anolis haquei	1	0	0
Anolis hobartsmithi	1	1	0
Anolis humilis	1	1	0
Anolis ibanezi	1	1	0
Anolis immaculogularis	1	1	0
Anolis insignis	1	1	0
Anolis johnmeyeri	1	1	0
Anolis kathydayae	1	1	0
Anolis kemptoni	1	1	0
Anolis kreutzi	1	1	0
Anolis kunayalae	1	1	0
Anolis laeviventris	1	1	0
Anolis latifrons	1	1	0
Anolis leditzigorum	1	1	0
Anolis lemurinus	1	1	0
Anolis limifrons	1	1	0
Anolis liogaster	1	1	0
Anolis lionotus	1	1	1
Anolis loveridgei	1	1	0
Anolis macrinii	1	1	0
Anolis macrophallus	1	1	0
Anolis maculiventris	1	1	0
Anolis magnaphallus	1	1	0
Anolis maia	1	0	0
Anolis marsupialis	1	1	0
Anolis matudai	1	1	0
Anolis mccraniei	1	1	0
Anolis megapholidotus	1	1	0
Anolis microlepidotus	1	1	0
Anolis microlepis	1	0	0
Anolis microtus	1	1	0
Anolis milleri	1	1	0
Anolis monteverde	1	1	0
Anolis morazani	1	1	0
Anolis muralla	1	1	0
Anolis naufragus	1	1	0
Anolis nebuloides	1	1	0
Anolis nebulosus	1	1	1

Anolis nietoi	1	1	0
Anolis ocelloscapularis	1	1	0
Anolis omiltemanus	1	1	0
Anolis osa	1	1	0
Anolis oxylophus	1	1	0
Anolis pachypus	1	1	0
Anolis parvicirculatus	1	1	0
Anolis pentaprion	1	1	0
Anolis petersii	1	1	0
Anolis peucephilus	1	1	0
Anolis pijolense	1	1	0
Anolis poecilopus	1	1	0
Anolis polylepis	1	1	0
Anolis pseudokemptoni	1	1	0
Anolis pseudopachypus	1	1	0
Anolis purpurescens	1	0	0
Anolis purpurgularis	1	1	0
Anolis purpuronectes	1	0	0
Anolis pygmaeus	1	0	0
Anolis quaqqulus	1	1	0
Anolis quercorum	1	1	0
Anolis rodriquezii	1	1	0
Anolis rubiginosus	1	1	0
Anolis rubribarbaris	1	1	0
Anolis sacamecatensis	1	1	0
Anolis sagrei	1	1	0
Anolis salvini	1	1	0
Anolis savagei	1	0	0
Anolis schiedii	1	1	0
Anolis sericeus	1	1	0
Anolis serranoi	1	1	0
Anolis sminthus	1	1	0
Anolis spilorhipis	1	1	0
Anolis stevepoei	1	1	0
Anolis subocularis	1	1	0
Anolis taylori	1	1	0
Anolis tenorioensis	1	1	0
Anolis triumphalis	1	0	0
Anolis tropidogaster	1	1	0
Anolis tropidolepis	1	1	0
Anolis tropidonotus	1	1	0
Anolis uniformis	1	1	0
Anolis unilobatus	1	1	0
Anolis ustus	1	1	0
Anolis vittigerus	1	1	0
Anolis wampuensis	1	1	0
Anolis wellbornae	1	1	0
Anolis wermuthi	1	1	0
Anolis wilsoni	1	1	0
Anolis woodi	1	1	0
Anolis yoroensis	1	1	0
Anolis zapotecorum	1	1	0
Anolis zeus	1	1	0
Aristelliger georgeensis	1	1	0
Aspidoscelis angusticeps	1	1	0
Aspidoscelis burti	1	1	1
Aspidoscelis calidipes	1	1	0
Aspidoscelis communis	1	1	0
Aspidoscelis costatus	1	1	0
Aspidoscelis cozumela	1	0	0
Aspidoscelis deppii	1	1	0
Aspidoscelis exsanguis	1	0	0
Aspidoscelis flagellicaudus	1	0	0
Aspidoscelis gularis	1	1	1
Aspidoscelis guttatus	1	1	0
Aspidoscelis hyperythrus	1	1	0

Aspidoscelis inornatus	1	1	0
Aspidoscelis labialis	1	1	0
Aspidoscelis laredoensis	1	0	0
Aspidoscelis lineattissimus	1	1	0
Aspidoscelis marmoratus	1	1	0
Aspidoscelis maslini	1	0	0
Aspidoscelis maximus	1	1	0
Aspidoscelis mexicanus	1	1	0
Aspidoscelis motaguae	1	0	0
Aspidoscelis neomexicanus	1	0	0
Aspidoscelis neotesselatus	1	0	0
Aspidoscelis opatae	1	0	0
Aspidoscelis pai	1	1	0
Aspidoscelis parvisocius	1	1	0
Aspidoscelis rodecki	1	0	0
Aspidoscelis sackii	1	1	0
Aspidoscelis scalaris	1	1	0
Aspidoscelis sexlineatus	1	1	0
Aspidoscelis sonorae	1	0	0
Aspidoscelis stictogrammus	1	0	0
Aspidoscelis tesselatus	1	0	0
Aspidoscelis tigris	1	1	1
Aspidoscelis uniparens	1	0	0
Aspidoscelis velox	1	0	0
Aspidoscelis xanthonotus	1	0	0
Bachia blairi	1	0	0
Bachia pallidiceps	1	0	0
Barisia ciliaris	1	0	0
Barisia herrerae	1	1	1
Barisia imbricata	1	1	1
Barisia jonesi	1	0	0
Barisia levicollis	1	0	0
Barisia planifrons	1	0	0
Barisia rudicollis	1	1	1
Basiliscus basiliscus	1	1	0
Basiliscus galeritus	1	0	0
Basiliscus plumifrons	1	1	1
Basiliscus vittatus	1	1	0
Cachryx alfredschmidti	1	1	0
Cachryx defensor	1	0	0
Callisaurus draconoides	1	1	1
Celestus adercus	1	0	0
Celestus bivittatus	1	1	1
Celestus cyanochloris	1	0	0
Celestus enneagrammus	1	0	0
Celestus hylaius	1	0	0
Celestus ingridae	1	1	0
Celestus laf	1	0	0
Celestus legnotus	1	1	0
Celestus montanus	1	0	0
Celestus orobius	1	0	0
Celestus rozellae	1	0	0
Celestus scansorius	1	0	0
Cnemidophorus duellmani	1	1	0
Cnemidophorus lemniscatus	1	1	0
Cnemidophorus ruatanus	1	1	0
Coleonyx brevis	1	1	1
Coleonyx elegans	1	1	1
Coleonyx fasciatus	1	0	0
Coleonyx mitratus	1	1	1
Coleonyx reticulatus	1	1	1
Coleonyx switaki	1	0	0
Coleonyx variegatus	1	1	1
Coloptychon rhombifer	1	0	0
Copeoglossum nigropunctatum	1	1	0
Cophosaurus texanus	1	1	1

Corytophanes cristatus	1	1	0
Corytophanes hernandesii	1	0	0
Corytophanes percarinatus	1	0	0
Crotaphytus antiquus	1	1	0
Crotaphytus bicinctores	1	1	1
Crotaphytus collaris	1	1	1
Crotaphytus dickersonae	1	1	0
Crotaphytus grismeri	1	1	1
Crotaphytus insularis	1	1	0
Crotaphytus nebrius	1	1	0
Crotaphytus reticulatus	1	1	1
Crotaphytus vestigium	1	1	0
Ctenosaura acanthura	1	0	0
Ctenosaura clarki	1	1	0
Ctenosaura flavidorsalis	1	1	0
Ctenosaura hemilopha	1	1	0
Ctenosaura macrolopha	1	1	0
Ctenosaura melanosterna	1	1	1
Ctenosaura oaxacana	1	1	0
Ctenosaura palearis	1	1	0
Ctenosaura pectinata	1	1	0
Ctenosaura quinquecarinata	1	1	0
Ctenosaura similis	1	1	1
Diploglossus atitlanensis	1	0	0
Diploglossus bilobatus	1	1	1
Diploglossus monotropis	1	1	0
Diploglossus montisilvestris	1	0	0
Dipsosaurus dorsalis	1	1	1
Echinosaura horrida	1	1	0
Echinosaura palmeri	1	1	0
Echinosaura panamensis	1	1	0
Elgaria cedrosensis	1	0	0
Elgaria coerulea	1	1	1
Elgaria kingii	1	0	0
Elgaria multicarinata	1	1	1
Elgaria panamintina	1	1	0
Elgaria paucicarinata	1	1	0
Elgaria velazquezi	1	0	0
Enyalioides heterolepis	1	1	0
Gambelia copeii	1	1	0
Gambelia sila	1	1	1
Gambelia wislizenii	1	1	1
Gerrhonotus farri	1	0	0
Gerrhonotus infernalis	1	1	1
Gerrhonotus lazcanoi	1	0	0
Gerrhonotus liocephalus	1	1	0
Gerrhonotus lugoi	1	0	0
Gerrhonotus ophiurus	1	1	0
Gerrhonotus parvus	1	0	0
Gonatodes albogularis	1	1	0
Gymnophthalmus speciosus	1	1	0
Heloderma horridum	1	1	1
Heloderma suspectum	1	1	1
Holbrookia approximans	1	1	0
Holbrookia elegans	1	1	0
Holbrookia lacerata	1	0	0
Holbrookia maculata	1	1	1
Holbrookia propinqua	1	1	1
Holcosus anomalus	1	1	0
Holcosus chaitzami	1	1	0
Holcosus festivus	1	1	0
Holcosus leptophrys	1	1	0
Holcosus quadrilineatus	1	1	1
Holcosus undulatus	1	1	1
Iguana iguana	1	1	0
Laemanctus longipes	1	1	1

Laemanctus serratus	1	0	0
Lepidoblepharis emberawoundule	1	0	0
Lepidoblepharis rufigularis	1	0	0
Lepidoblepharis sanctaemartae	1	0	0
Lepidoblepharis victormartinezi	1	0	0
Lepidoblepharis xanthostigma	1	1	0
Lepidophyma chicoasensis	1	0	0
Lepidophyma cuicateca	1	0	0
Lepidophyma dontomasi	1	1	0
Lepidophyma flavimaculatum	1	1	1
Lepidophyma gaigeae	1	1	0
Lepidophyma lineri	1	0	0
Lepidophyma lipetzi	1	0	0
Lepidophyma lowei	1	0	0
Lepidophyma mayae	1	0	0
Lepidophyma micropholis	1	1	0
Lepidophyma occulor	1	1	0
Lepidophyma pajapanensis	1	0	0
Lepidophyma radula	1	0	0
Lepidophyma reticulatum	1	0	0
Lepidophyma smithii	1	0	0
Lepidophyma sylvaticum	1	1	0
Lepidophyma tarascae	1	1	0
Lepidophyma tuxtlae	1	1	0
Lepidophyma zongolica	1	0	0
Loxopholis ruginceps	1	1	0
Loxopholis southi	1	1	0
Marisora alliacea	1	1	0
Marisora brachypoda	1	1	0
Marisora unimarginata	1	1	0
Mesaspis antauges	1	1	0
Mesaspis cuchumatanus	1	1	0
Mesaspis gadovii	1	1	1
Mesaspis juarezi	1	1	1
Mesaspis monticola	1	1	1
Mesaspis moreletii	1	1	1
Mesaspis viridiflava	1	0	0
Mesoscincus altamirani	1	1	0
Mesoscincus managuae	1	0	0
Mesoscincus schwartzei	1	1	0
Morunasaurus groi	1	1	0
Ophisaurus attenuatus	1	1	1
Ophisaurus ceroni	1	0	0
Ophisaurus compressus	1	1	1
Ophisaurus incomptus	1	0	0
Ophisaurus mimicus	1	1	0
Ophisaurus ventralis	1	0	0
Petrosaurus mearnsi	1	0	0
Petrosaurus repens	1	0	0
Petrosaurus thalassinus	1	1	0
Pholidobolus vertebralis	1	1	0
Phrynosoma asio	1	0	0
Phrynosoma bauri	1	1	0
Phrynosoma blainvillii	1	1	0
Phrynosoma braconnieri	1	1	0
Phrynosoma brevirostris	1	1	0
Phrynosoma cerroense	1	1	0
Phrynosoma cornutum	1	1	1
Phrynosoma coronatum	1	1	1
Phrynosoma diminutum	1	1	0
Phrynosoma ditmarsi	1	1	1
Phrynosoma douglasii	1	0	1
Phrynosoma goodei	1	0	0
Phrynosoma hernandesi	1	1	1
Phrynosoma mcallii	1	1	1
Phrynosoma modestum	1	1	1

Phrynosoma orbiculare	1	1	0
Phrynosoma ornatissimum	1	0	0
Phrynosoma platyrhinos	1	1	1
Phrynosoma sherbrookei	1	1	0
Phrynosoma solare	1	1	1
Phrynosoma taurus	1	1	0
Phyllodactylus bordai	1	1	0
Phyllodactylus davisi	1	0	0
Phyllodactylus delcampoi	1	0	0
Phyllodactylus duellmani	1	0	0
Phyllodactylus homolepidurus	1	0	0
Phyllodactylus lanei	1	1	1
Phyllodactylus muralis	1	1	0
Phyllodactylus nocticolus	1	1	0
Phyllodactylus papenfussi	1	0	0
Phyllodactylus paucituberculatus	1	0	0
Phyllodactylus tuberculosus	1	1	1
Phyllodactylus unctus	1	1	0
Phyllodactylus xanti	1	1	0
Plestiodon anthracinus	1	1	1
Plestiodon bilineatus	1	0	0
Plestiodon brevirostris	1	1	0
Plestiodon callicephalus	1	1	0
Plestiodon colimensis	1	0	0
Plestiodon copei	1	1	1
Plestiodon dicei	1	0	0
Plestiodon dugesii	1	1	0
Plestiodon egregius	1	1	1
Plestiodon fasciatus	1	1	1
Plestiodon gilberti	1	1	1
Plestiodon indubitus	1	1	0
Plestiodon inexpectatus	1	1	1
Plestiodon lagunensis	1	1	0
Plestiodon laticeps	1	1	1
Plestiodon lotus	1	0	0
Plestiodon lynxe	1	1	1
Plestiodon multilineatus	1	0	0
Plestiodon multivirgatus	1	1	1
Plestiodon nietoi	1	0	0
Plestiodon obsoletus	1	1	1
Plestiodon ochoterenae	1	1	0
Plestiodon parviauriculatus	1	1	1
Plestiodon parvulus	1	0	0
Plestiodon reynoldsi	1	1	0
Plestiodon septentrionalis	1	1	1
Plestiodon skiltonianus	1	1	1
Plestiodon sumichrasti	1	1	1
Plestiodon tetragrammus	1	1	1
Polychrus gutturosus	1	1	0
Polychrus marmoratus	1	1	0
Potamites apodemus	1	1	0
Ptychoglossus festae	1	1	0
Ptychoglossus myersi	1	1	0
Ptychoglossus plicatus	1	1	0
Sauromalus ater	1	1	1
Sauromalus hispidus	1	1	0
Sauromalus varius	1	1	0
Sceloporus acanthinus	1	0	0
Sceloporus adleri	1	1	0
Sceloporus aeneus	1	1	1
Sceloporus albiventris	1	0	0
Sceloporus anahuacus	1	0	0
Sceloporus arenicolus	1	1	0
Sceloporus asper	1	0	0
Sceloporus aurantius	1	0	0
Sceloporus aureolus	1	1	0

Sceloporus bicanthalis	1	1	1
Sceloporus bimaculosus	1	1	0
Sceloporus brownorum	1	1	0
Sceloporus bulleri	1	1	0
Sceloporus caeruleus	1	0	0
Sceloporus carinatus	1	0	0
Sceloporus cautus	1	1	0
Sceloporus chaneyi	1	0	0
Sceloporus chrysostictus	1	1	1
Sceloporus clarkii	1	1	1
Sceloporus consobrinus	1	1	0
Sceloporus couchii	1	1	0
Sceloporus cowlesi	1	1	0
Sceloporus cozumelae	1	1	1
Sceloporus cryptus	1	1	0
Sceloporus cupreus	1	0	0
Sceloporus cyanogenys	1	1	0
Sceloporus cyanostictus	1	1	0
Sceloporus druckercolini	1	0	0
Sceloporus dugesii	1	1	1
Sceloporus edbelli	1	1	0
Sceloporus edwardtaylori	1	0	0
Sceloporus exsul	1	0	0
Sceloporus formosus	1	1	1
Sceloporus gadoviae	1	1	1
Sceloporus gadsdeni	1	1	0
Sceloporus goldmani	1	1	0
Sceloporus graciosus	1	1	1
Sceloporus grammicus	1	1	1
Sceloporus grandaevus	1	1	0
Sceloporus halli	1	0	0
Sceloporus heterolepis	1	1	0
Sceloporus horridus	1	1	1
Sceloporus hunsakeri	1	1	0
Sceloporus insignis	1	1	0
Sceloporus internasalis	1	0	0
Sceloporus jalapae	1	1	1
Sceloporus jarrovii	1	1	0
Sceloporus lemosespinali	1	1	0
Sceloporus licki	1	0	0
Sceloporus lunae	1	0	0
Sceloporus lundelli	1	1	0
Sceloporus macdougalli	1	1	0
Sceloporus maculosus	1	0	0
Sceloporus magister	1	1	1
Sceloporus malachiticus	1	1	1
Sceloporus megalepidurus	1	1	0
Sceloporus melanorhinus	1	1	0
Sceloporus merriami	1	1	1
Sceloporus minor	1	1	0
Sceloporus mucronatus	1	1	1
Sceloporus nelsoni	1	1	0
Sceloporus oberon	1	1	0
Sceloporus occidentalis	1	1	1
Sceloporus ochoterenae	1	1	1
Sceloporus olivaceus	1	1	1
Sceloporus omiltemanus	1	1	0
Sceloporus orcutti	1	1	1
Sceloporus ornatus	1	1	0
Sceloporus palaciosi	1	1	0
Sceloporus parvus	1	1	0
Sceloporus poinsettii	1	1	1
Sceloporus pyrocephalus	1	1	1
Sceloporus salvini	1	0	0
Sceloporus samcolemani	1	1	0
Sceloporus scalaris	1	1	1

Sceloporus serrifer	1	0	0
Sceloporus shannonorum	1	1	0
Sceloporus siniferus	1	1	1
Sceloporus slevini	1	1	0
Sceloporus smaragdinus	1	1	0
Sceloporus smithi	1	0	0
Sceloporus spinosus	1	1	1
Sceloporus squamosus	1	1	0
Sceloporus stejnegeri	1	1	0
Sceloporus subpictus	1	1	0
Sceloporus sugillatus	1	1	0
Sceloporus taeniocnemis	1	1	0
Sceloporus tanneri	1	0	0
Sceloporus teapensis	1	1	0
Sceloporus torquatus	1	1	1
Sceloporus tristichus	1	1	0
Sceloporus undulatus	1	1	1
Sceloporus unicanthalis	1	0	0
Sceloporus uniformis	1	1	0
Sceloporus utiformis	1	1	1
Sceloporus variabilis	1	1	1
Sceloporus virgatus	1	1	1
Sceloporus woodi	1	1	1
Sceloporus zosteromus	1	1	1
Scincella assatus	1	0	0
Scincella caudaequinae	1	1	0
Scincella cherriei	1	1	0
Scincella forbesora	1	1	0
Scincella gemmingeri	1	1	0
Scincella incerta	1	0	0
Scincella kikaapoa	1	0	0
Scincella lateralis	1	1	1
Scincella silvicola	1	1	1
Sphaerodactylus argus	1	1	0
Sphaerodactylus continentalis	1	0	0
Sphaerodactylus dunni	1	0	0
Sphaerodactylus glaucus	1	1	1
Sphaerodactylus graptolaemus	1	1	0
Sphaerodactylus homolepis	1	1	1
Sphaerodactylus lineolatus	1	1	0
Sphaerodactylus millepunctatus	1	1	1
Sphaerodactylus notatus	1	1	0
Sphenomorphus rarus	1	0	0
Thecadactylus rapicauda	1	1	0
Tretioscincus bifasciatus	1	0	0
Tupinambis tequixin	1	1	0
Uma cowlesi	1	1	0
Uma exsul	1	1	1
Uma inornata	1	1	0
Uma notata	1	1	1
Uma paraphygas	1	1	1
Uma scoparia	1	1	1
Urosaurus bicarinatus	1	1	1
Urosaurus gadovi	1	1	0
Urosaurus graciosus	1	1	1
Urosaurus lahtelai	1	0	0
Urosaurus nigricaudus	1	1	0
Urosaurus ornatus	1	1	1
Uta stansburiana	1	1	1
Xantusia arizonae	1	1	1
Xantusia bezyi	1	1	0
Xantusia bolsonae	1	1	1
Xantusia extorris	1	1	1
Xantusia gilberti	1	0	0
Xantusia gracilis	1	0	0
Xantusia henshawi	1	1	1

Xantusia jaycolei	1	0	0
Xantusia sanchezi	1	1	1
Xantusia sherbrookei	1	0	0
Xantusia sierrae	1	1	0
Xantusia vigilis	1	1	1
Xantusia wigginsi	1	1	0
Xenosaurus agrenon	1	0	0
Xenosaurus arboreus	1	0	0
Xenosaurus grandis	1	1	1
Xenosaurus mendozai	1	1	0
Xenosaurus newmanorum	1	1	1
Xenosaurus penai	1	1	0
Xenosaurus phalaroanthereon	1	0	0
Xenosaurus platyceps	1	1	1
Xenosaurus rackhami	1	0	0
Xenosaurus rectocollaris	1	1	1
Xenosaurus tzacualtipantecus	1	0	0

Appendix 2: Fossils, phylogenies and the evolving climate niche

Adam C. Algar[1] & Simon Tarr[1]

[1]School of Geography, University of Nottingham, Nottingham UK, NG7 2RD

A dataset that links geographical occurrences, phylogenies, fossils and climate reconstructions for more than 10,000 vertebrate species reveals accelerated rates of climate niche evolution in warm-blooded animals.

Climate represents a fundamental challenge for all organisms. With few exceptions, species are restricted to a subset of climatic conditions where they can maintain evolutionary fitness and viable populations, i.e. their climate niche. Determining why climate niches have evolved quickly in some groups but slowly in others is central to understanding the uneven geographical distribution of life on Earth, and how it will respond to future climate change (Wiens et al., 2010). Writing in Nature Ecology & Evolution, Rolland et al. (Rolland et al., 2018) find evidence that metabolic heat production—endothermy—has allowed mammals and birds to weaken climate's evolutionary shackles. In a study of unprecedented breadth, the authors combined data on climate niches for over 10,000 species of terrestrial vertebrates to estimate past rates of climate niche evolution. They found that climate niches of endotherms evolved more rapidly than those of ectotherms.

Climate niche conservatism—the retention of climate niche characteristics through ecological and evolutionary time—is thought to have played an important role in the origin of multiple biogeographic patterns, including

global diversity gradients (Wiens et al., 2010). It will also play a key role in determining the effects of rapid climate change on species' future survival (Jezkova and Wiens, 2016). However, climate niches are not uniformly conserved: their rate of evolution can vary greatly among clades, with implications for species richness, lineage diversification and trait evolution (Cooney et al., 2016; Cooper et al., 2011; Lawson and Weir, 2014; Title and Burns, 2015). Previous work has hypothesized that the ability to produce metabolic heat, and thus decouple internal body temperature from the external environment, may have allowed endotherms to more easily invade hostile climates, enhancing rates of climate niche evolution (Jezkova and Wiens, 2016).

Rolland et al. test this hypothesis on an impressive scale. They estimated climate niches using geo-referenced occurrences for over 11,465 bird, mammal, reptile and amphibian species. Traditionally, to estimate rates of divergence, evolution of these climate niches would be modelled along a phylogeny. While this approach can detect niche divergence between species, it is poor at detecting directional evolution (Slater et al., 2012) and it ignores climate change throughout Earth's history. Recent work with morphological traits has demonstrated that linking fossils with phylogenies can improve estimates of past trait evolution (Slater et al., 2012) but to apply this approach to climate niches, Rolland et al. had to overcome a major barrier. Climate niches, unlike some morphological traits, cannot be directly measured from fossils. Even if you know where a fossil was found, climate change and plate tectonics mean that the climate experienced by that species may be very different from present-day conditions. Rolland et al. resolved this problem by

integrating plate tectonics, mountain uplift and past climate change to estimate fossil niches. They then integrated modern and fossil niches to reconstruct niche change along each branch of a phylogeny, allowing them to estimate both rate and direction of climate niche evolution. They found that endotherms (mammals and birds) had much higher rates of climate niche evolution than the ectotherms (reptiles and amphibians). However, even these higher rates of climate niche evolution could not completely decouple biogeography from climatic constraints. By reconstructing historical latitudinal diversity gradients, Rolland et al. found that all groups expanded toward the poles during warmer periods in the Earth's history and contracted toward the equator as the Earth cooled, with stronger effects in ectotherms.

The integration of fossil and extant species' niches provides new insights but also presents challenges. In particular is the need to rely on estimates of climate niches from species' occurrences and climate maps. This approach measures the realised niche which may reflect biotic interactions or dispersal limitation rather than fundamental, physiological, limits (Saupe et al., 2018). While fundamental niches can be estimated for extant species (Kearney and Porter, 2004), the relevant physiological and behavioural traits are not preserved in the fossil record. Realised niches may shift faster than fundamental niches (Saupe et al., 2018), which could produce apparent differences in evolutionary rates if endotherms fill their fundamental niches less than ectotherms. Whether this is the case, especially at the broad taxonomic breadth studied by Rolland et al., merits further attention. A second area for further enquiry is using fossils to not just inform ancestral climate niche reconstructions, but to test them. Rolland et al. tested the reliability of

their method using simulations with known rates. However, evaluation of ancestral climate niche reconstructions by predicting climate niches of fossil species not included in model fitting will go further in determining the potential of fossils to inform estimates of climate niche evolution. Finally, as Rolland et al. recognise, future consideration of multiple climate niche axes—beyond average temperature—will provide a more detailed picture of niche evolution through time.

The centrality of niche conservatism for understanding the past and future of Earth's biogeography makes understanding climate niche evolution more important than ever. The integration of fossils and phylogenetic data to estimate rates of climate niche evolution represents an exciting step forward. The discovery, for such an extensive range of species, of endothermy's relationship with accelerated niche evolution unlocks substantial potential for further investigation of how metabolic heat production interacts with other intrinsic (organismal traits) and extrinsic (environmental) drivers of climate niche evolution. As Rolland et al. note, their results suggest that endotherms' responses to future climate change may be less predictable than those of ectotherms. However, a cautionary note: while ecologists can look to the past to understand the future, the past is not a panacea. Whether integrating fossils and phylogenies can improve future predictions is still very much unknown but Rolland et al.'s work brings us closer to answering such questions.

References

Please refer to the main references section starting on page 143.